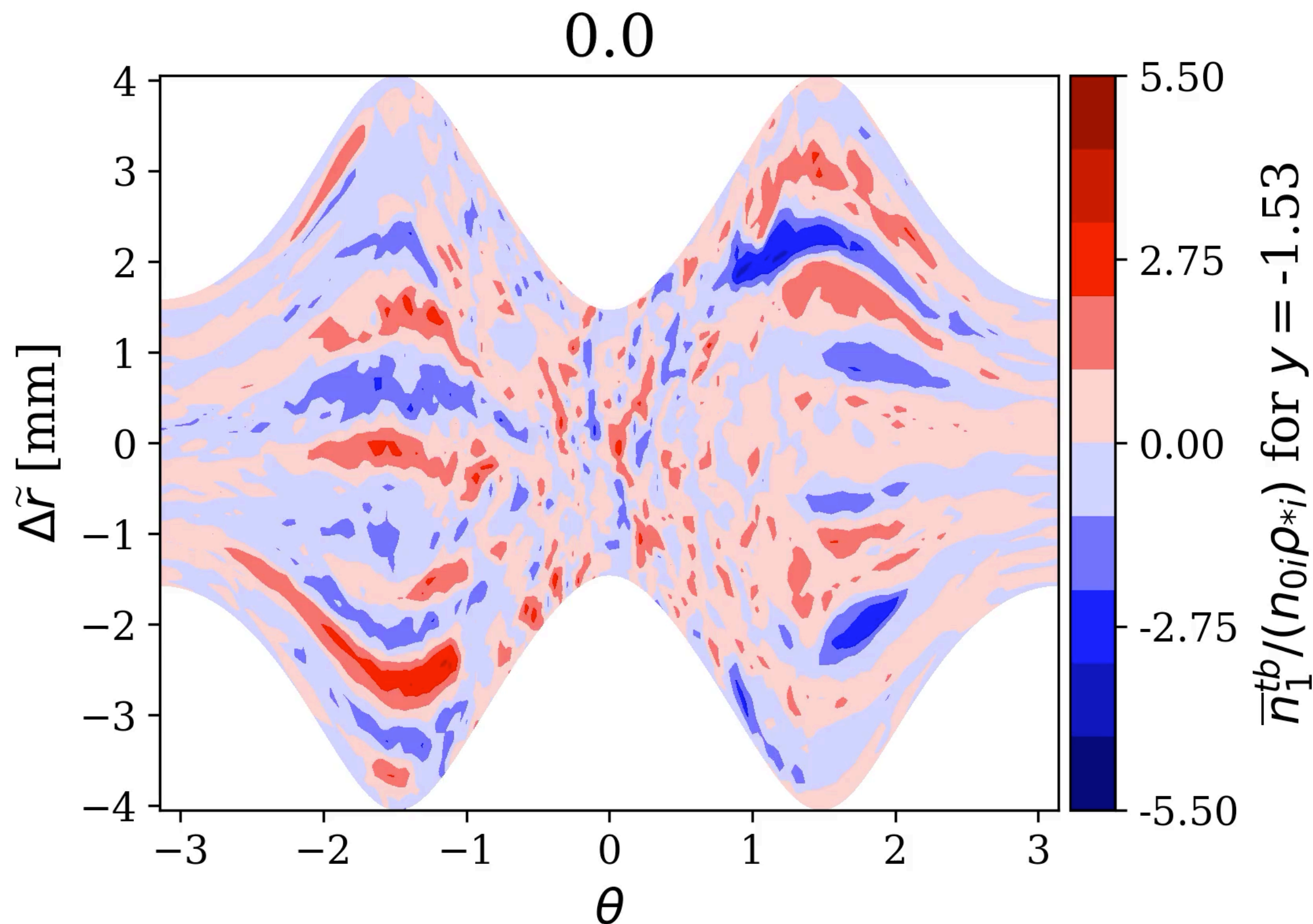


Microstability in fusion plasmas with steep temperature gradients



Gyrokinetic simulation of turbulent density perturbations versus a radial ($\Delta\tilde{r}$) and poloidal (θ) coordinate in a JET-ILW pedestal.

Jason Parisi

*Culham Centre for Fusion Energy
University of Oxford*

Thanks to my collaborators:

Felix Parra, Colin Roach, Michael Hardman,
Michael Barnes, Denis St-Onge, Justin Ball,
David Hatch, Bill Dorland, Ian Abel,
David Dickinson, Carine Giroud, Ben Chapman,
Jon Hillesheim, Plamen Ivanov, Nobuyuki Aiba

PPPL Seminar, May 3, 2021

Outline

- The pedestal
- Linear pedestal physics
- Nonlinear pedestal physics
- Stellarator physics
- Discussion

Main conclusions

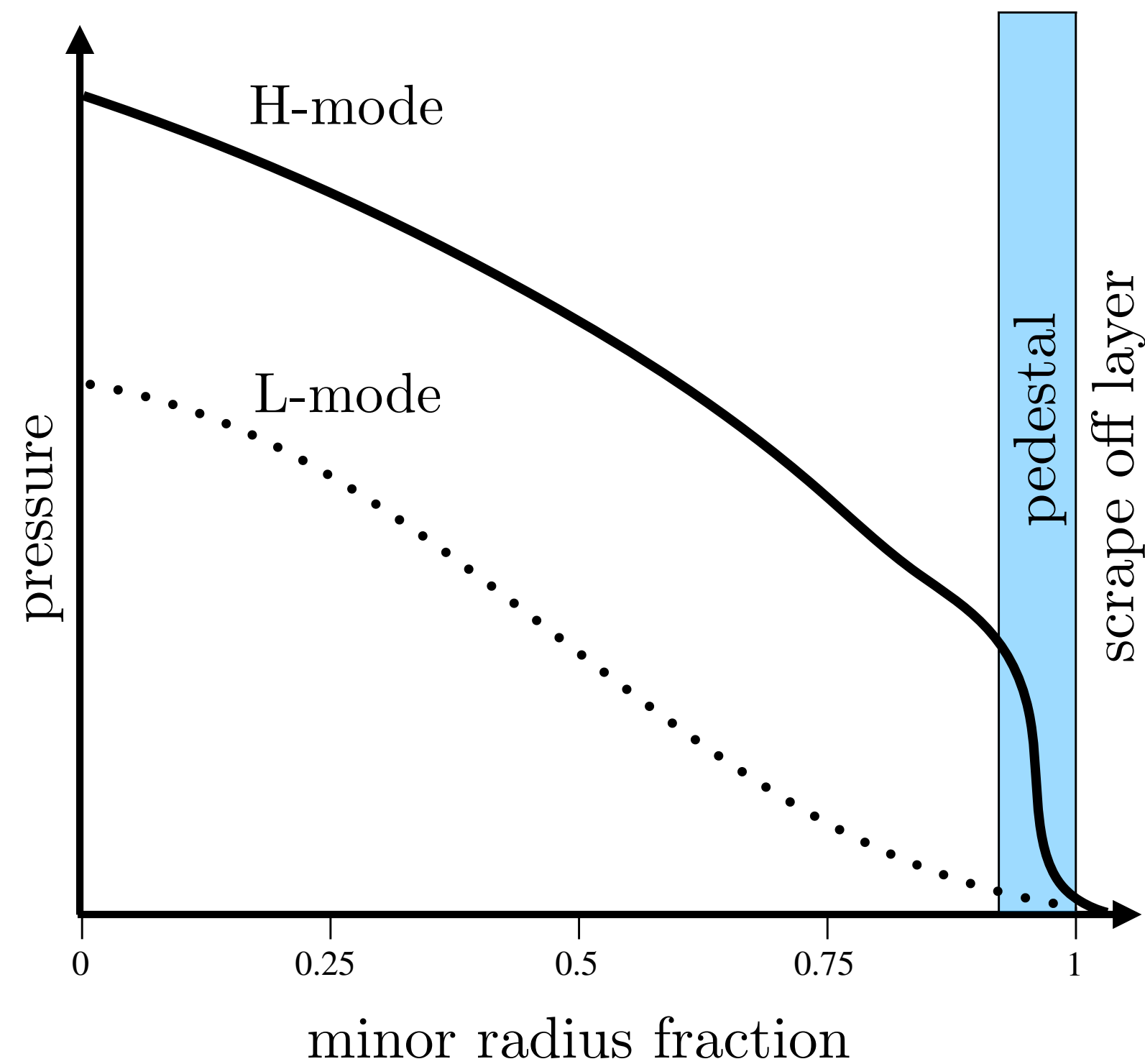
- Steep temperature gradients can cause ETG turbulence to be located at the top and bottom of the poloidal cross section.
- Steep temperature gradients significantly increase the range of scales to be resolved, making even single kinetic species gyrokinetic simulations 'multiscale'.
- Nonlinear gyrokinetic simulations need to be run for sufficiently 'long' to capture slowest growing modes in box, which modify fluctuations/transport at 'long' times.

The pedestal

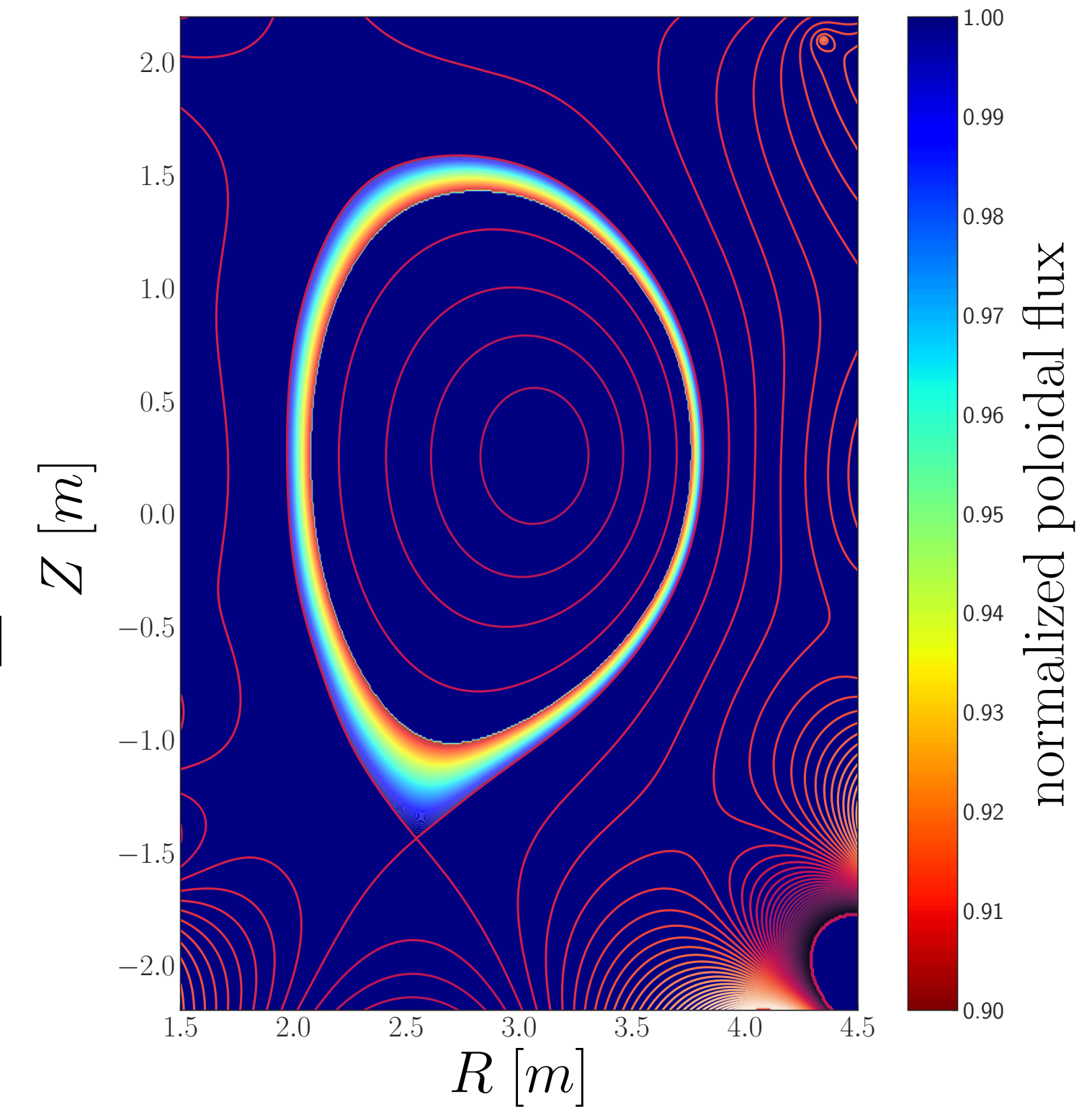
The pedestal

- Region at plasma edge with significantly increased equilibrium temperature and density gradients. Appears once external heating crosses threshold (Wagner, 1982).

a) Typical tokamak pressure profiles.



b) Pedestal highlighted by colored contours representing poloidal flux.



- For geometry in this work, we use a Miller equilibrium from a steep gradient region in a JET-ILW discharge. Here, $R/L_{Te} \simeq 130$, where R is major radius and $L_{Te} = |\nabla \ln T_e|^{-1}$.

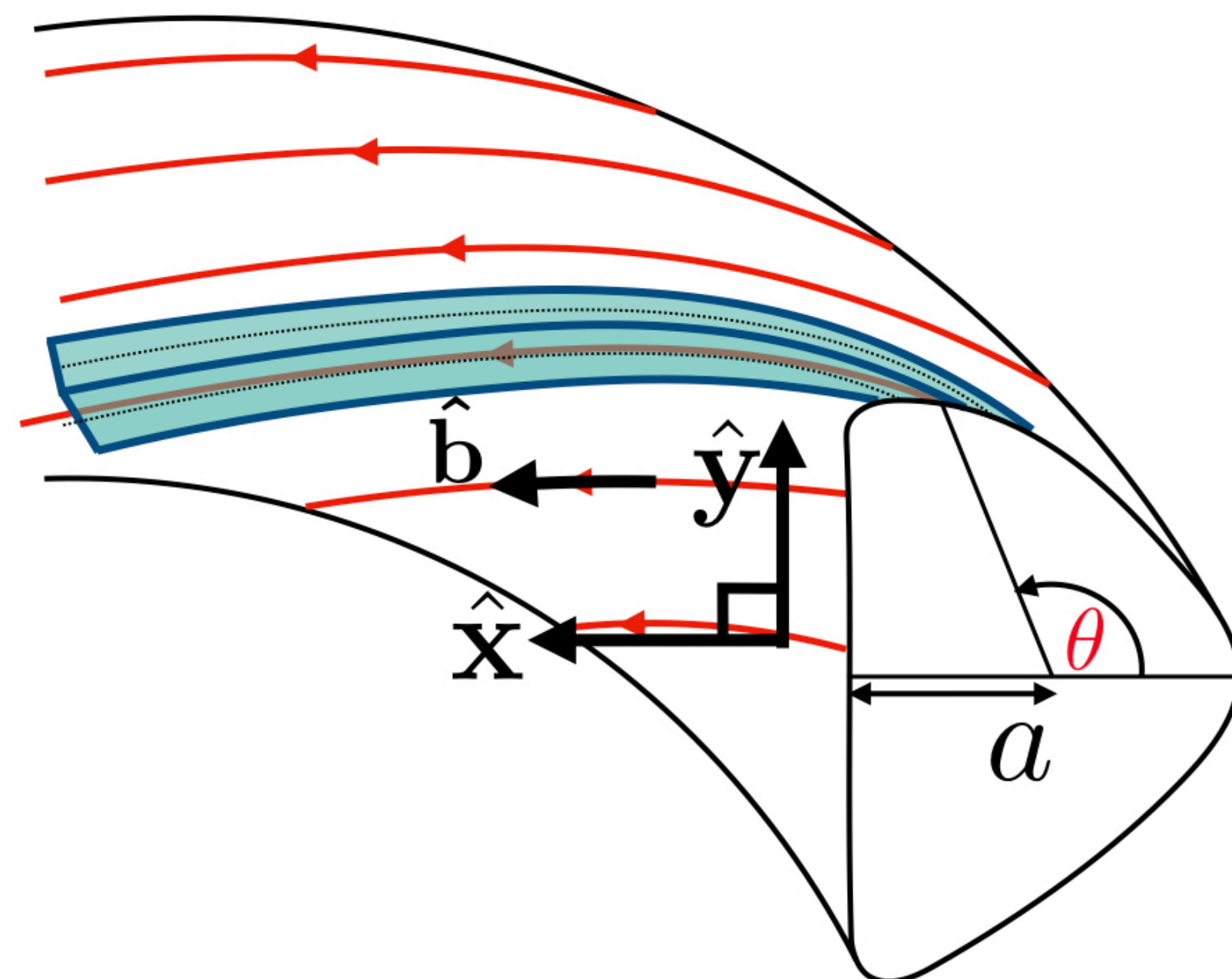
Nomenclature

- Use $\{x, y, \theta\}$ real space coordinates: x radial, y field line label, θ parallel ballooning arclength.
- Perpendicular wavenumber k_{\perp} , with magnetic shear \hat{s} , and effective radial wavenumber $K_x \approx k_y \hat{s} \theta$,

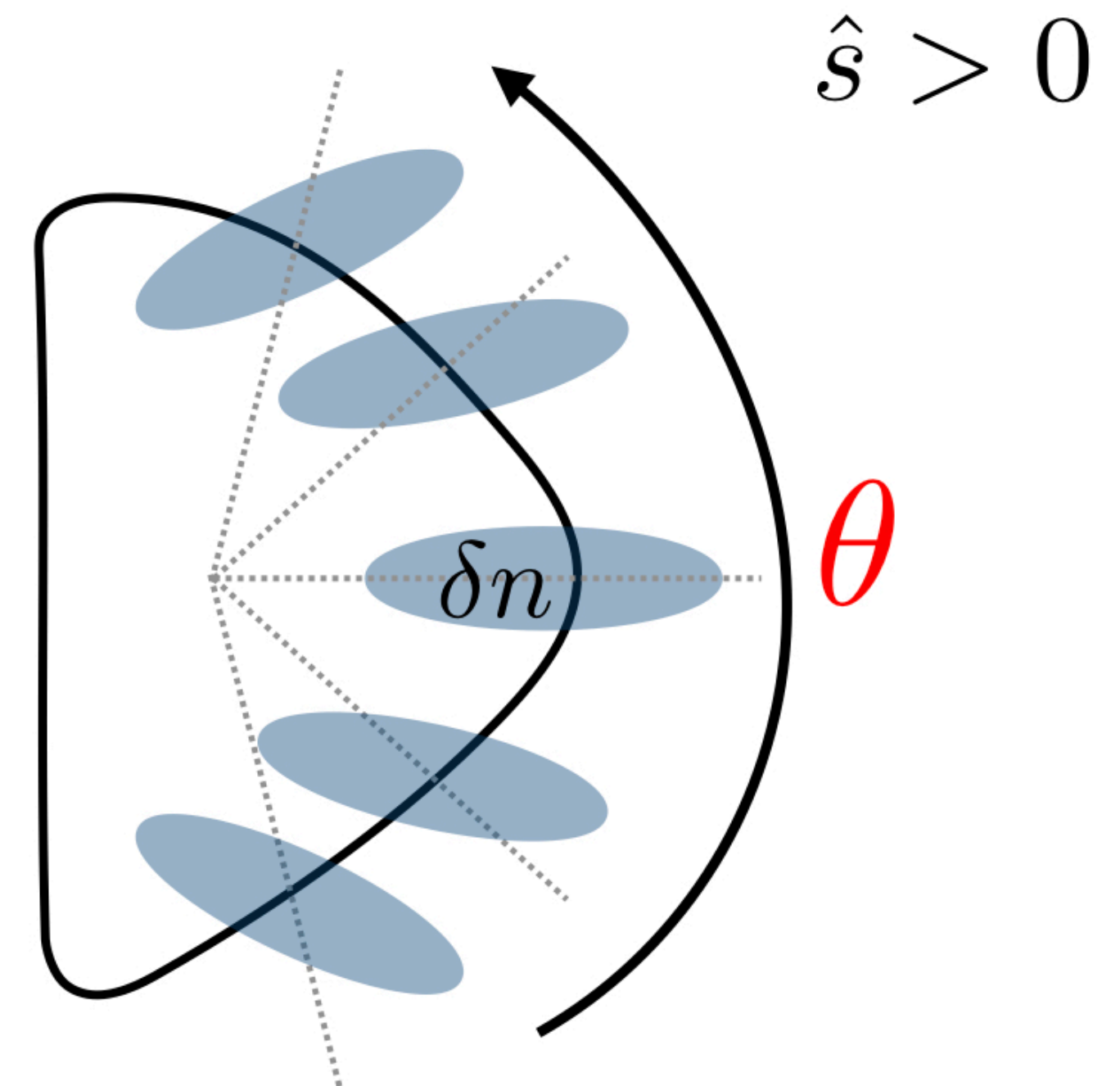
$$k_{\perp} \approx \sqrt{K_x^2 + k_y^2} \approx k_y \sqrt{(\hat{s} \theta)^2 + 1}.$$

- Frequencies, $\omega_{Me} = \mathbf{k}_{\perp} \cdot \mathbf{v}_{Me}$, $\omega_{*e}^T = \nabla \ln(T_e) \cdot \mathbf{v}_E^{tb} T_e / e \phi^{tb} = k_y v_{te} \rho_e / L_{Te}$, where the electrostatic magnetic drift is $\mathbf{v}_{Me} = (\hat{\mathbf{b}} \times \nabla \ln B)(v_{\parallel}^2 + v_{\perp}^2/2) / \Omega_e$, ϕ^{tb} is the turbulent electrostatic potential, and $\hat{\mathbf{b}} = \mathbf{B}/B$.

a) Coordinate system.



b) Magnetic shear acting on a perturbation.

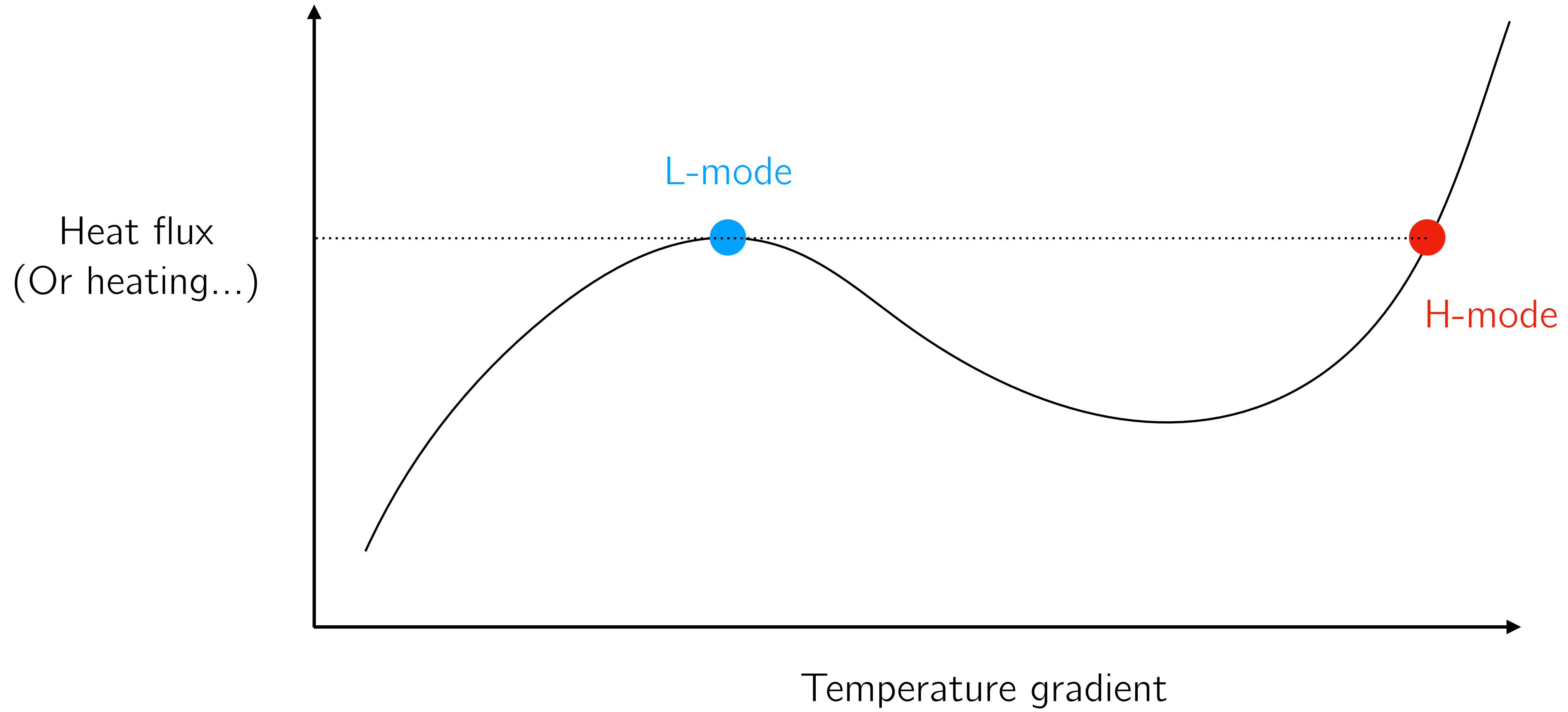


Pedestal microstability

- Zoo of pedestal microinstabilities: KBM, ITG, MTM, ETG (Dickinson, 2013; Hatch, 2016; Kotschenreuther, 2019; Pueschel, 2019; Parisi, 2020; Guttenfelder, 2021).
- We focus on **toroidal ETG** modes, which dominate in steep gradient region of linear and nonlinear JET-ILW pedestal discharges we have investigated. Note: these pedestal toroidal ETG modes are very different to core toroidal ETG modes.
- We care about these toroidal ETG modes because they dominate fluctuations and transport in simulations we have performed (and because they are interesting!).

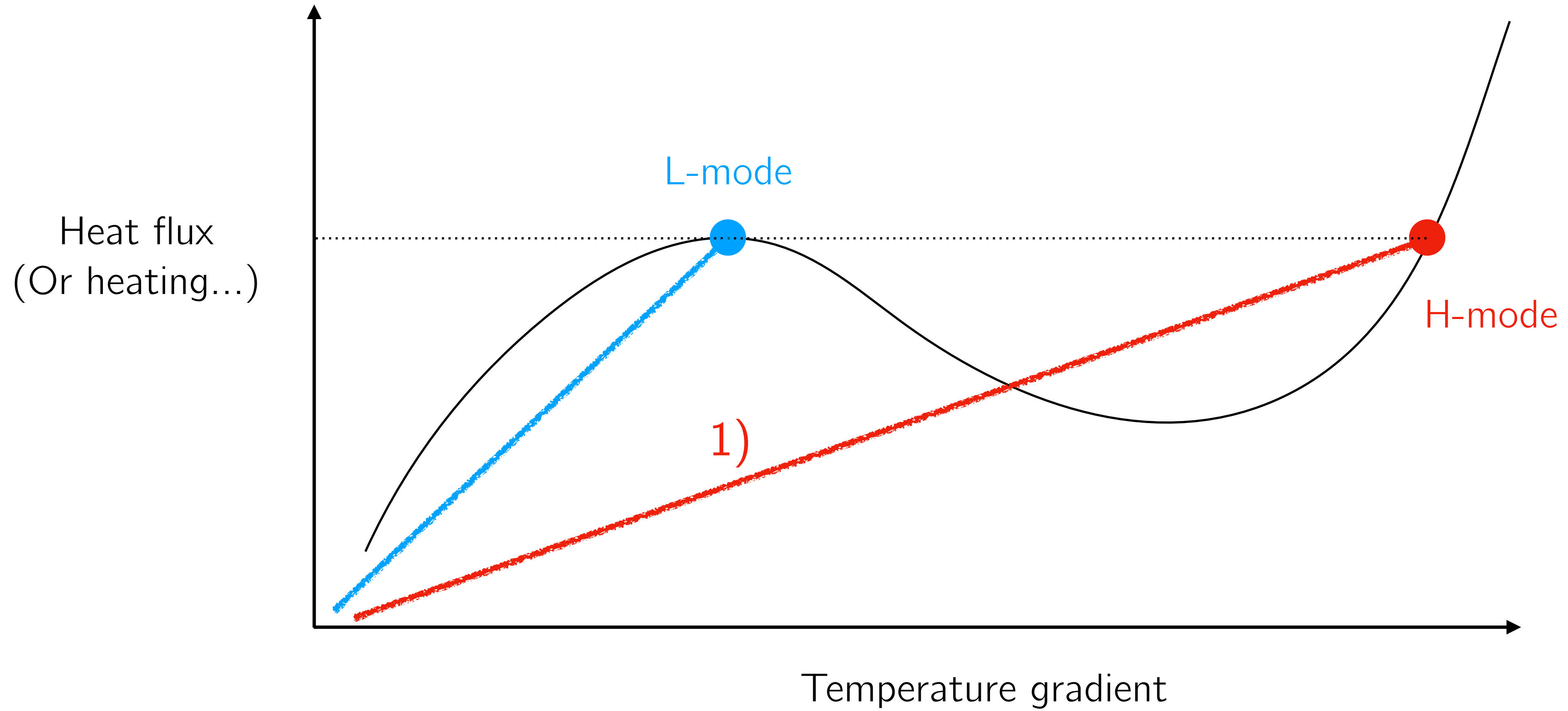
Motivation

Cartoon of H-mode pedestal bifurcation



Motivation Cartoon of H-mode pedestal bifurcation

2 possible ways to get to H-mode transport 1) H-mode transport less stiff

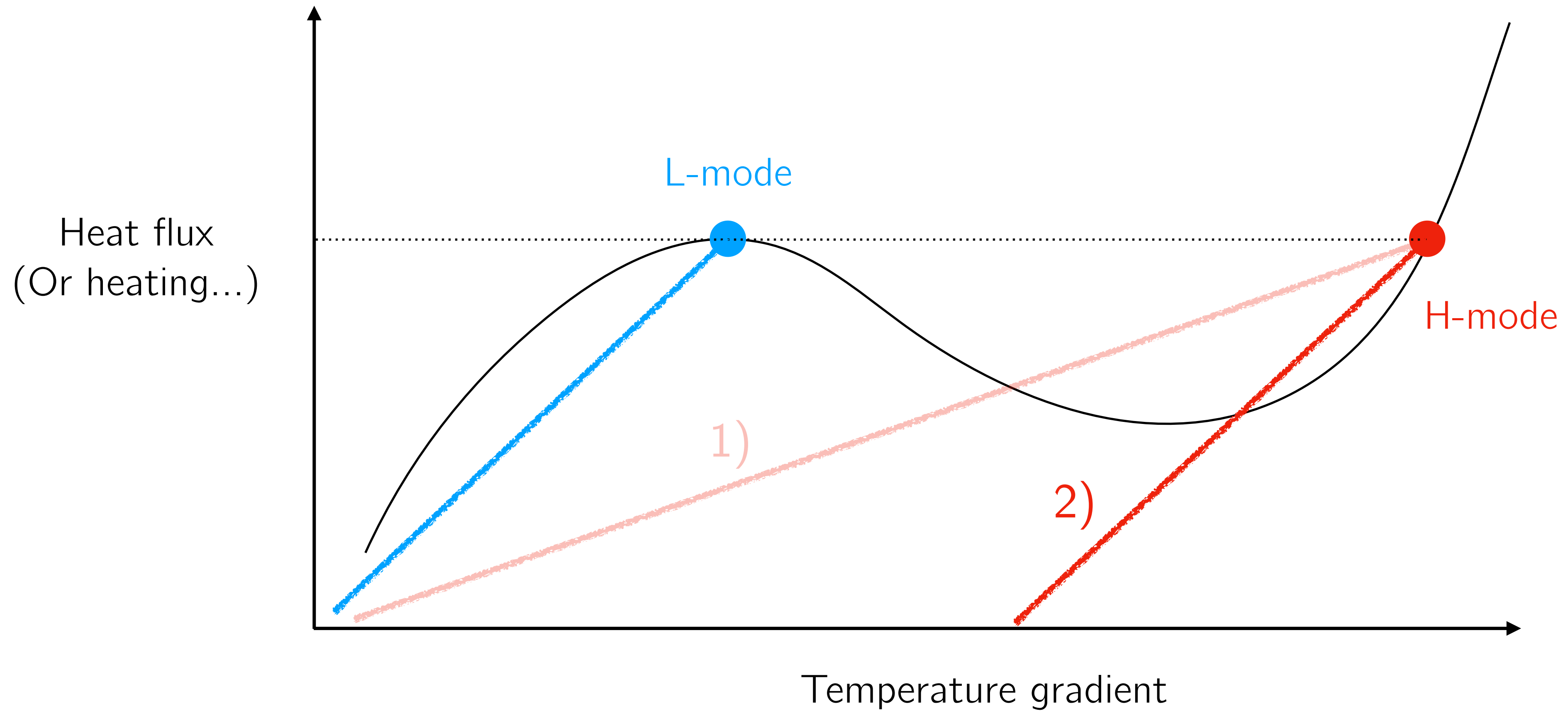


Motivation Cartoon of H-mode pedestal bifurcation

2 possible ways to get to H-mode transport

1) H-mode transport less stiff

2) Higher linear critical gradients

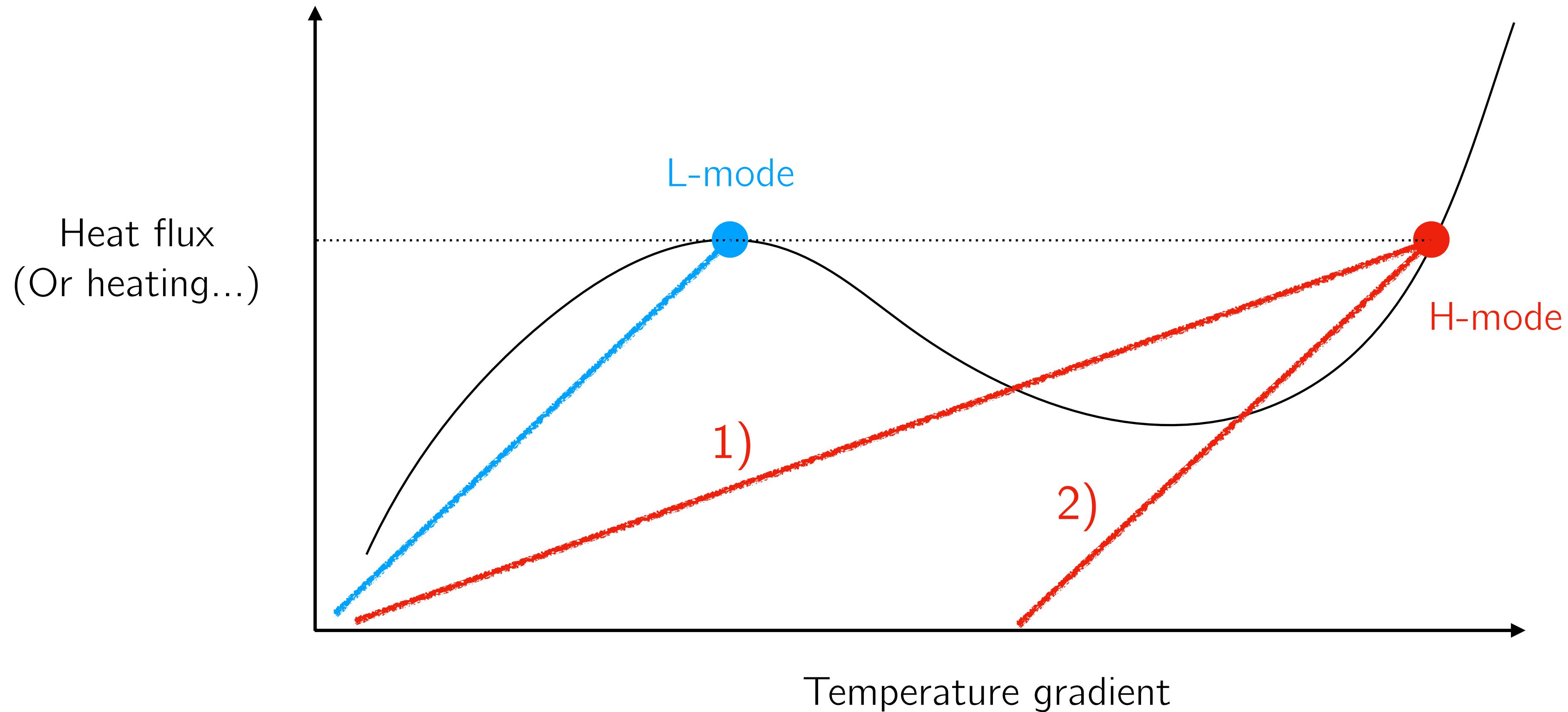


Motivation Cartoon of H-mode pedestal bifurcation

2 possible ways to get to H-mode transport

1) H-mode transport less stiff

2) Higher linear critical gradients



Pedestal toroidal ETG modes satisfy 2), and possibly 1) \rightarrow candidates for electron pedestal transport.

Linear physics

Pedestal microstability

- Fast growing toroidal ETG modes require balance of ExB drift frequency ω_{*e}^T and magnetic drift frequency ω_{ke} ,

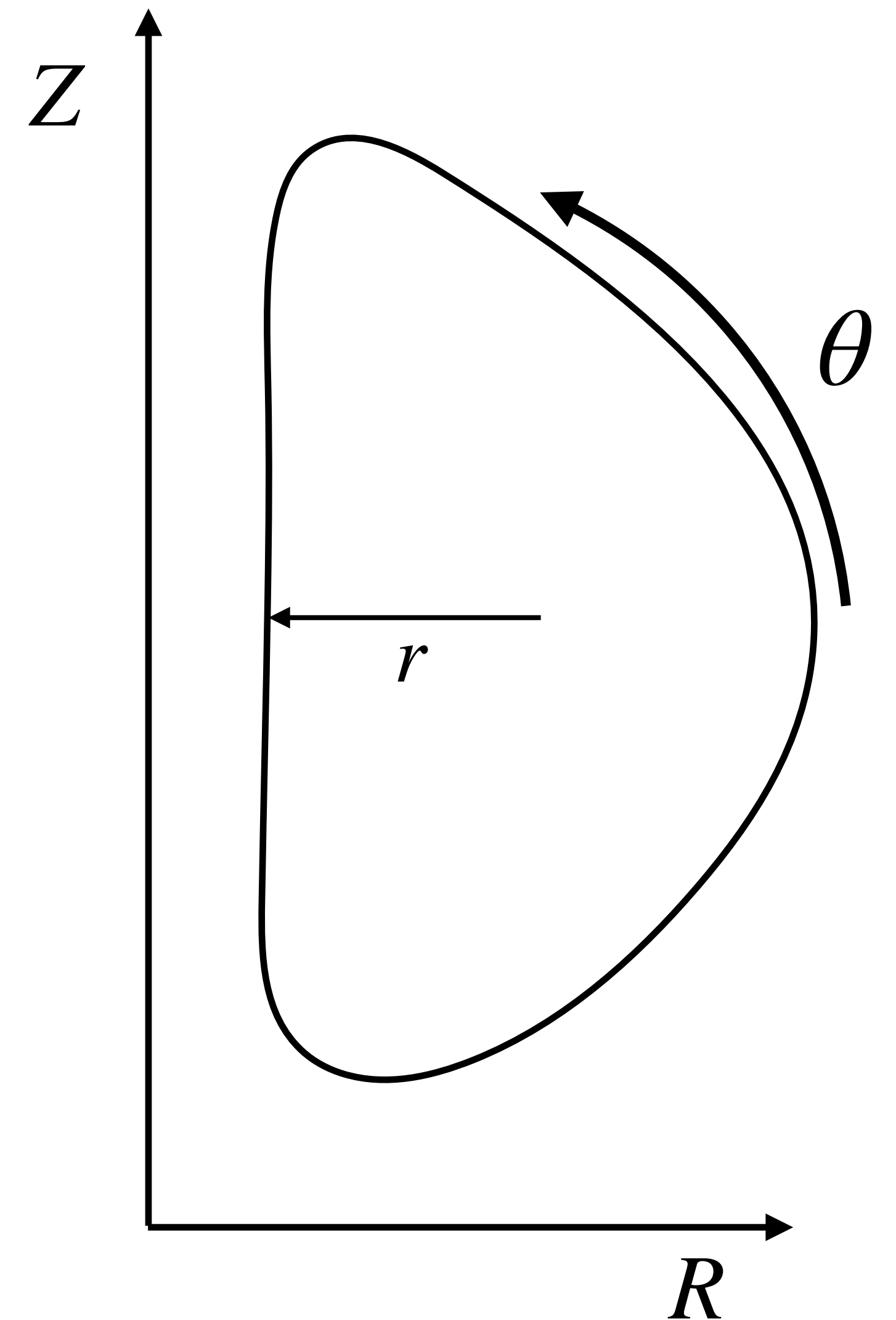
$$\frac{\omega_{*e}^T}{\omega_{ke}} \sim 1$$

- Because of steep pedestal gradients, require perpendicular wavenumber $k_{\perp} \simeq k_y \hat{s} \theta \gg k_y$,

$$\frac{\omega_{*e}^T}{\omega_{ke}} \sim \frac{k_y R}{k_{\perp} \underbrace{L_{Te}}_{\gg 1}} \sim \frac{1}{\hat{s} \theta} \frac{R}{L_{Te}} \sim 1, \text{ so } \theta \sim \frac{1}{\hat{s}} \frac{R}{L_{Te}},$$

where \hat{s} is global magnetic shear, θ is the poloidal ballooning angle, R is the major radial distance to mode, $L_{Te} = |\partial_r \ln T_e|^{-1}$ is a flux function, and r is the minor radius at the midplane.

- This causes instability to live away from outboard (and usually near **top/bottom** of flux surface due to flux expansion and drifts).



A flux surface with coordinates R, Z, θ .

Pedestal microstability

- We also expect the scales for toroidal instability to satisfy $k_{\perp}\rho_e \sim 1$ due to FLR damping.
- Using (from our previous slide)

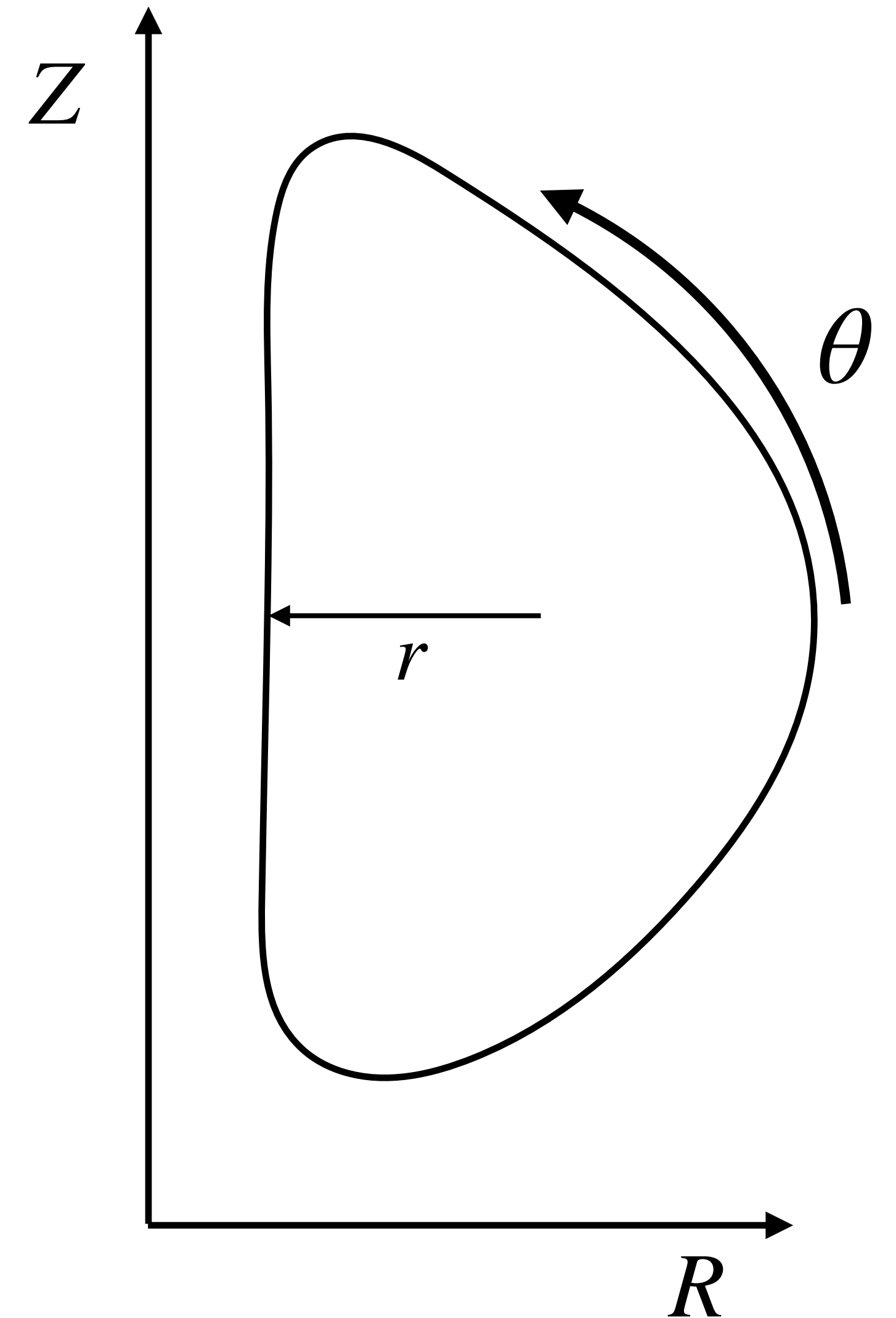
$$\frac{\omega_{*e}^T}{\omega_{ke}} \sim \frac{k_y R}{k_{\perp} L_{Te}} \sim 1$$

we find

$$k_y \rho_e \sim k_{\perp} \rho_e \frac{L_{Te}}{R}$$

and therefore using $k_{\perp}\rho_e \sim 1$ we find that strongly driven toroidal ETG turbulence satisfies

$$k_y \rho_e \sim \frac{L_{Te}}{R}.$$



A flux surface with coordinates R, Z, θ .

Pedestal microstability

- To summarize, toroidal ETG modes in steep temperature gradients satisfy:

Relatively large radial wavenumber:

$$k_{\perp} \gg k_y \text{ (follows from } R/L_{Te} \gg 1)$$

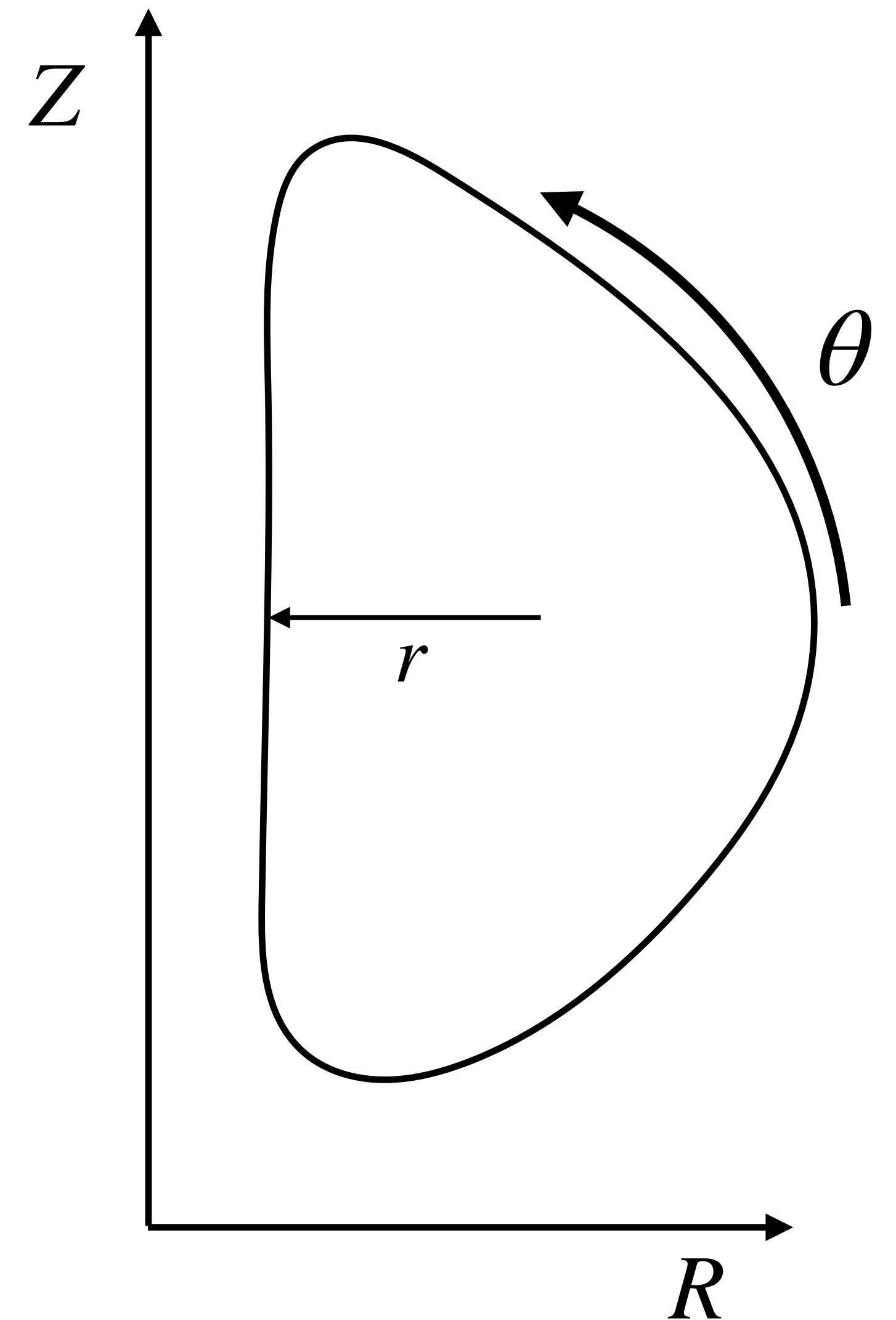
Far along a field line:

$$\theta \sim \frac{1}{\hat{s}} \frac{R}{L_{Te}} \text{ (follows from } k_{\perp} \gg k_y)$$

Long wavelength in binormal direction:

$$k_y \rho_e \sim \frac{L_{Te}}{R} \text{ (follows from } k_{\perp} \rho_e \sim 1)$$

- There are important additional effects that we will skip, but you can ask me/read about them in (Parisi, 2020).

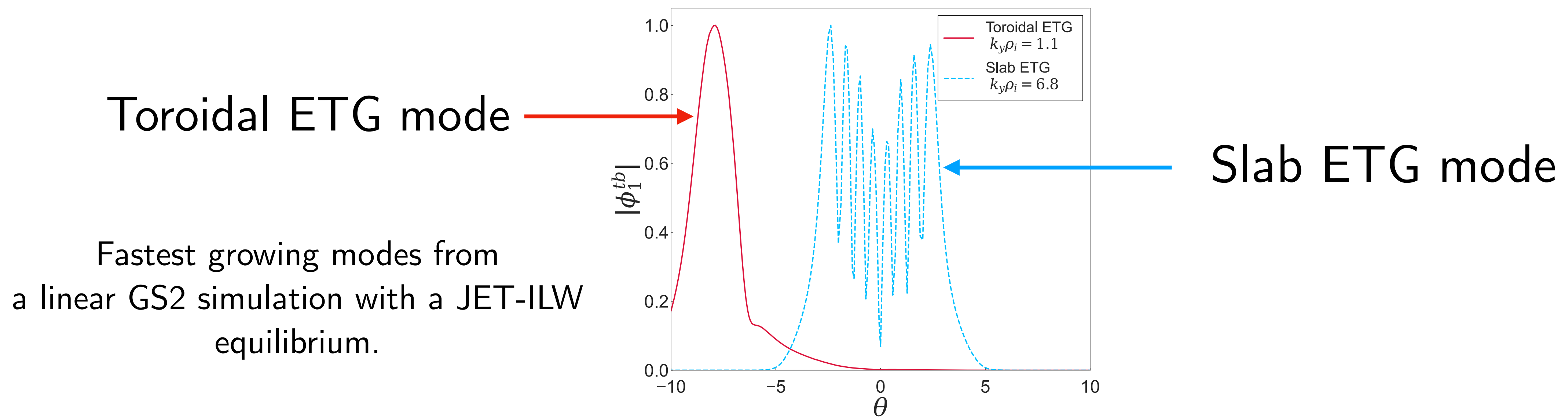


A flux surface with coordinates R, Z, θ .

Linear pedestal physics review

Important to resolve all θ locations in pedestal simulations

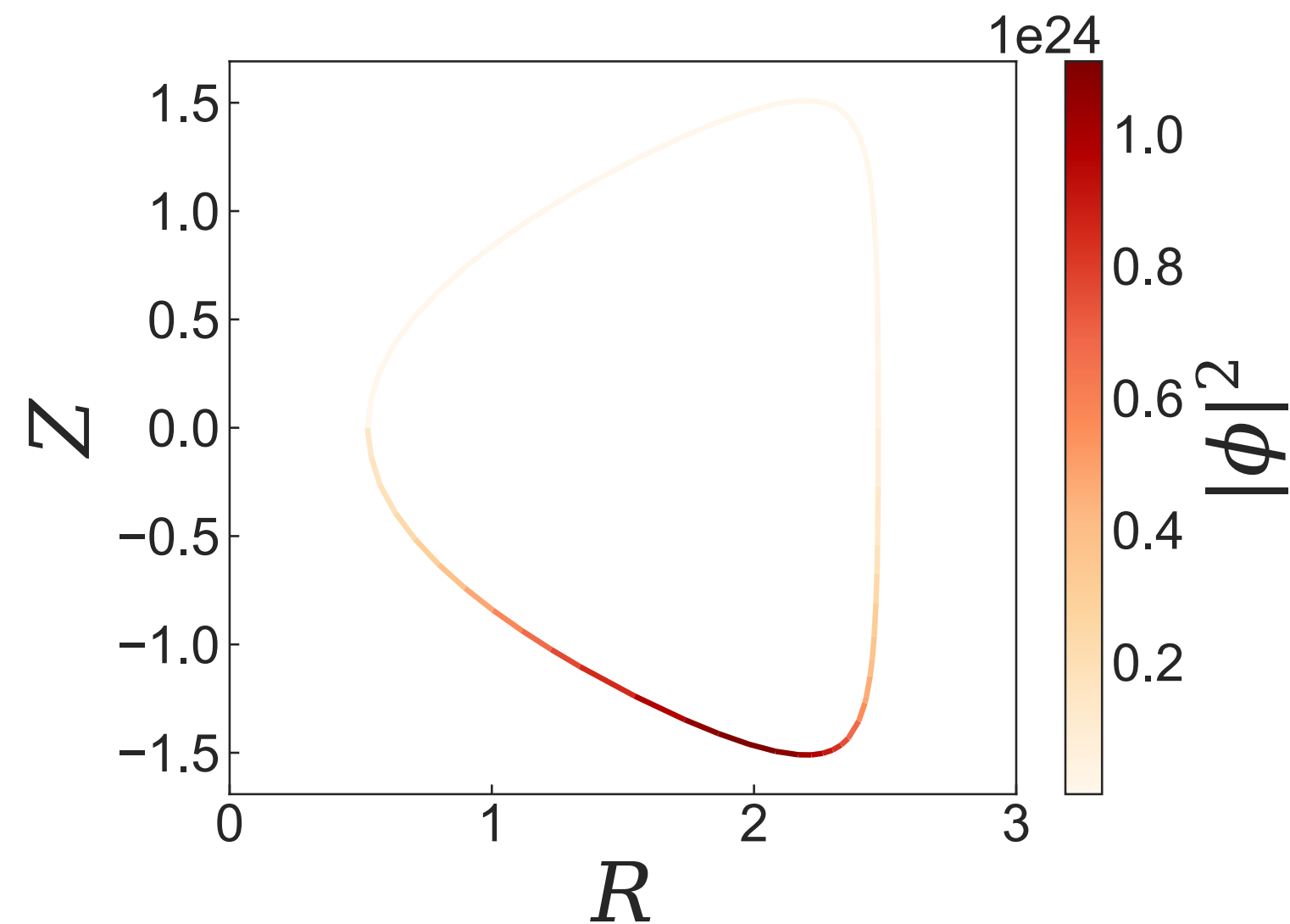
- Toroidal ETG requires $\theta \sim \frac{1}{\hat{s}} \frac{R}{L_{Te}}$.
- Slab ETG branch cannot extend too far in θ , otherwise ω_{Me} dominates.
- Expect slab and toroidal ETG turbulence to have highly distinct characters!



Toroidal ETG mode location

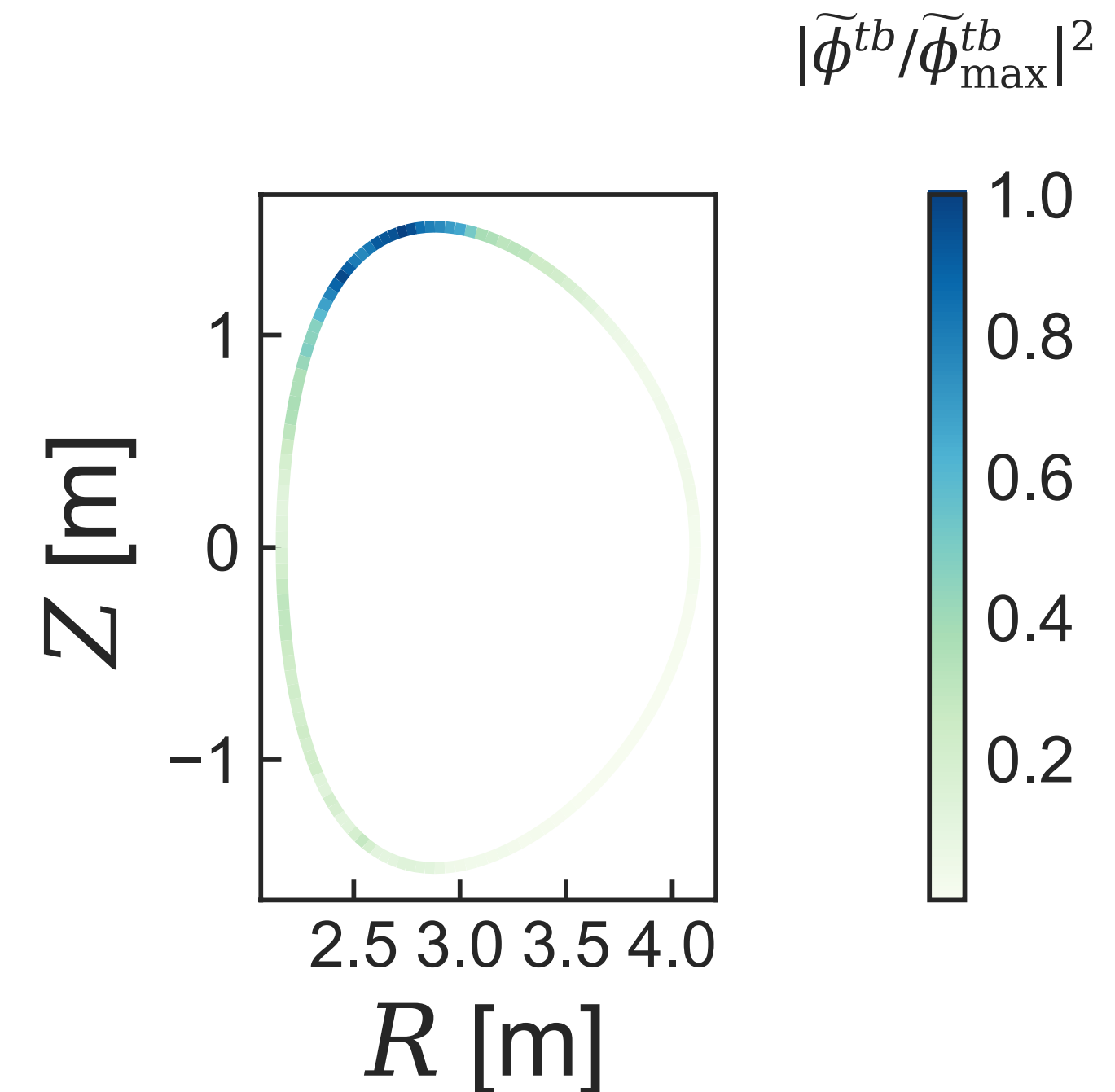
- Toroidal ETG instability lives roughly at the **top/bottom** of flux surface in variety of shapes linearly and nonlinearly...

Negative triangularity, **tight** aspect ratio,
linear simulation:



a) Toroidal ETG mode in **linear** gyrokinetic simulation of negative triangularity geometry (gs2).

Positive triangularity, **regular** aspect ratio,
nonlinear simulation:



b) Turbulent electrostatic potential in **nonlinear** gyrokinetic simulation of JET-ILW pedestal (stella).

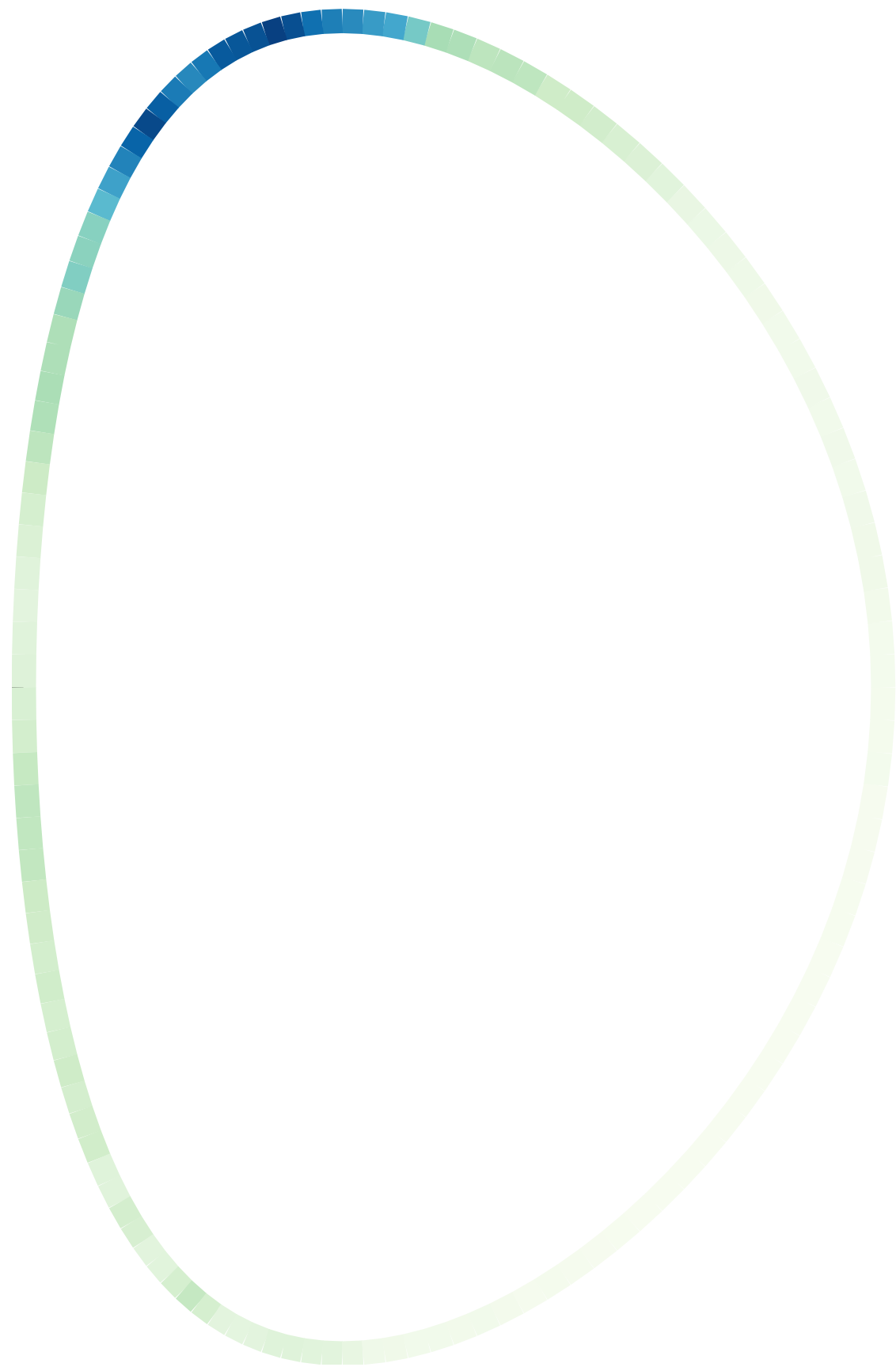
Toroidal ETG mode location cartoon

- Why does mode live at top/bottom?



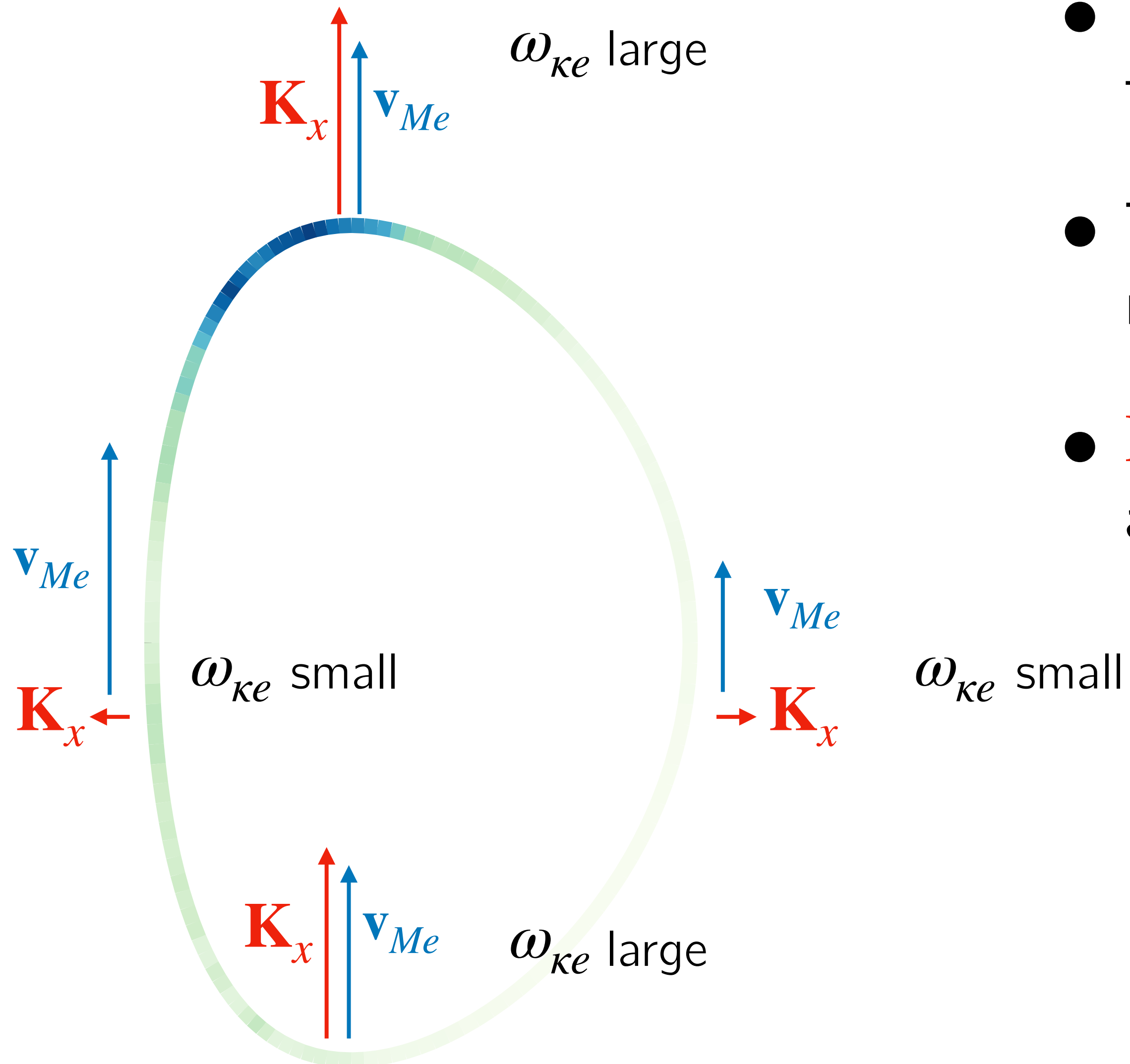
Toroidal ETG mode location cartoon

- Why does mode live at top/bottom?
- Recall, mode needs a very fast magnetic drift frequency $\omega_{\kappa e}$ because ω_{*e}^T is large in pedestal!



Toroidal ETG mode location cartoon

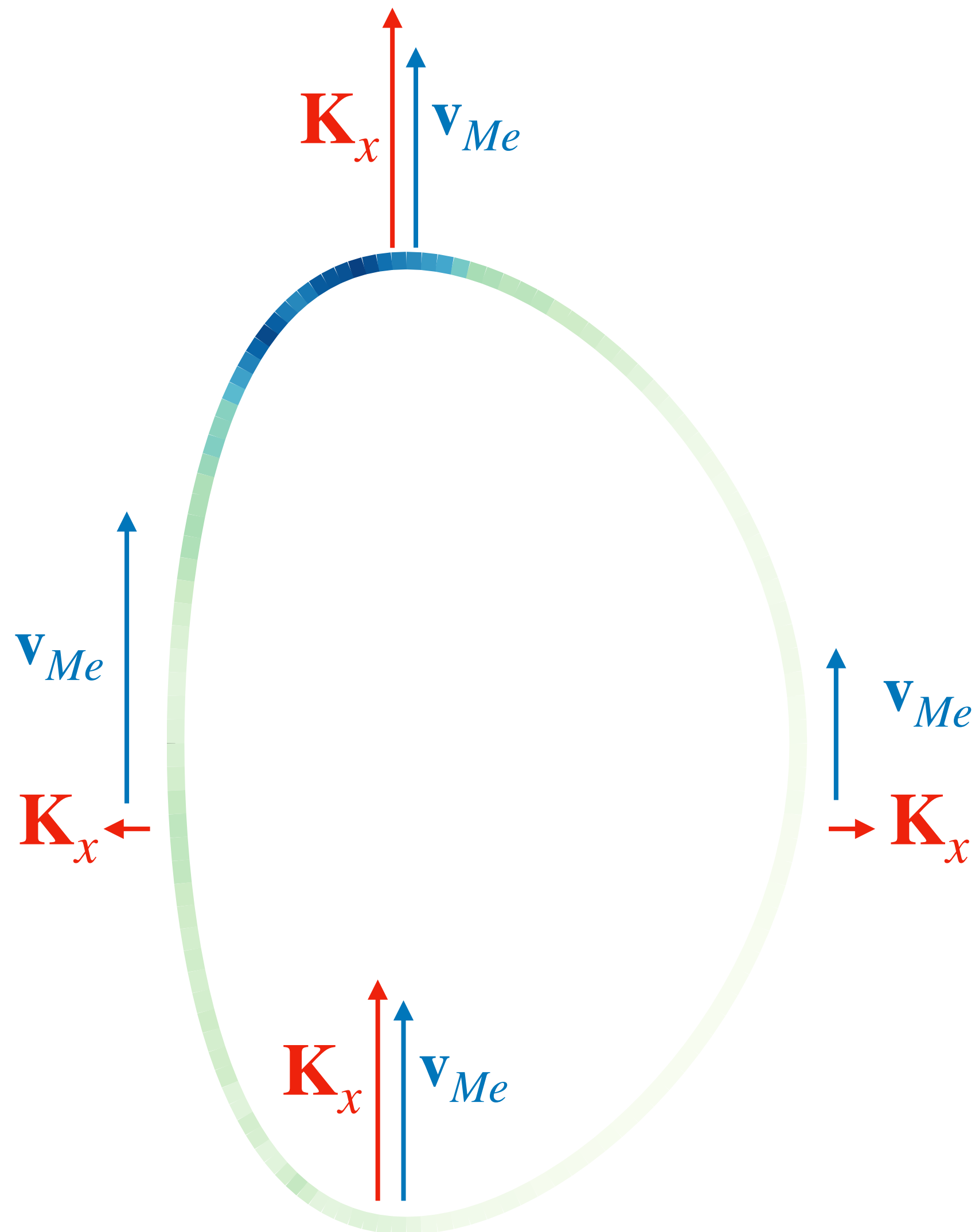
- Why does mode live at top/bottom?



- Recall, mode needs a very fast magnetic drift frequency ω_{ke} because ω_{*e}^T is large in pedestal!
- The quantity $\omega_{ke} = \mathbf{k}_\perp \cdot \mathbf{v}_{Me}$ becomes large by radial component of \mathbf{k}_\perp , \mathbf{K}_x , becoming large!
- $\mathbf{K}_x \simeq k_y \hat{s}\theta$ becomes large as mode moves along field line away from outboard midplane.

Toroidal ETG mode location cartoon

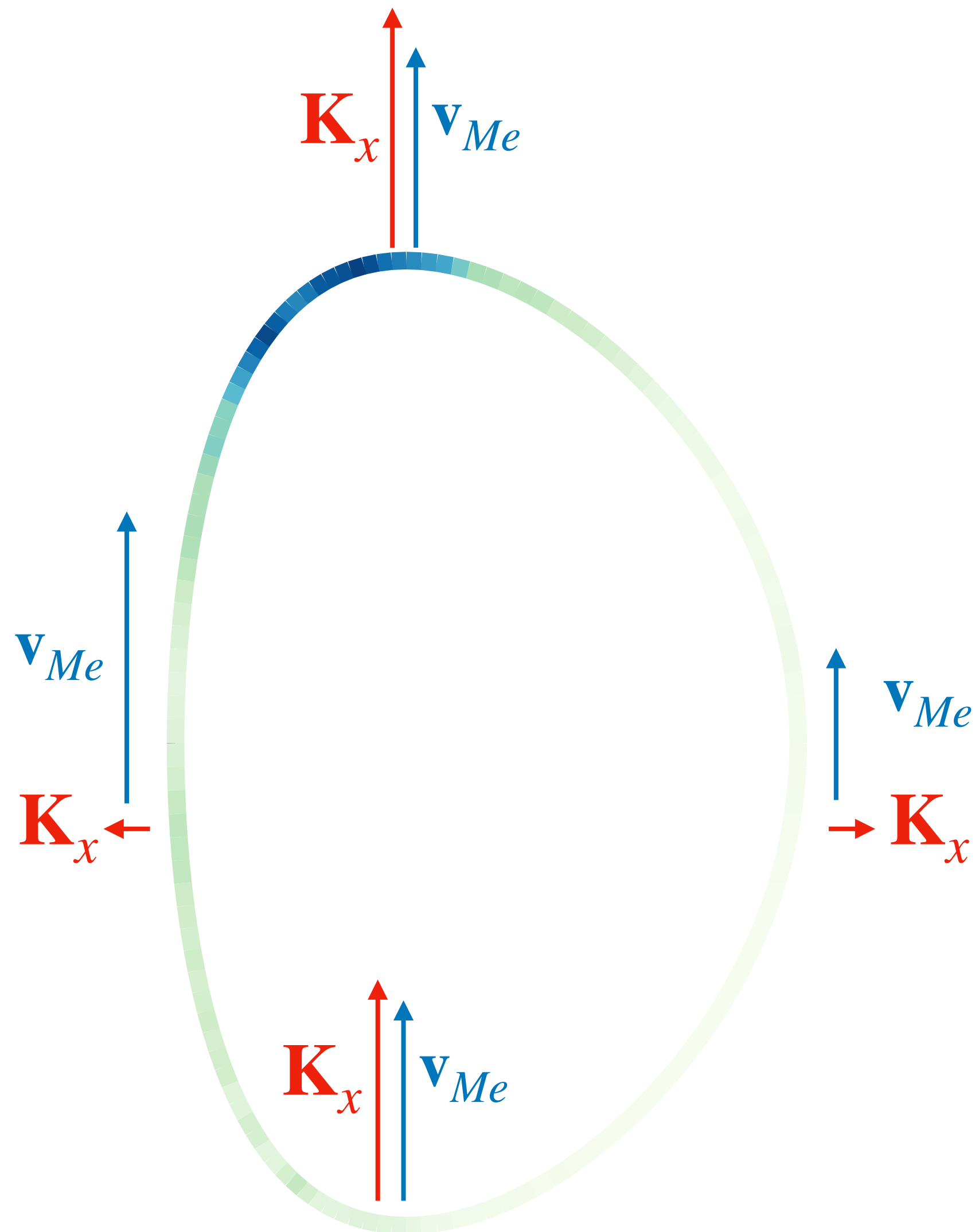
- Why does mode live at top/bottom?



- Recall, mode needs a very fast magnetic drift frequency ω_{ke} because ω_{*e}^T is large in pedestal!
- The quantity $\omega_{ke} = \mathbf{k}_\perp \cdot \mathbf{v}_{Me}$ becomes large by radial component of \mathbf{k}_\perp , K_x , becoming large!
- $K_x \simeq k_y \hat{s}\theta$ can become large as mode moves along field line away from outboard midplane.
- Hence, mode lives near **top/bottom**.

Toroidal ETG mode location cartoon

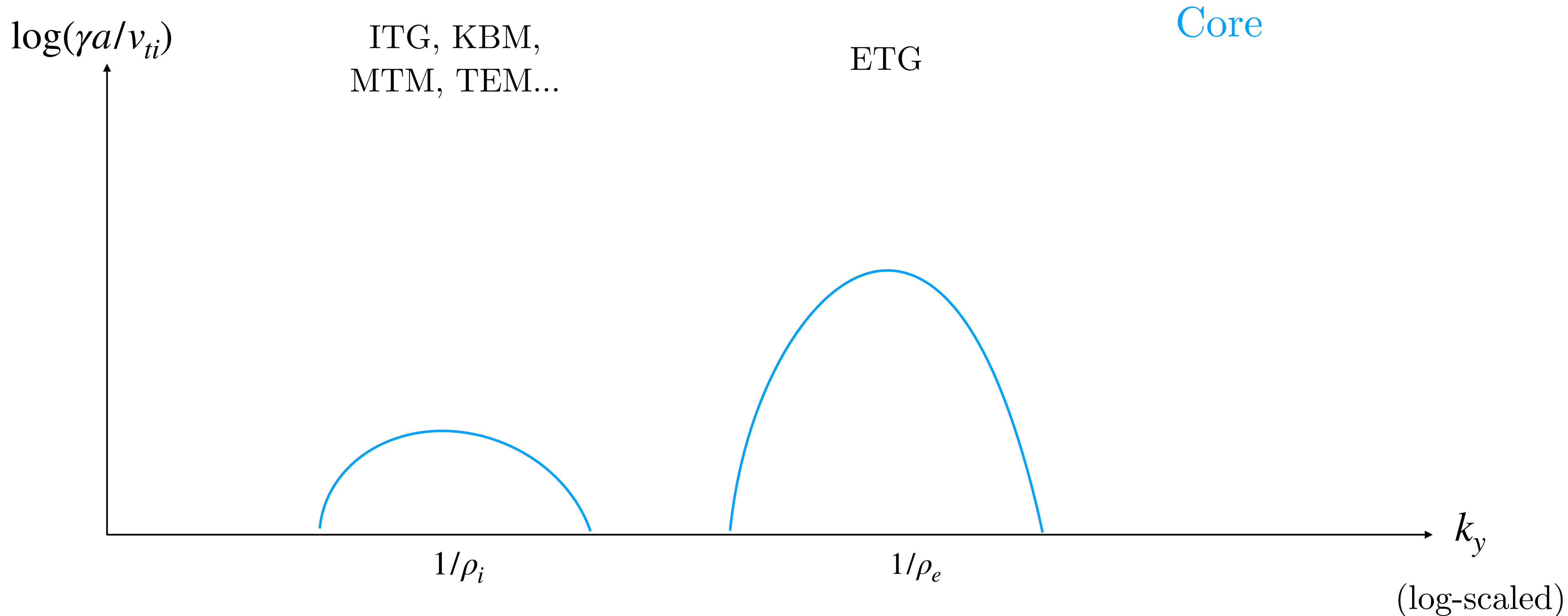
- Why does mode live at top/bottom?



- Recall, mode needs a very fast magnetic drift frequency ω_{ke} because ω_{*e}^T is large in pedestal!
- The quantity $\omega_{ke} = \mathbf{k}_\perp \cdot \mathbf{v}_{Me}$ becomes large by radial component of \mathbf{k}_\perp , \mathbf{K}_x , becoming large!
- $\mathbf{K}_x \simeq k_y \hat{s} \theta$ can become large as mode moves along field line away from outboard midplane.
- Hence, mode lives near **top/bottom**.
- Picture is slightly modified by additional subtleties such as finite Larmor radius (FLR) damping and ballooning coordinate $\theta_0 = k_x / k_y \hat{s} \dots$

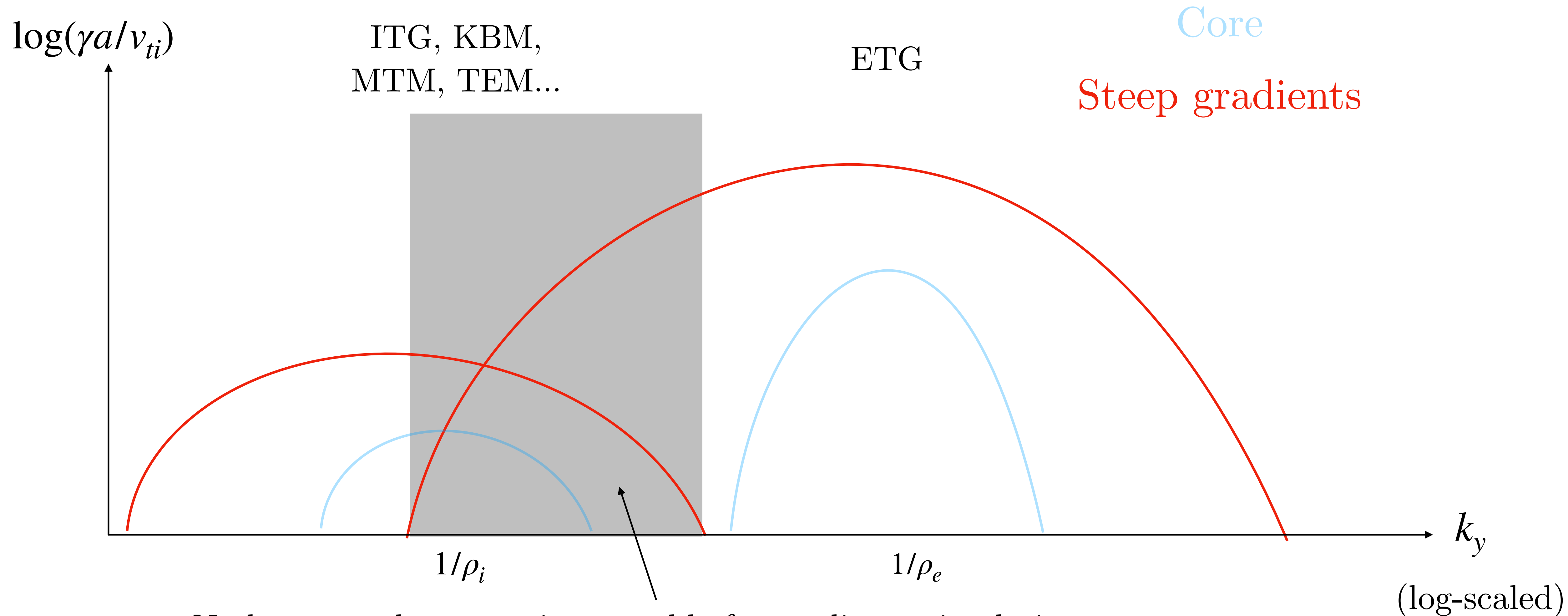
Effect of steep gradients on scale separation

Core: (hopefully!) some separation of ion-scale and ETG physics



Effect of steep gradients on scale separation

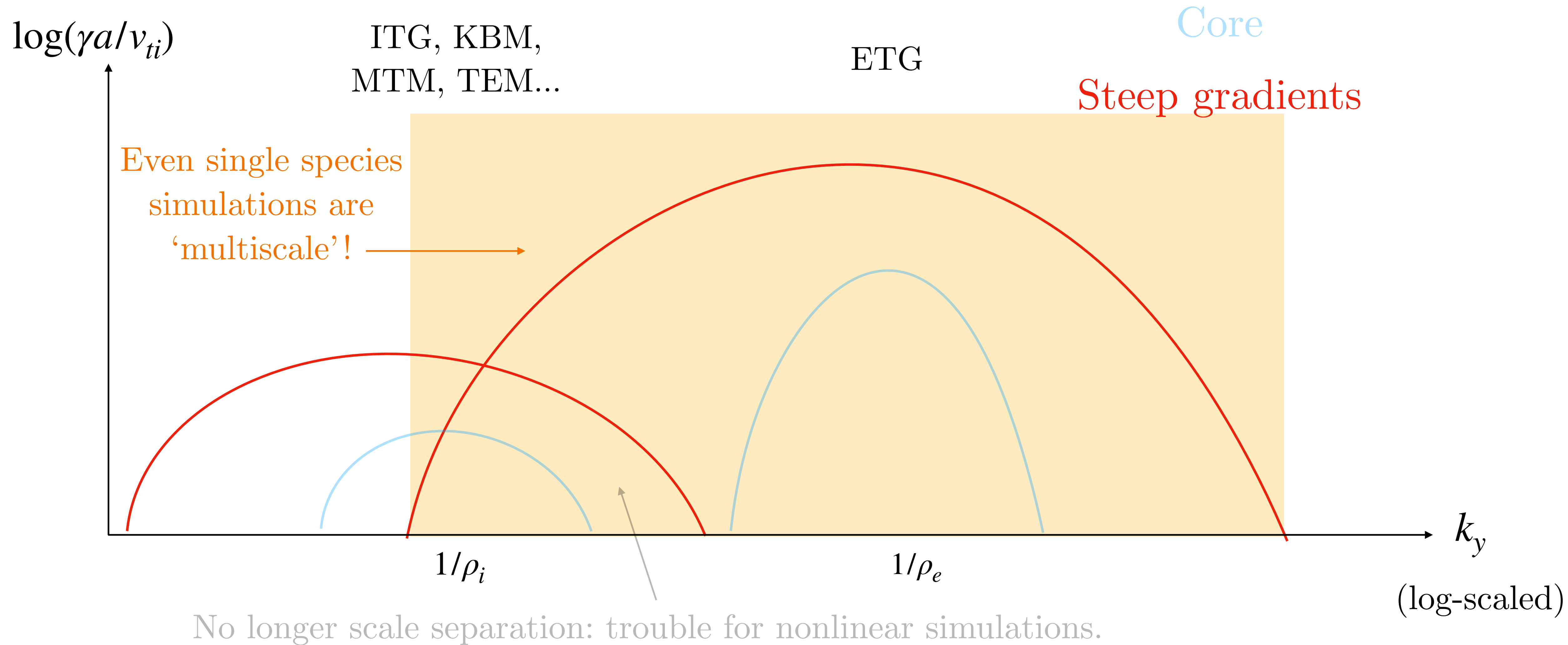
Steep gradients: typically no separation of ion-scale and ETG physics



No longer scale separation: trouble for nonlinear simulations.

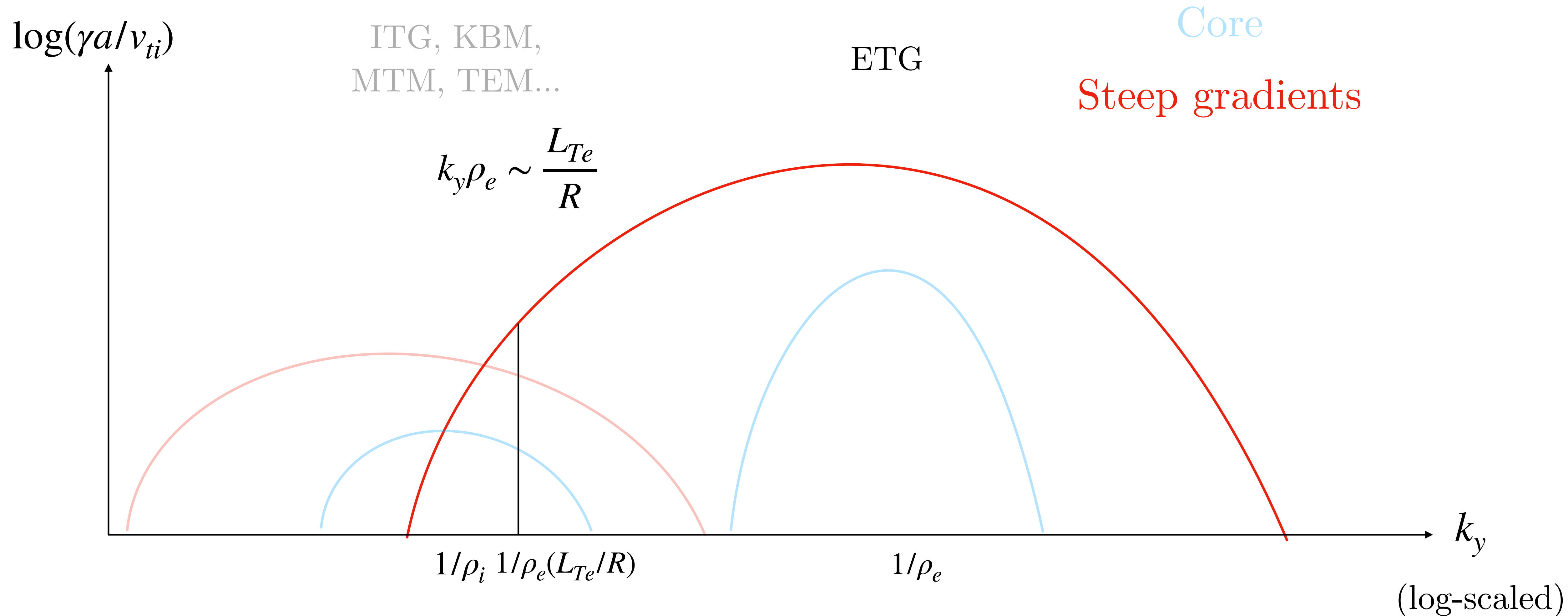
Effect of steep gradients on scale separation

Steep gradients: single species simulations become 'multiscale'



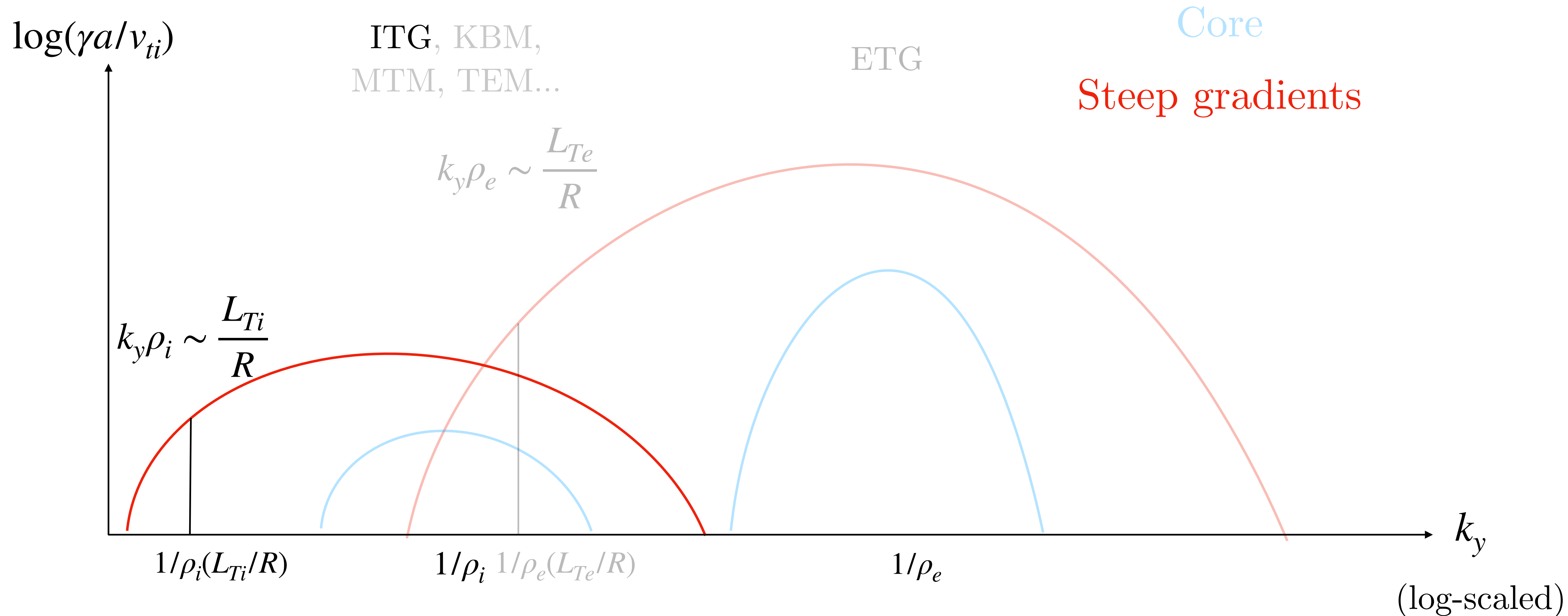
Effect of steep gradients on scale separation

Steep gradients: we can estimate the longest scales for ETG



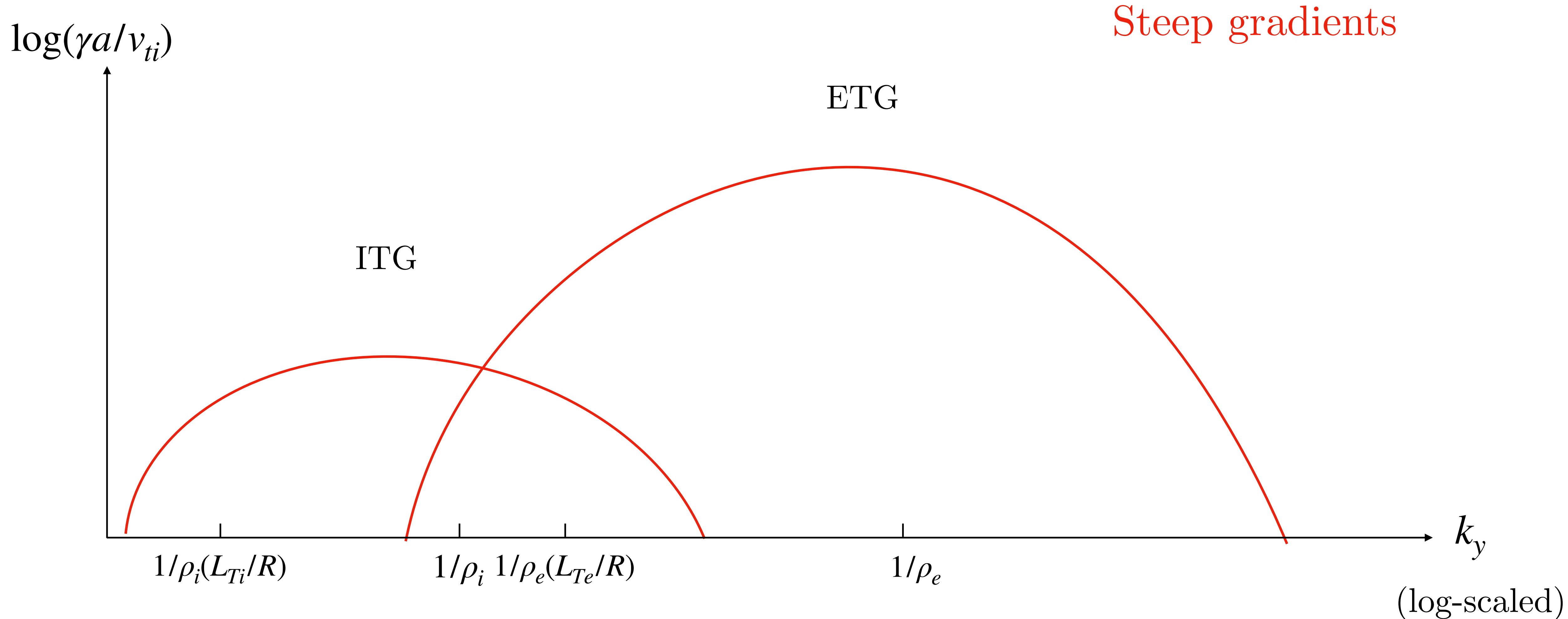
Effect of steep gradients on scale separation

Steep gradients: we can also estimate the longest scales for ITG



Effect of steep gradients on scale separation

Steep gradients summary



Important implications for simulating turbulence!

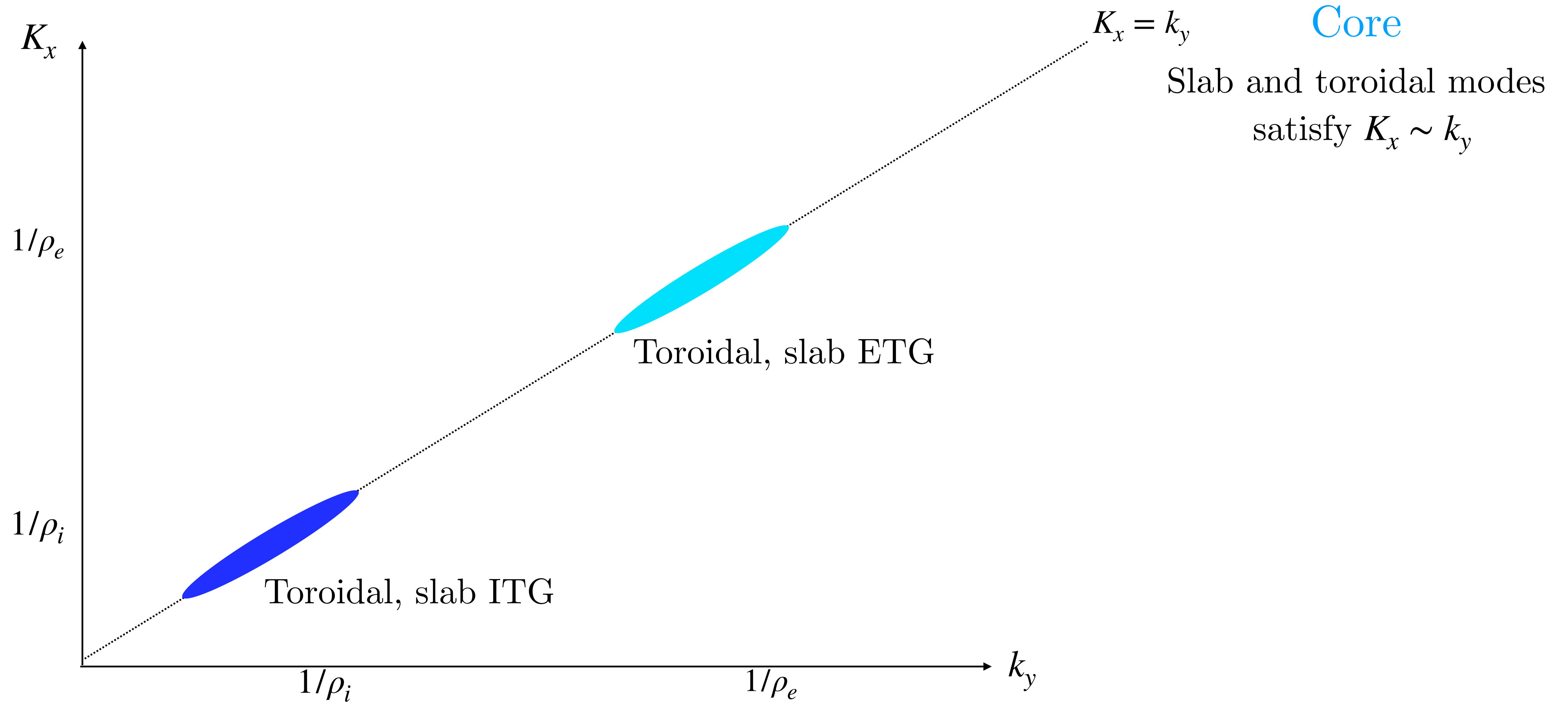
Effect of steep gradients on scale separation

Scale separation in the radial direction also matters

- So far we have talked mainly about scales in k_y (binormal scales).
- Because steep temperature gradients cause $K_x \gg k_y$ for toroidal ETG mode, must ensure that nonlinear simulations have sufficient radial resolution.

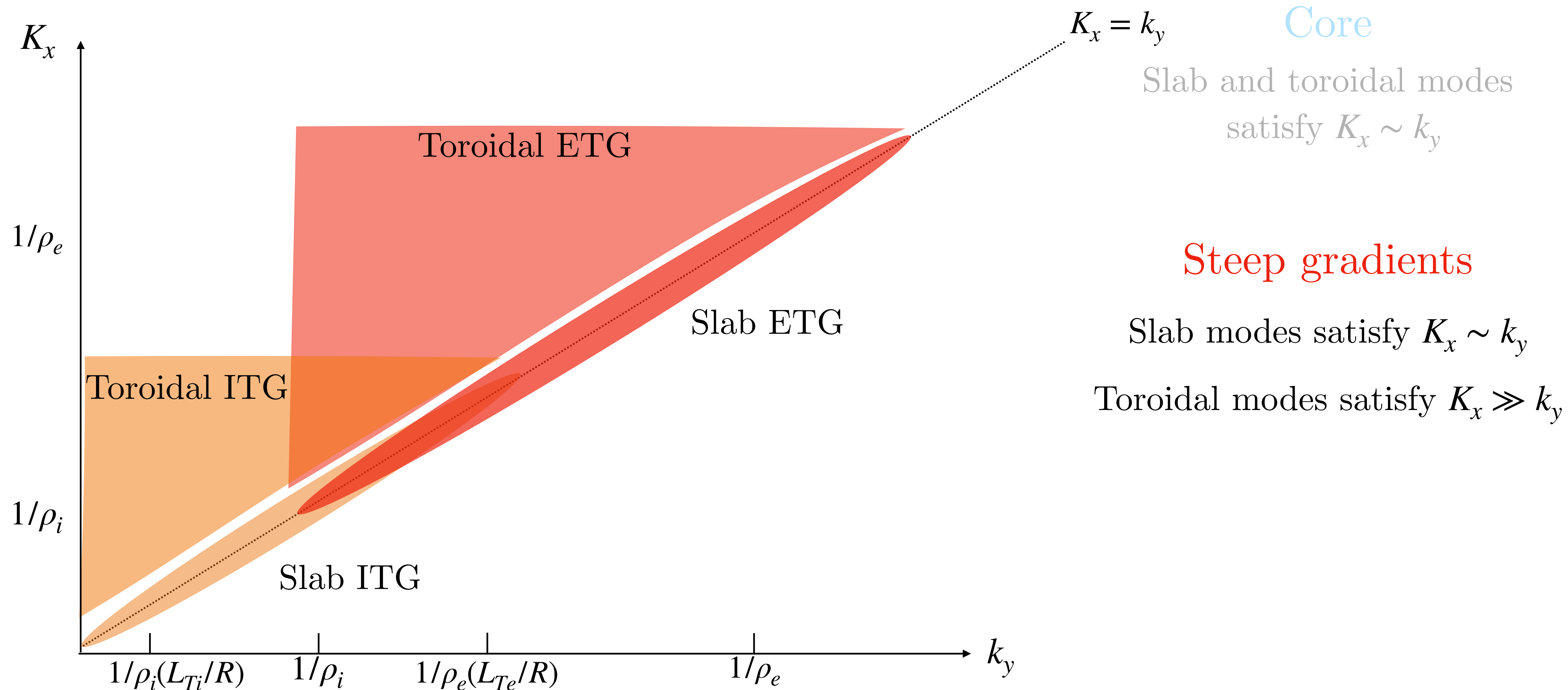
Effect of steep gradients on scale separation

Core gradients: k_y and K_x typically isotropic



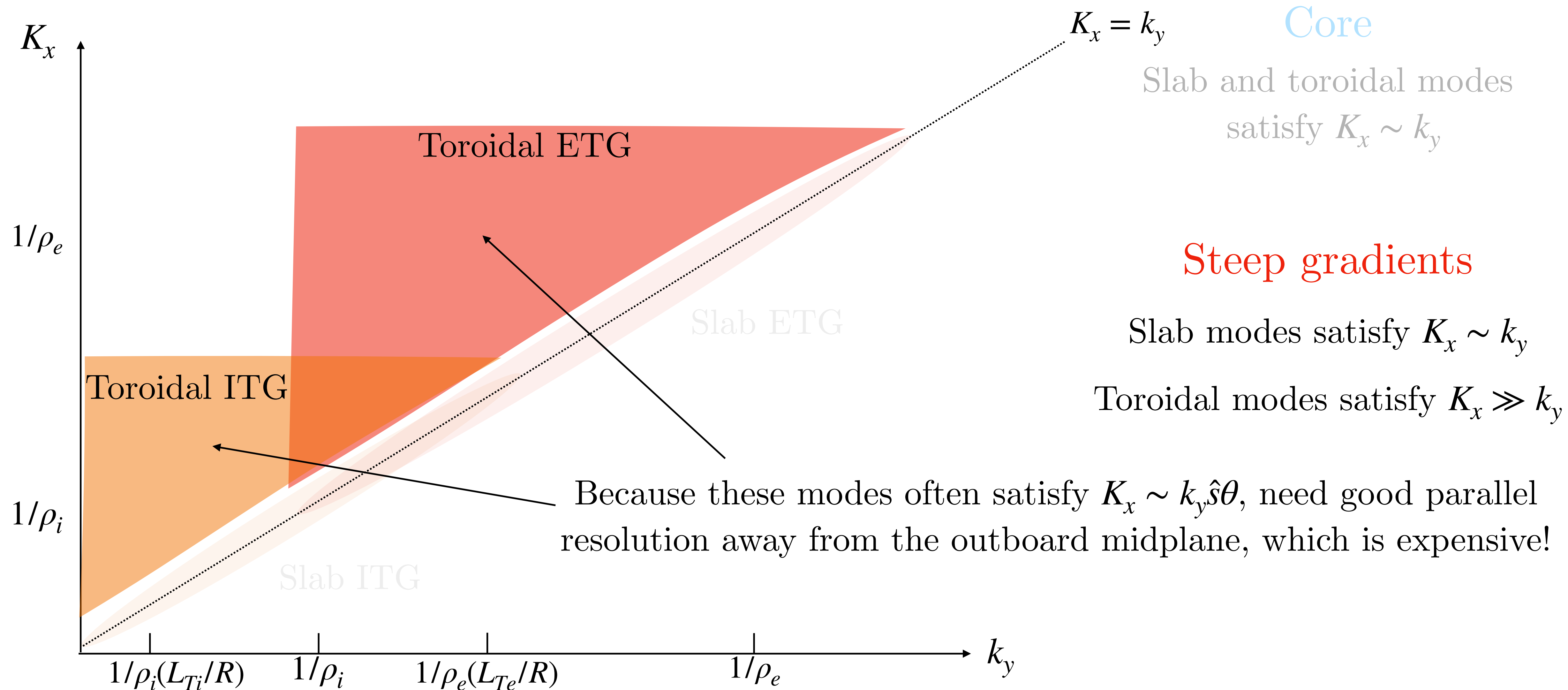
Effect of steep gradients on scale separation

Steep gradients: k_y and K_x can be highly anisotropic



Effect of steep gradients on scale separation

Steep gradients: k_y and K_x can be highly anisotropic



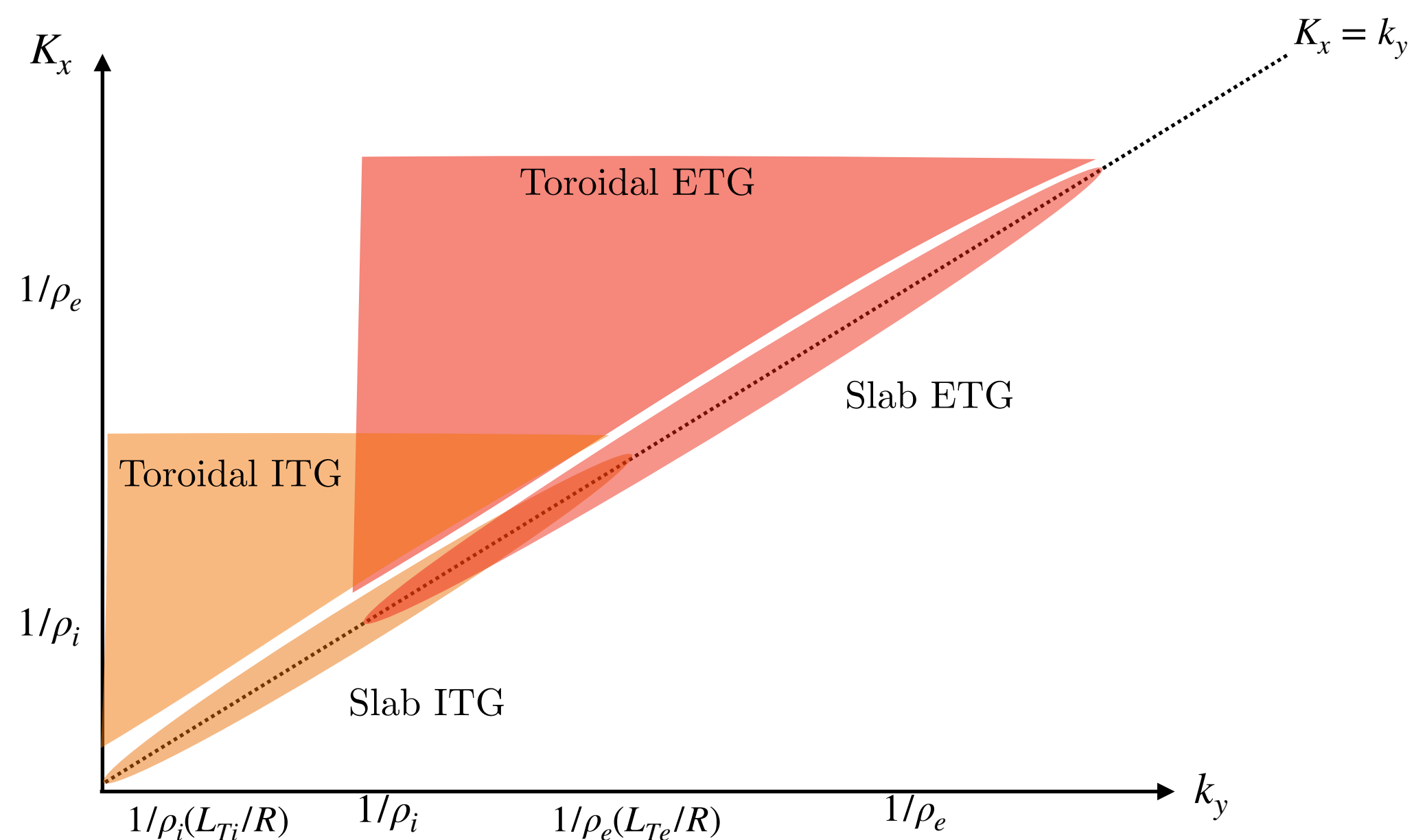
Effect of steep gradients on scale separation

Steep gradients: k_y and K_x can be highly anisotropic

Steep gradients

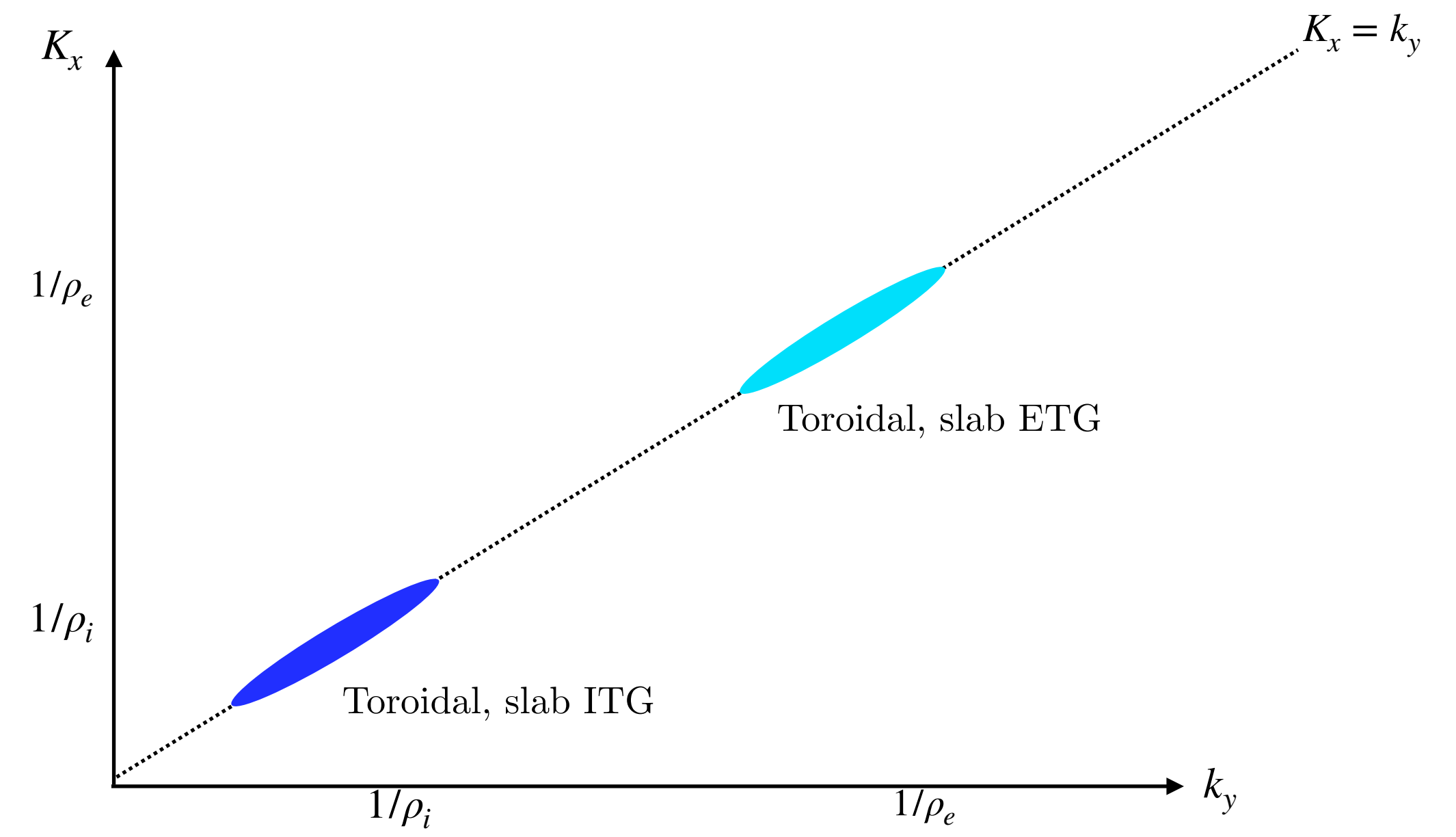
Slab modes satisfy $K_x \sim k_y$

Toroidal modes satisfy $K_x \gg k_y$



Core

Slab and toroidal modes satisfy $K_x \sim k_y$



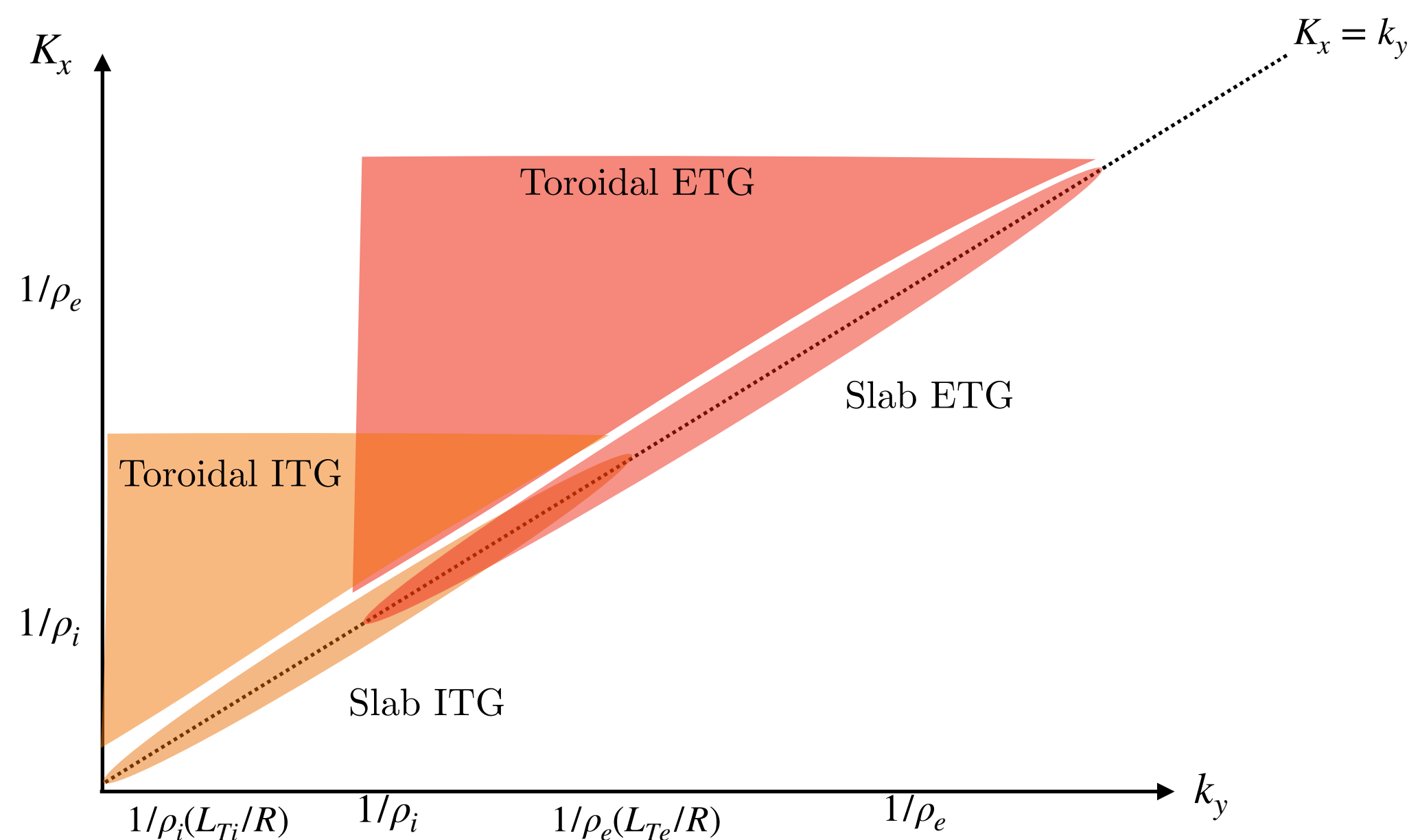
Effect of steep gradients on scale separation

Steep gradients: k_y and K_x can be highly anisotropic

Steep gradients

Slab modes satisfy $K_x \sim k_y$

Toroidal modes satisfy $K_x \gg k_y$



Some implications for nonlinear simulations:

- Need to capture wide range of k_y , K_x scales; currently impossible to perform nonlinear gyrokinetic simulations from $k_y\rho_i \sim L_{Ti}/R$ to $k_y\rho_e > 1$.
- Simulations require good parallel resolution away from outboard midplane.
- Require simulations are ‘multiscale’ in time as well as space \longrightarrow run simulations sufficiently long!

Nonlinear physics

Nonlinear pedestal physics

Resolving toroidal, slab physics nonlinearly is computationally challenging

- Linear γ/k_{\perp}^2 spectrum has strong $\theta_0 = k_x/\hat{s}k_y$ and $k_y\rho_i$ dependence.

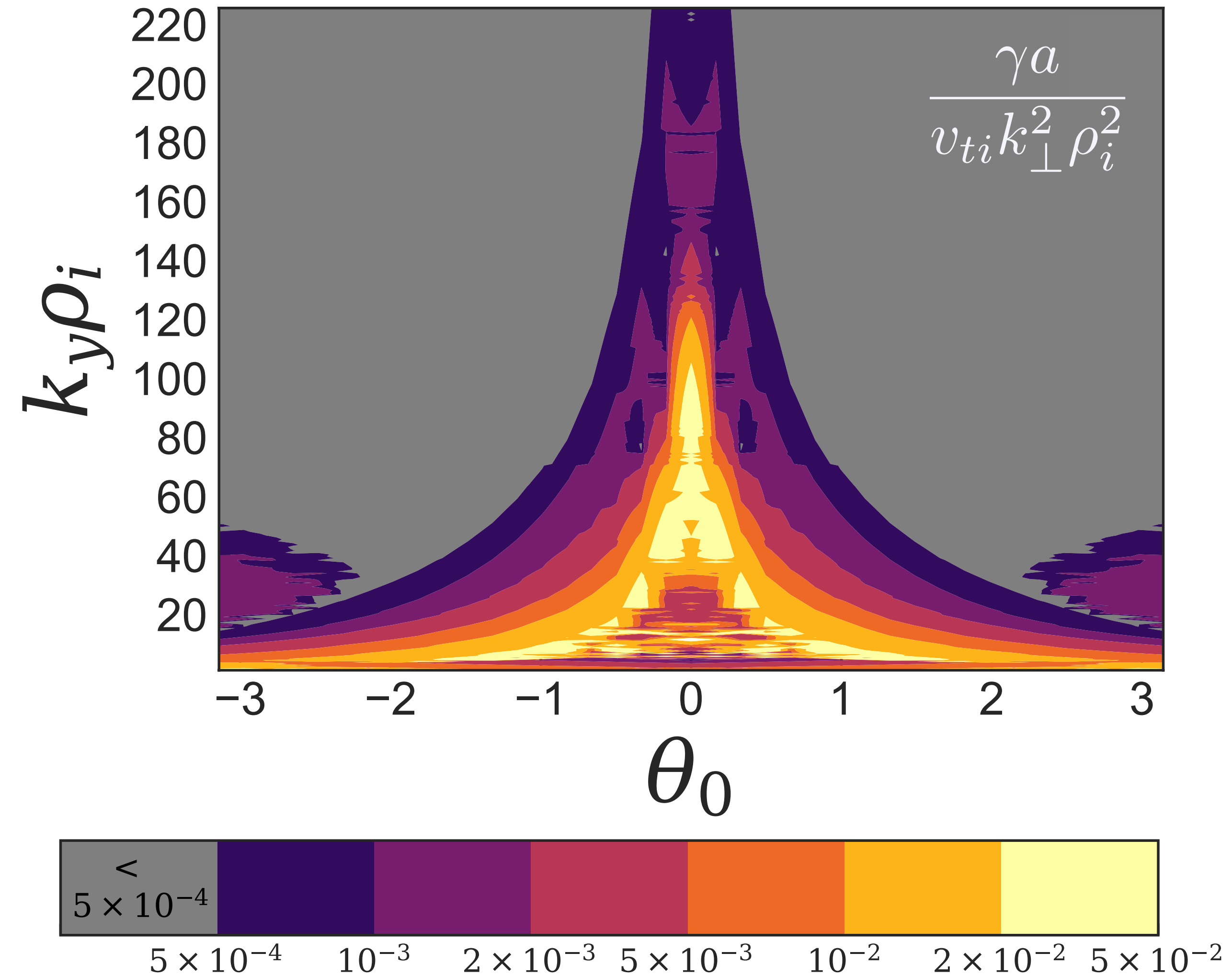


Figure: γ/k_{\perp}^2 from the linear spectrum, γ is linear growth rate.

Nonlinear pedestal physics

Resolving toroidal, slab physics nonlinearly is computationally challenging

- Linear γ/k_{\perp}^2 spectrum has strong $\theta_0 = k_x/\hat{s}k_y$ and $k_y\rho_i$ dependence.
- Expect **toroidal** ETG transport at small $k_y\rho_i \sim 1$ but $K_x\rho_e \sim 1$ and **slab** ETG transport at $k_y\rho_e \sim K_x\rho_e \sim 1$.
- Toroidal modes peak away from outboard midplane, slab near outboard midplane.

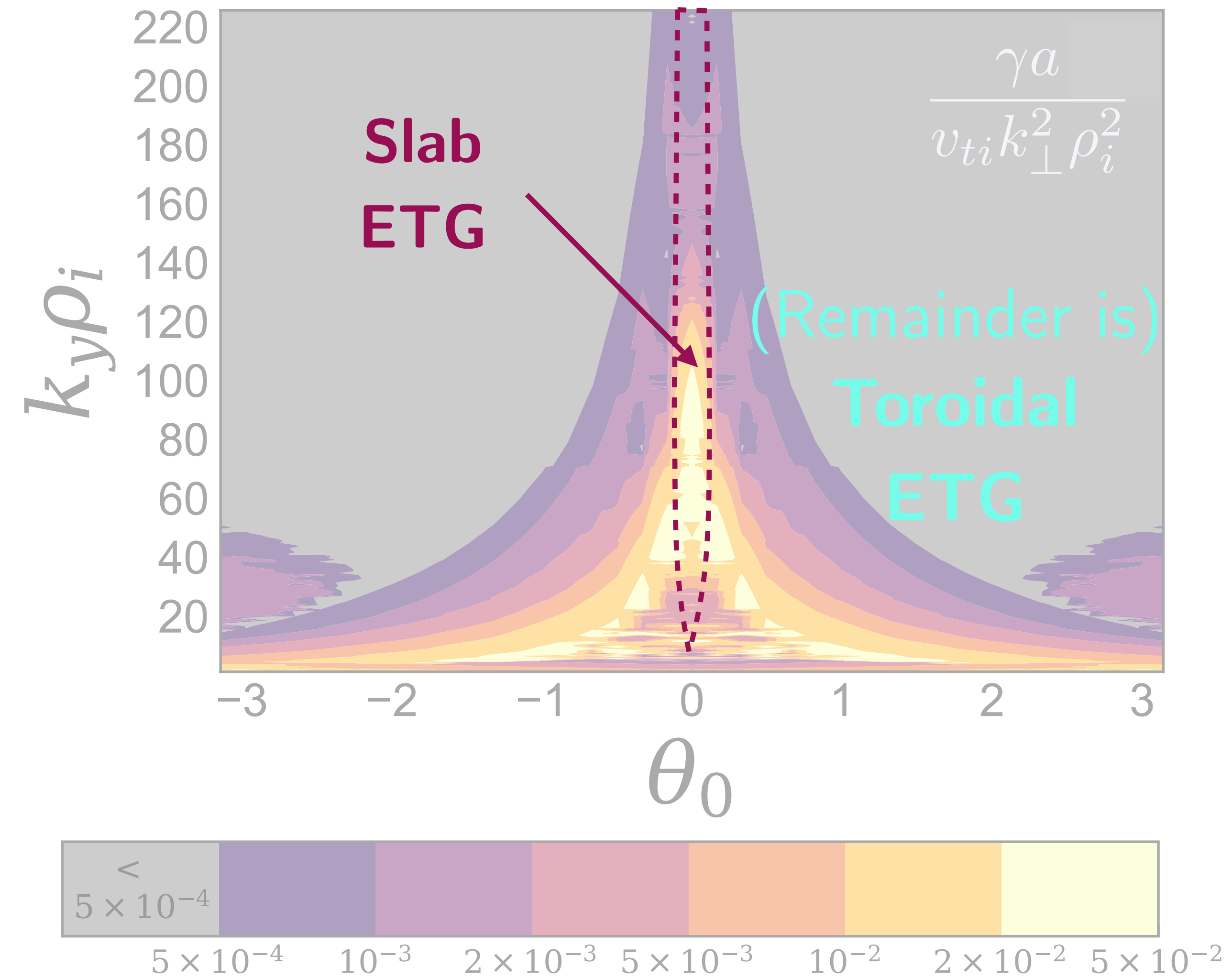


Figure: γ/k_{\perp}^2 from the linear spectrum, γ is linear growth rate.

Nonlinear pedestal physics

Resolving toroidal, slab physics nonlinearly is computationally challenging

- Linear γ/k_{\perp}^2 spectrum has strong $\theta_0 = k_x/\hat{s}k_y$ and $k_y\rho_i$ dependence.
- Expect **toroidal** ETG transport at small $k_y\rho_i \sim 1$ but $K_x\rho_e \sim 1$ and **slab** ETG transport at $k_y\rho_e \sim K_x\rho_e \sim 1$.
- Toroidal modes peak away from outboard midplane, slab near outboard midplane.
- Nonlinear grid requires:
 - 'small' Δk_y but large max k_y
 - 'small' $\Delta\theta_0$ but enough radial modes
 - large number of parallel gridpoints
- Currently infeasible to satisfactorily resolve all of these scales nonlinearly.

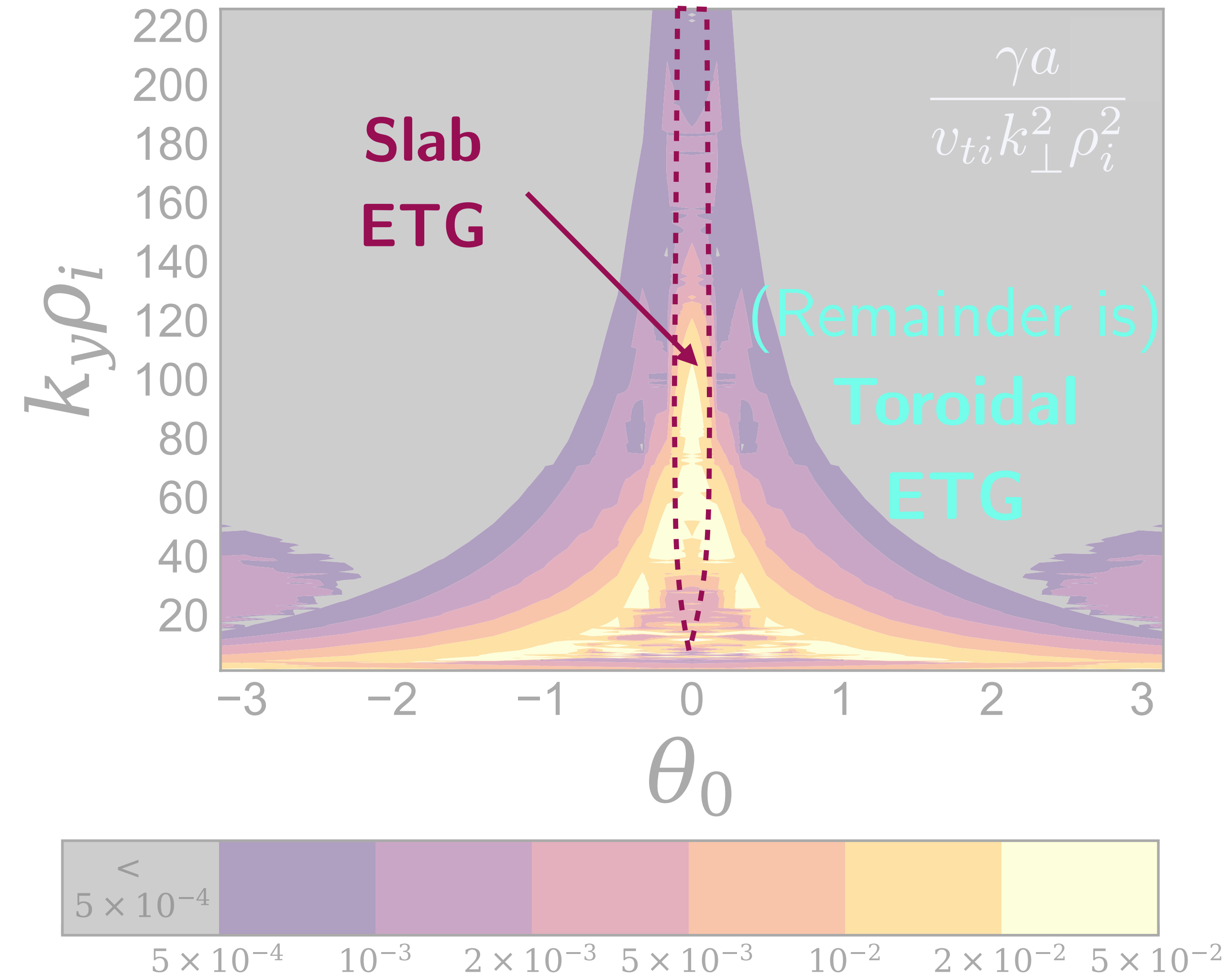


Figure: γ/k_{\perp}^2 from the linear spectrum, γ is linear growth rate.

Nonlinear pedestal physics

Resolving toroidal, slab physics nonlinearly is computationally challenging

- Dominant linear modes also exist at a range of θ locations, which need to be resolved!

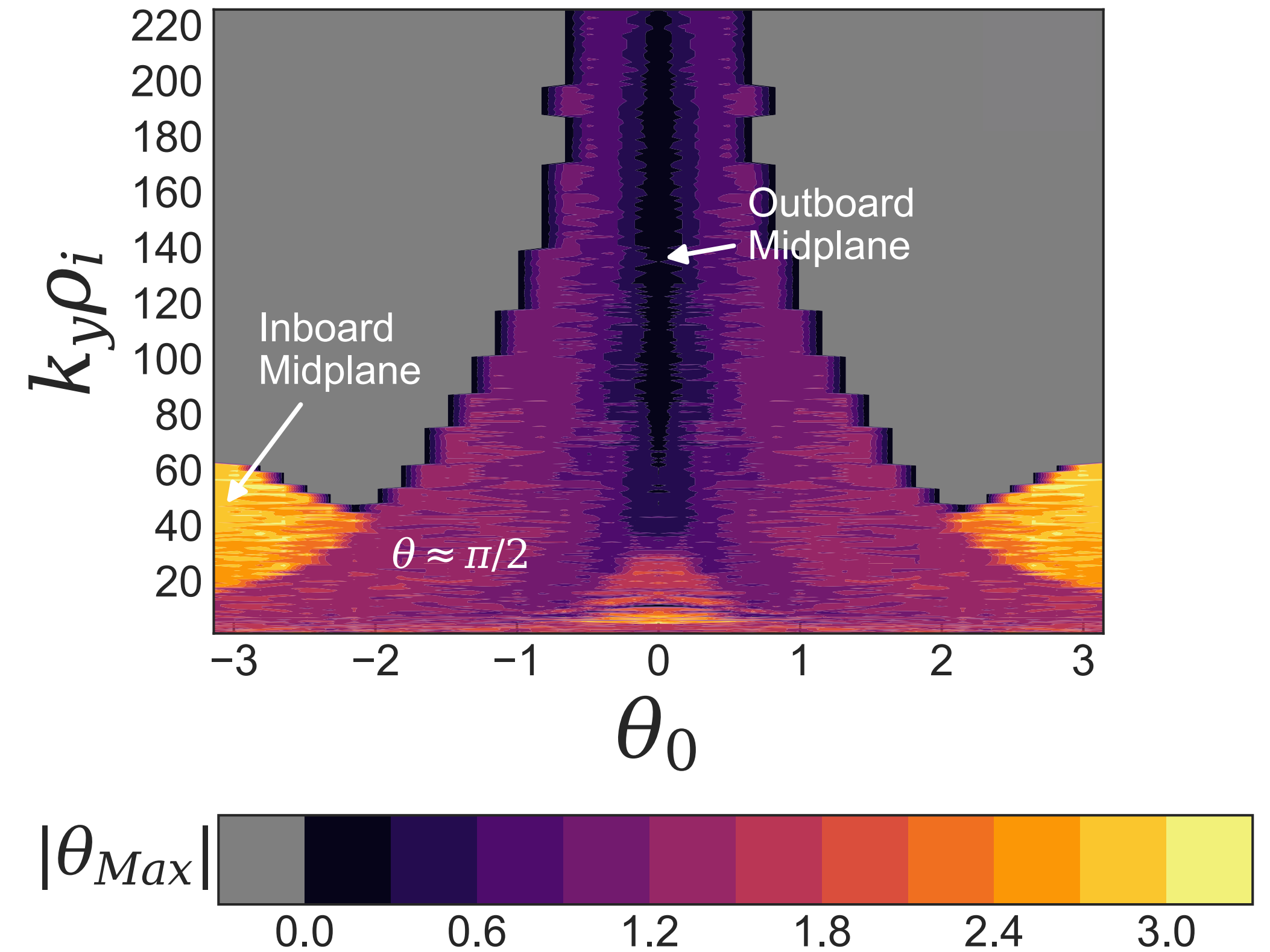


Figure: θ location of different modes in the growth rate spectrum.

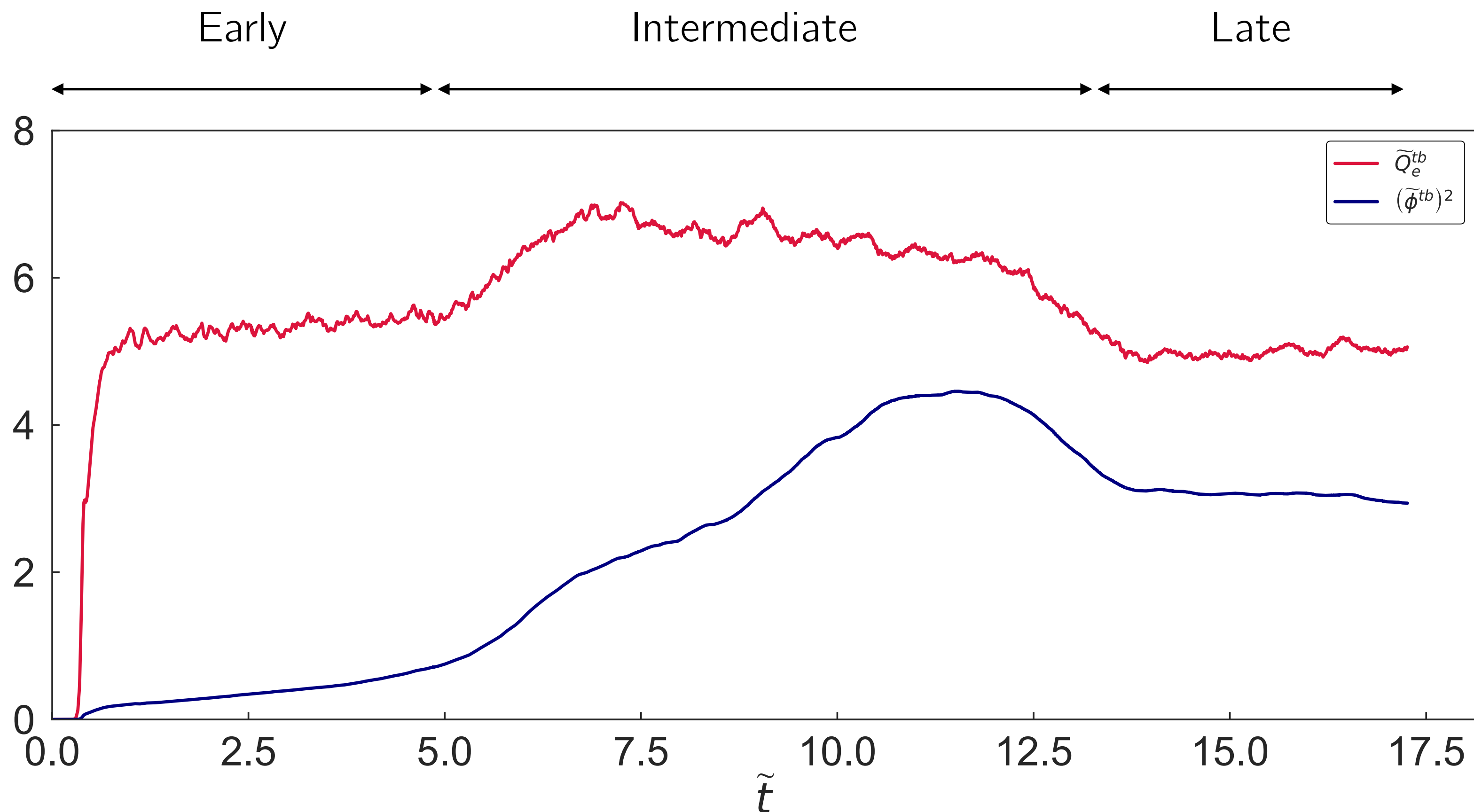
Nonlinear simulation

Parameters

- We perform electrostatic nonlinear gyrokinetic simulations using stella (Barnes, 2019).
- Steep gradient region of JET-ILW pedestal.
- 150 poloidal modes, 70 radial modes, 128 parallel gridpoints, 64 v_{\parallel} gridpoints, 12 μ gridpoints, some hyperviscosity, kinetic ions and electrons, Miller geometry fit to JET shot 92174.
- Minimum poloidal wavenumber $k_y \rho_i = 0.7$, minimum radial wavenumber $k_x \rho_i = 1.6$.
- Run simulation for roughly 1000 a/v_{te} times (5-10 linear growth times of slowest dominant linear modes in our box).
- **Health warning:** the simulation I will show here is not yet in a 'steady state,' but we have run lower resolution simulations that saturate and have similar properties.

Nonlinear simulation Split into early, intermediate, and late times

- **Early** times: slab ETG modes dominate (high $k_y \rho_i$ slab grows faster and so saturates faster).
- **Intermediate** times: toroidal modes have relatively large amplitudes, appear to suppress slab.
- **Late** times: state with both toroidal and slab modes and reduced fluxes (simulation needs more time!).

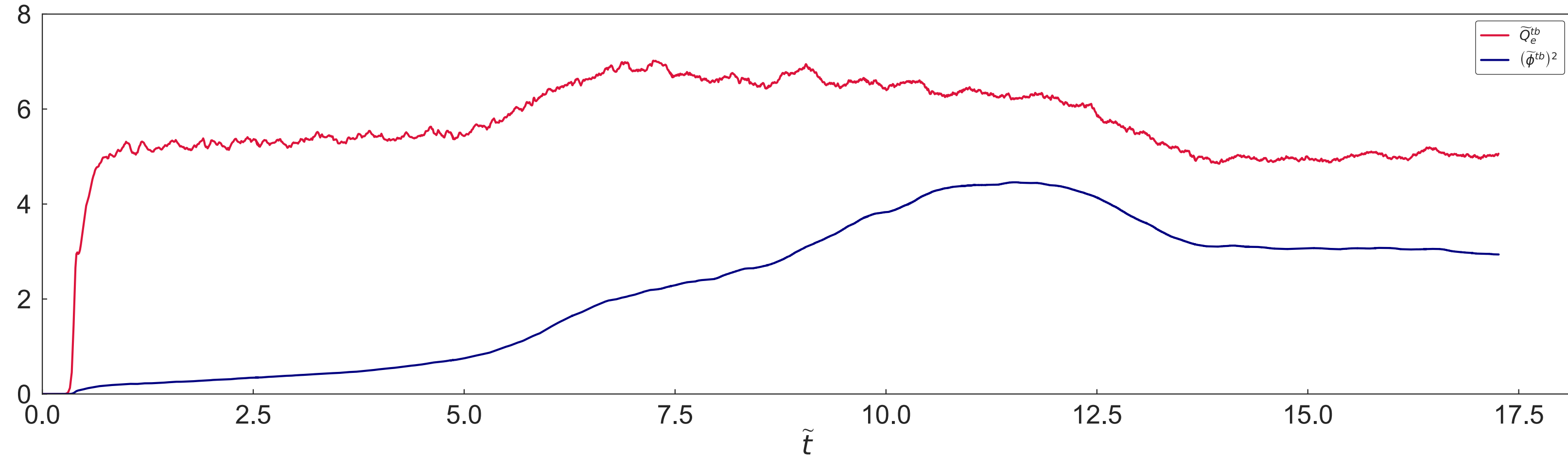


Normalization conventions:

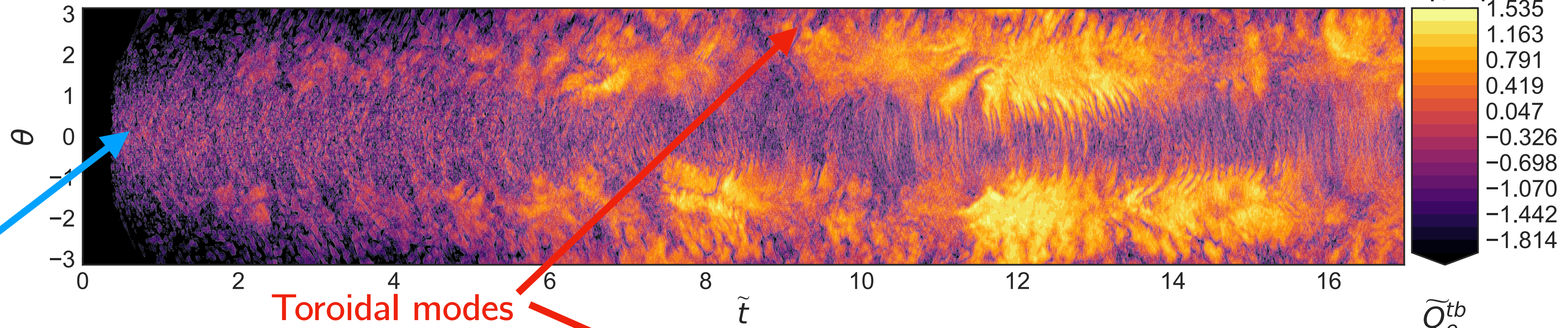
$$\tilde{t} = tv_{ti}/a \quad \widetilde{Q}_e^{tb} = Q_e^{tb}/Q_{gB}$$

$$\widetilde{\phi}^{tb} = e\phi^{tb}/T_i\rho_{*i}$$

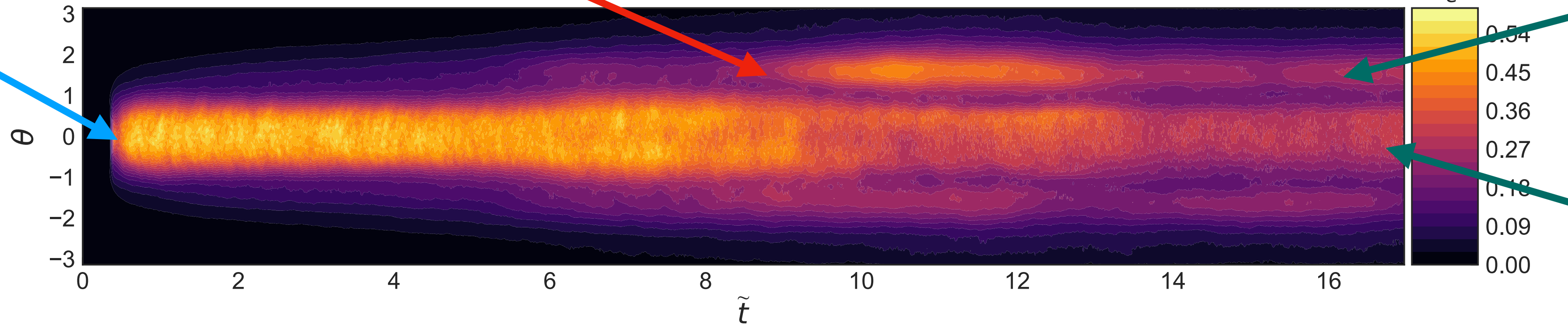
Nonlinear results Potential and heat flux time traces



← Early Intermediate Late → $\ln|\bar{\phi}^{tb}|$

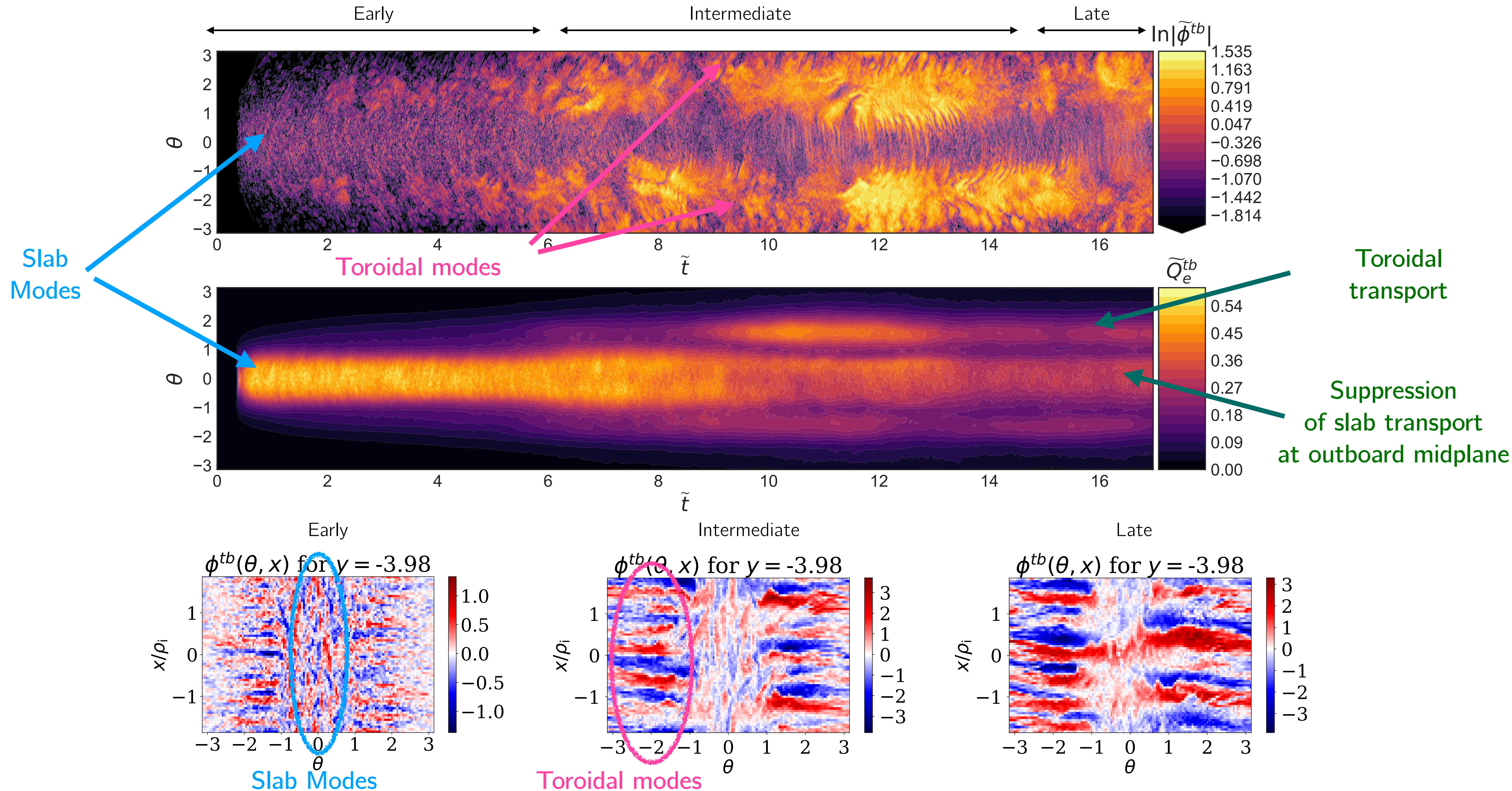


Slab Modes



Toroidal transport
Suppression of slab transport at outboard midplane

Nonlinear results Turbulence character



Nonlinear results Heat flux spectrum time evolution

- Heat flux spectra changes significantly with time. At **early times**, heat flux dominated by fast growing, high $k_y \rho_i$ modes near outboard midplane.

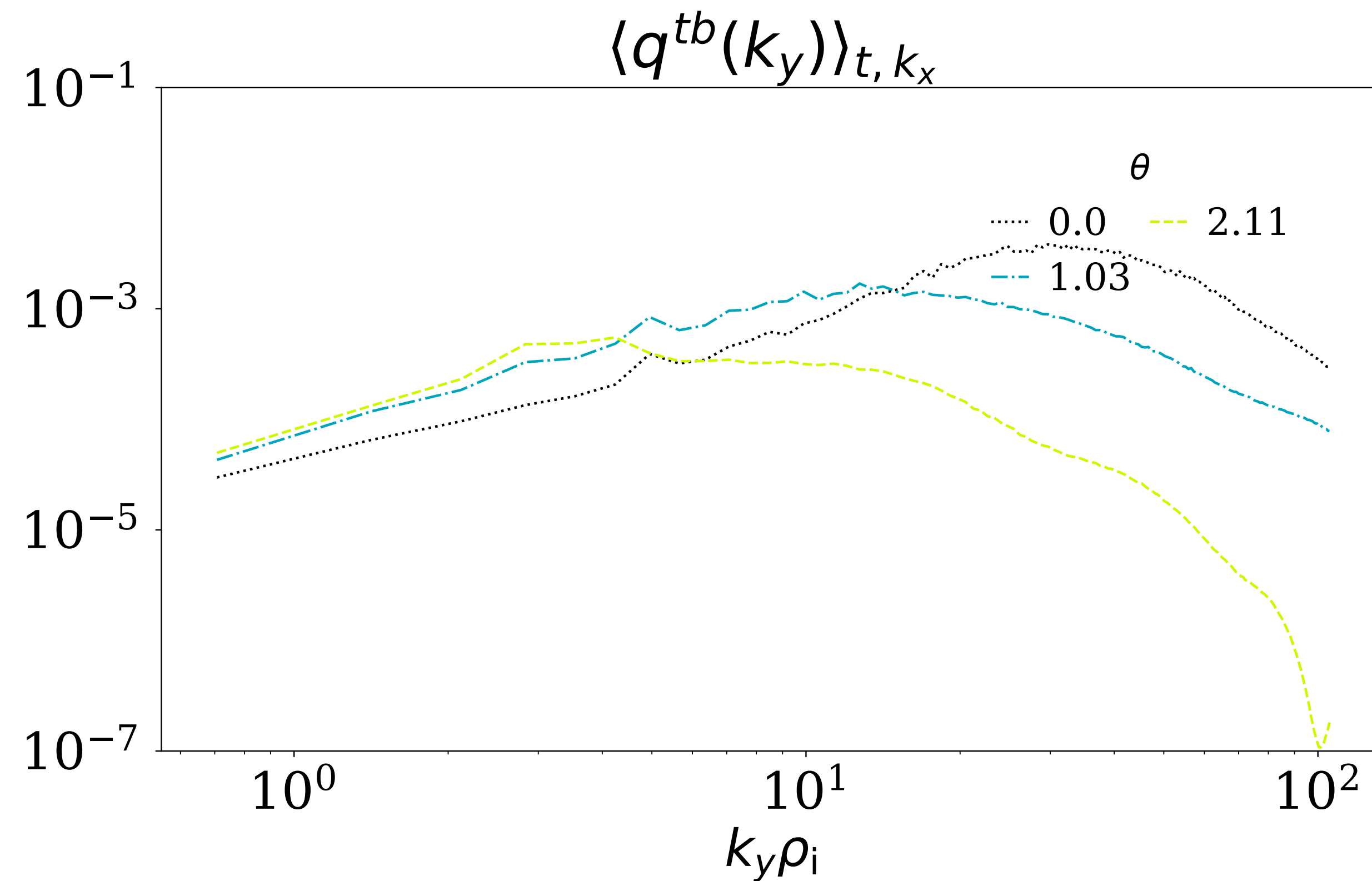


Figure: heat flux at 'early' times.

Nonlinear results Heat flux spectrum time evolution

- At **intermediate times**, heat flux gains low $k_y \rho_i$ contribution away from outboard midplane.

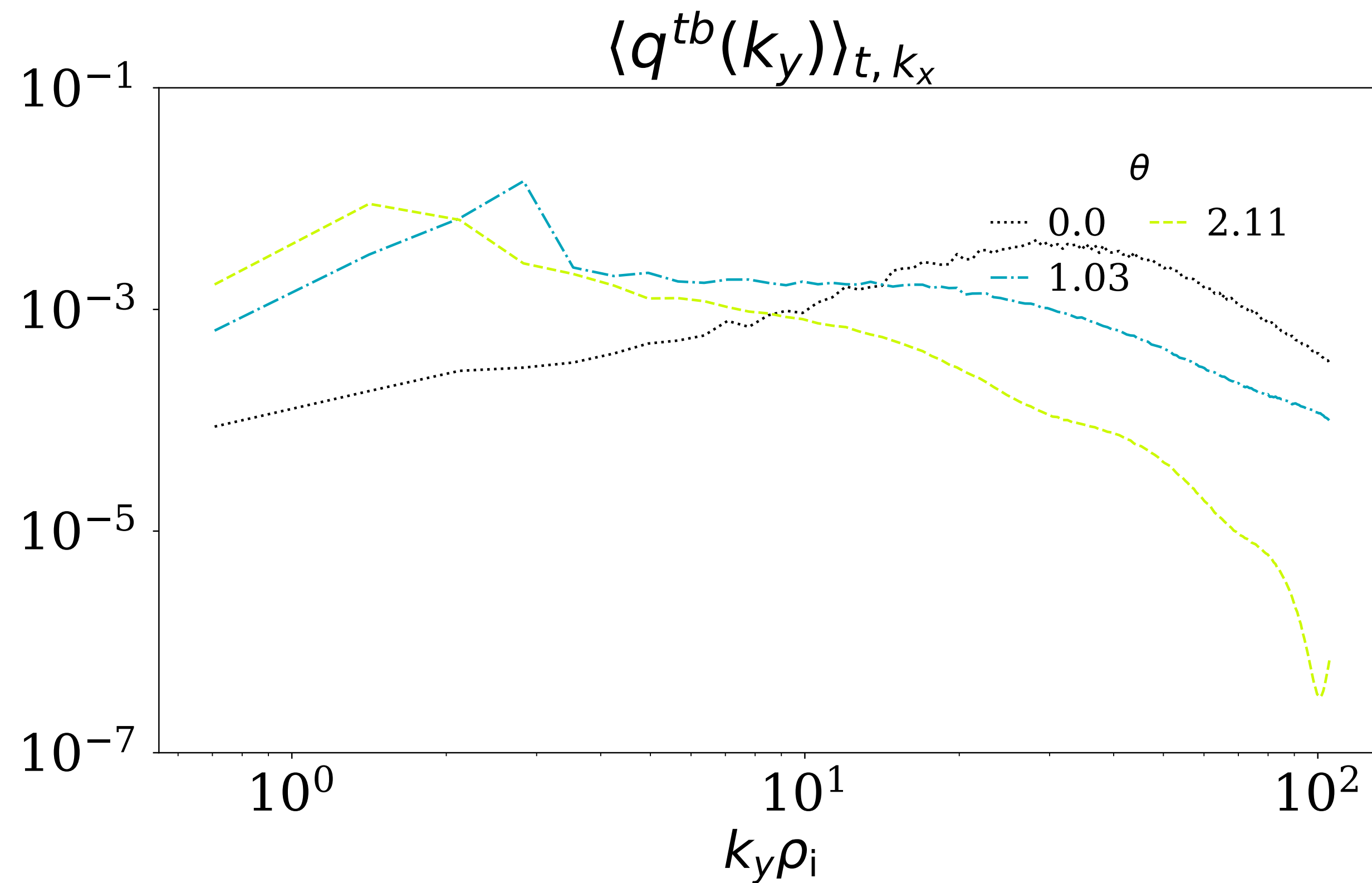


Figure: heat flux at 'intermediate' times.

Nonlinear results Heat flux spectrum time evolution

- At **late times**, heat flux dominated by low $k_y \rho_i$ contribution away from outboard midplane.

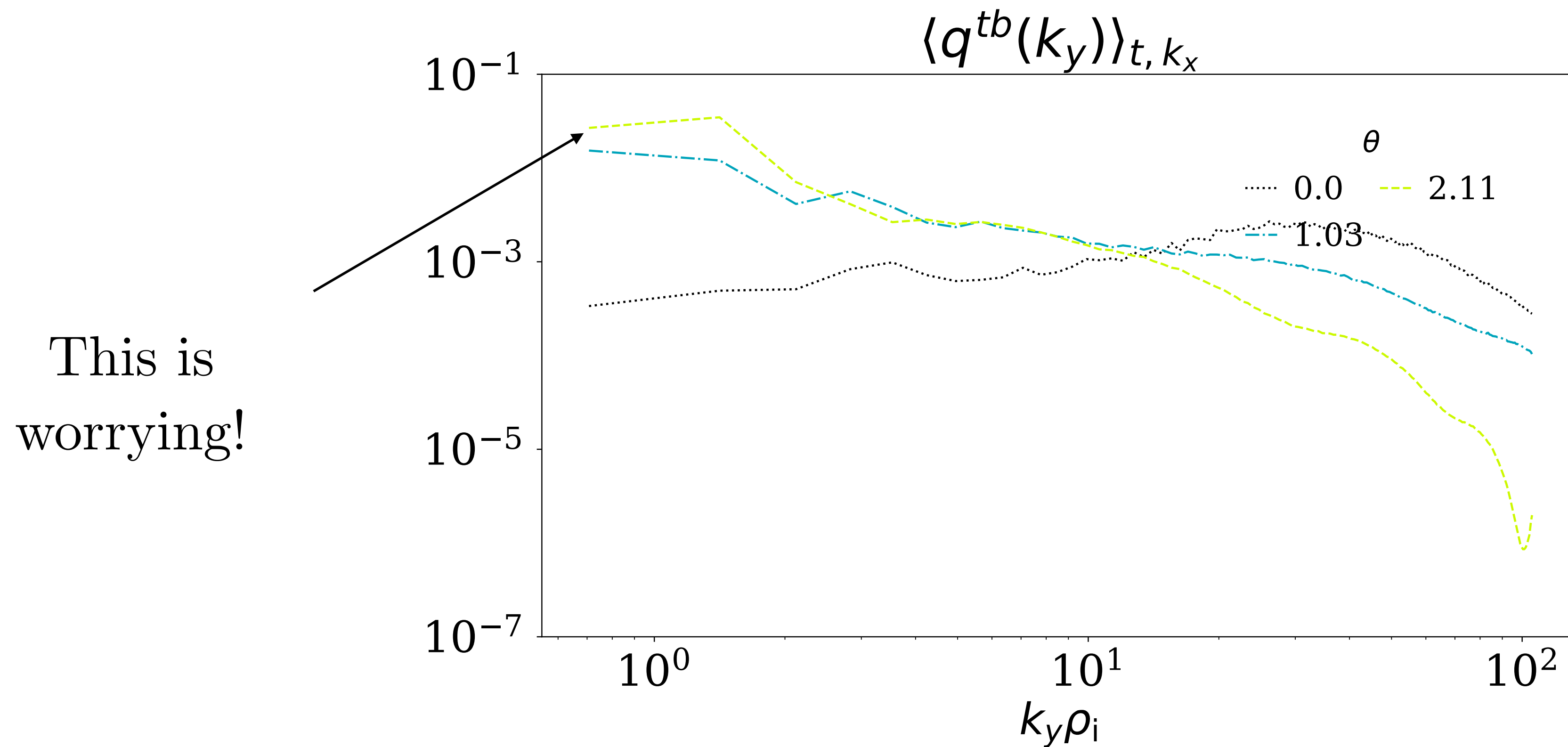


Figure: heat flux at 'late' times.

Nonlinear results Heat flux spectrum time evolution

- At **late times**, heat flux has significant low $k_y \rho_i$ contribution away from outboard midplane.

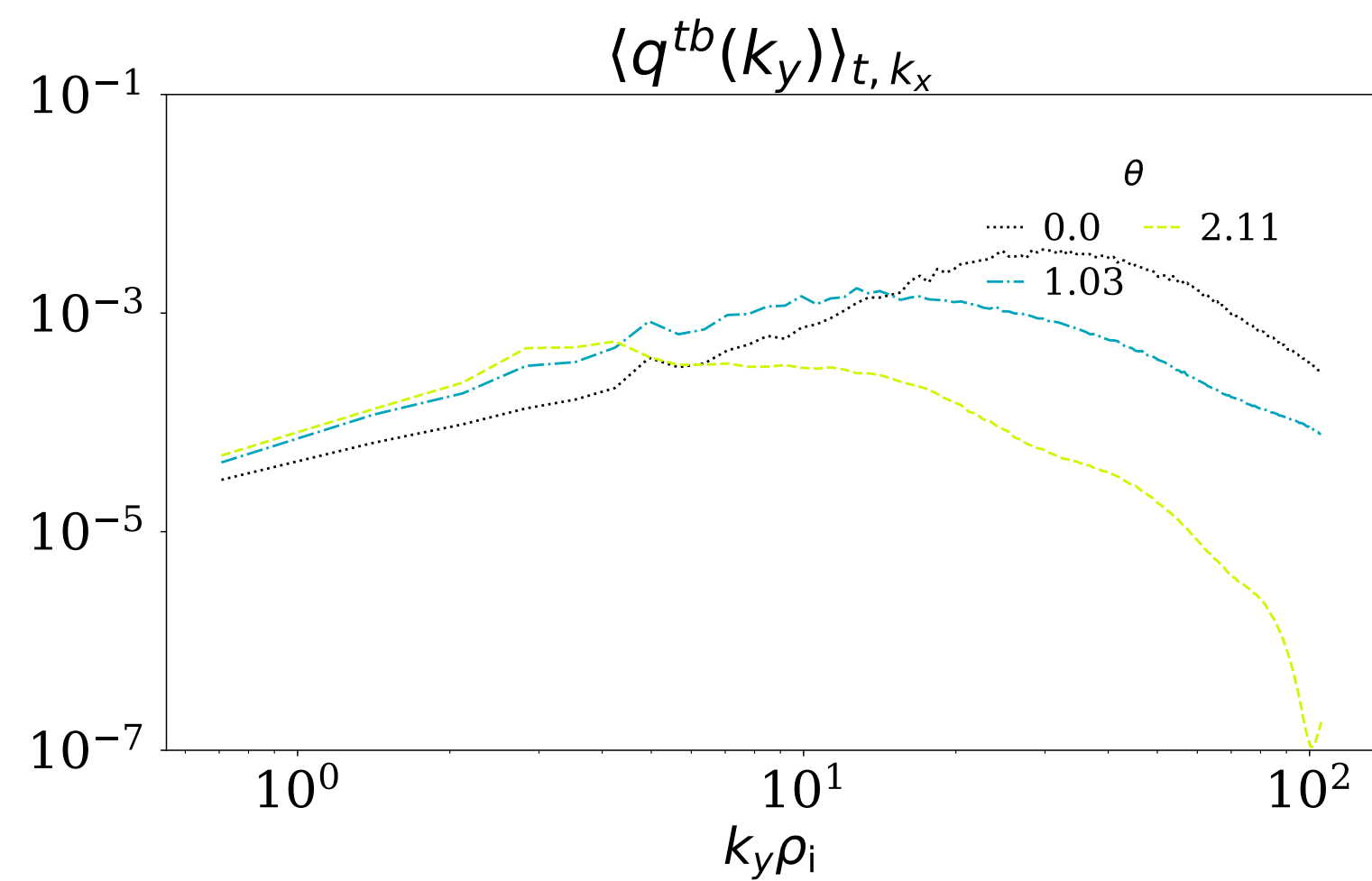


Figure: heat flux at 'early' times.

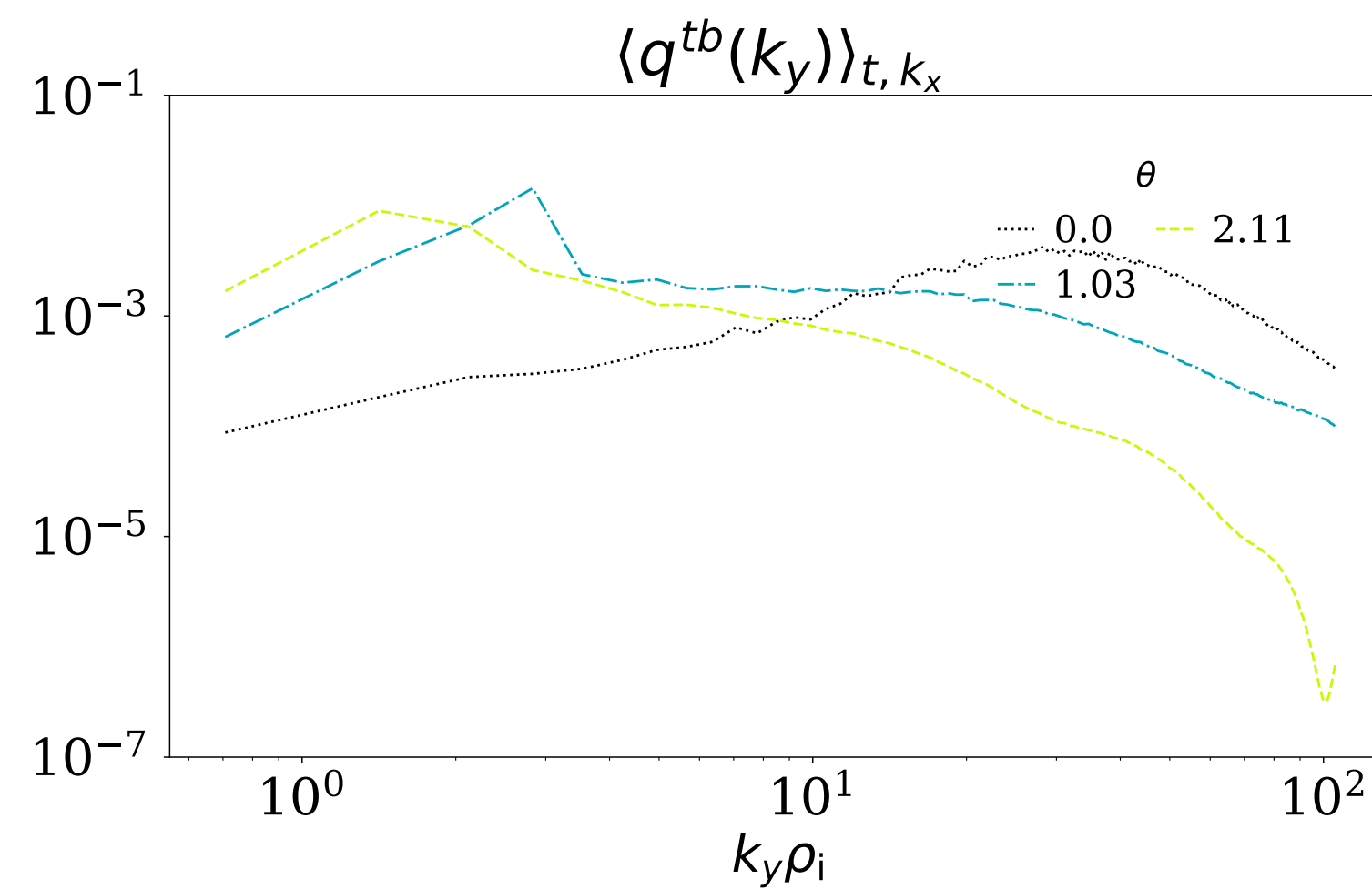


Figure: heat flux at 'intermediate' times.

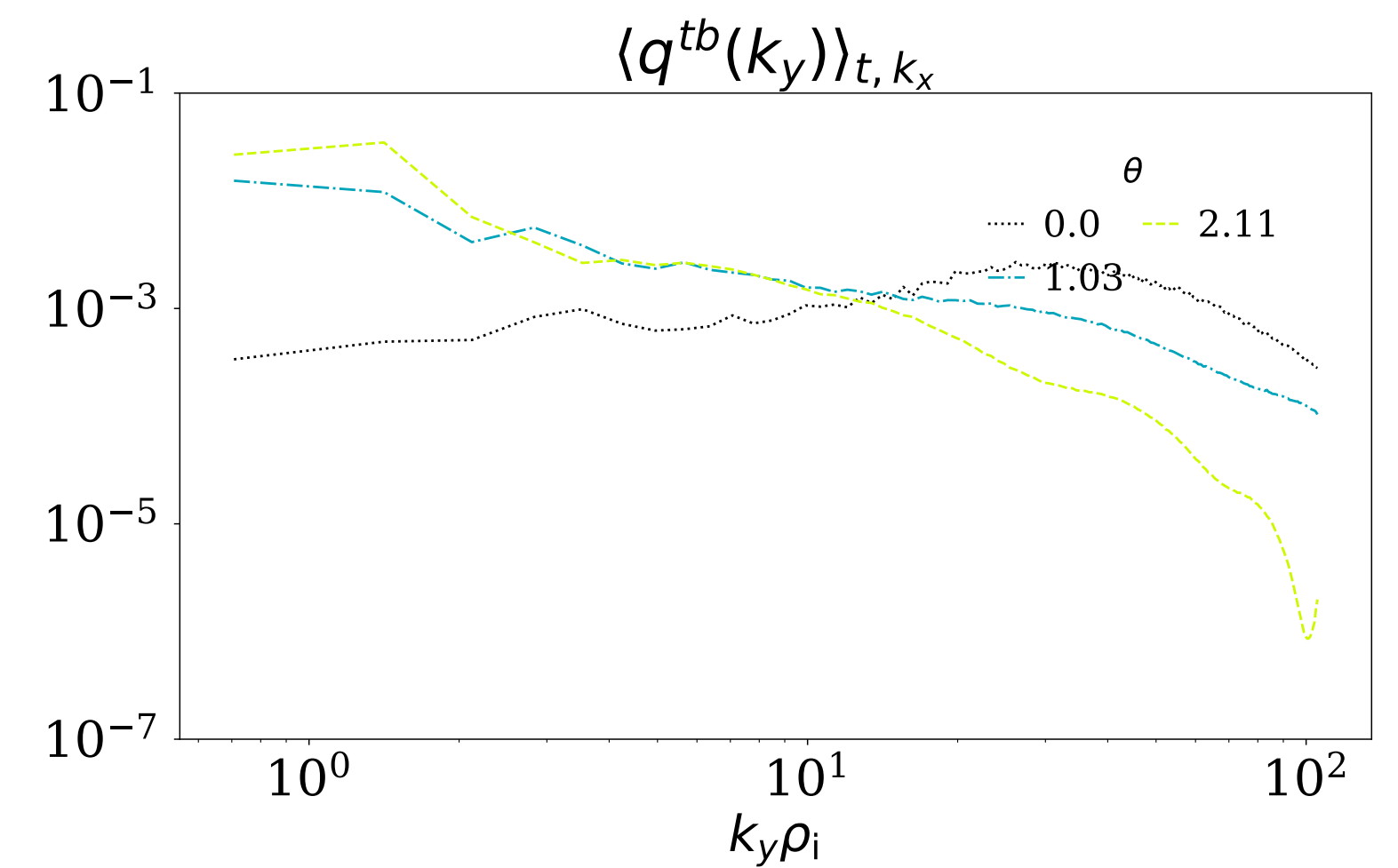
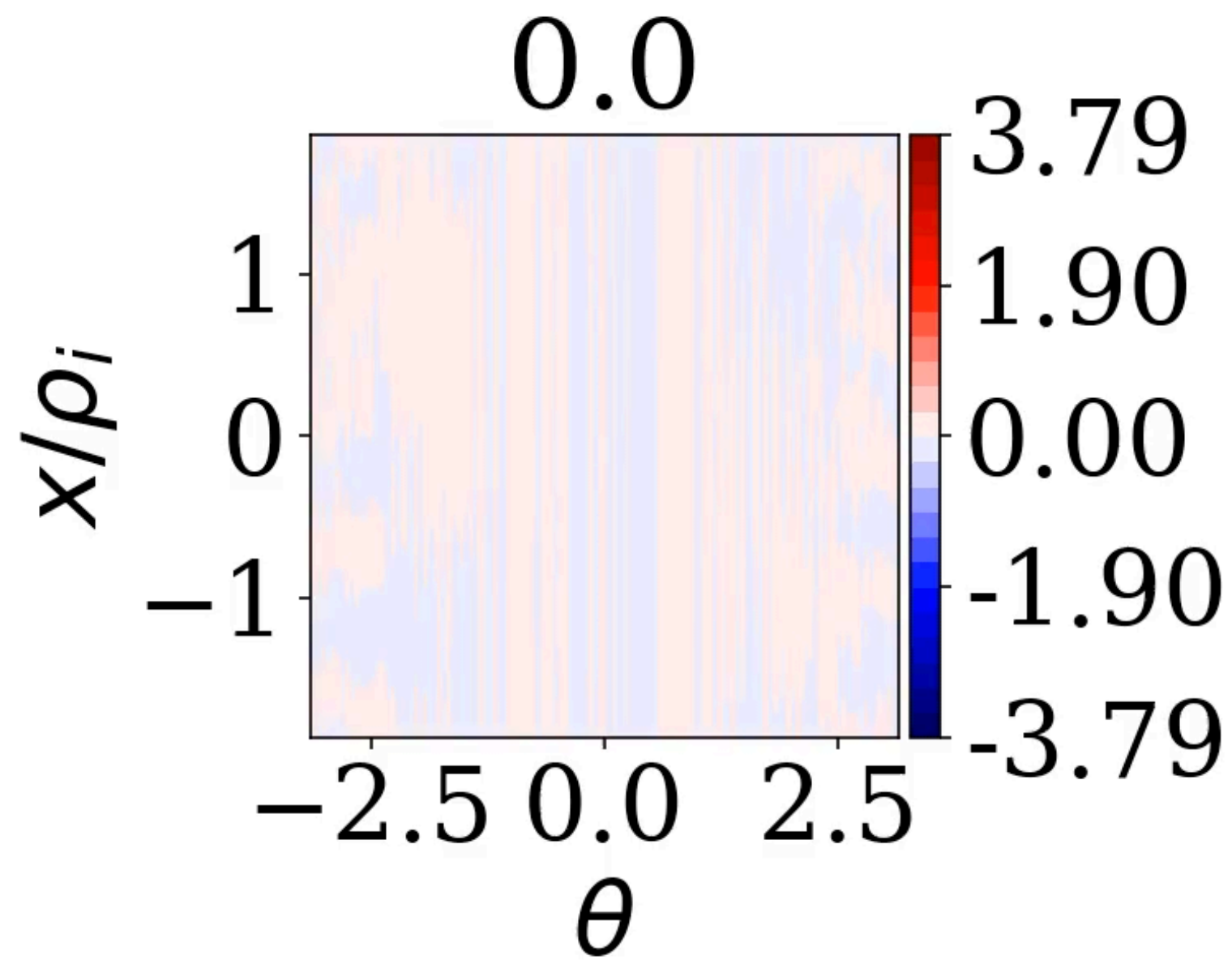


Figure: heat flux at 'late' times.

Nonlinear results Potential perturbation movies.

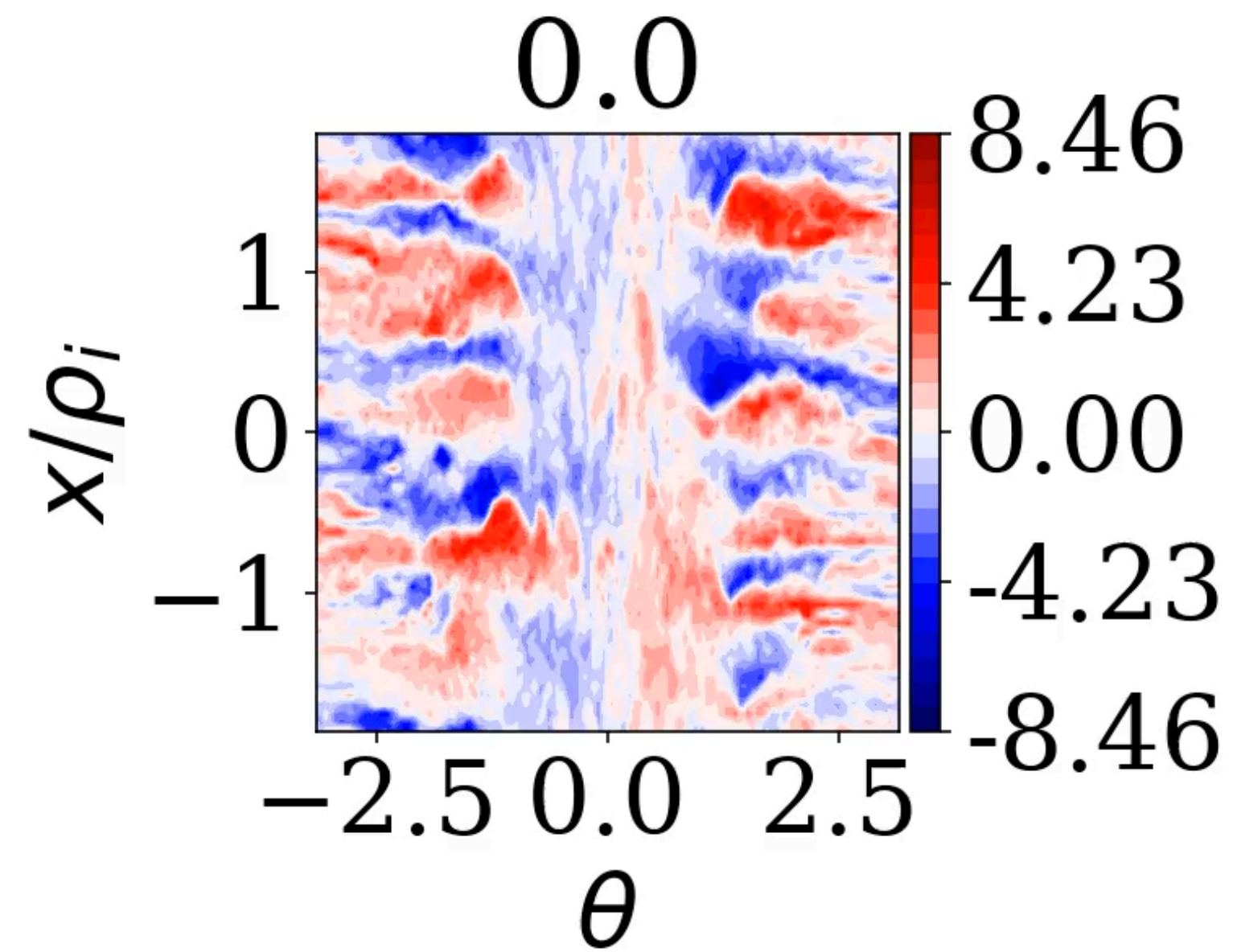
Early

Slab modes dominant
and transporting heat



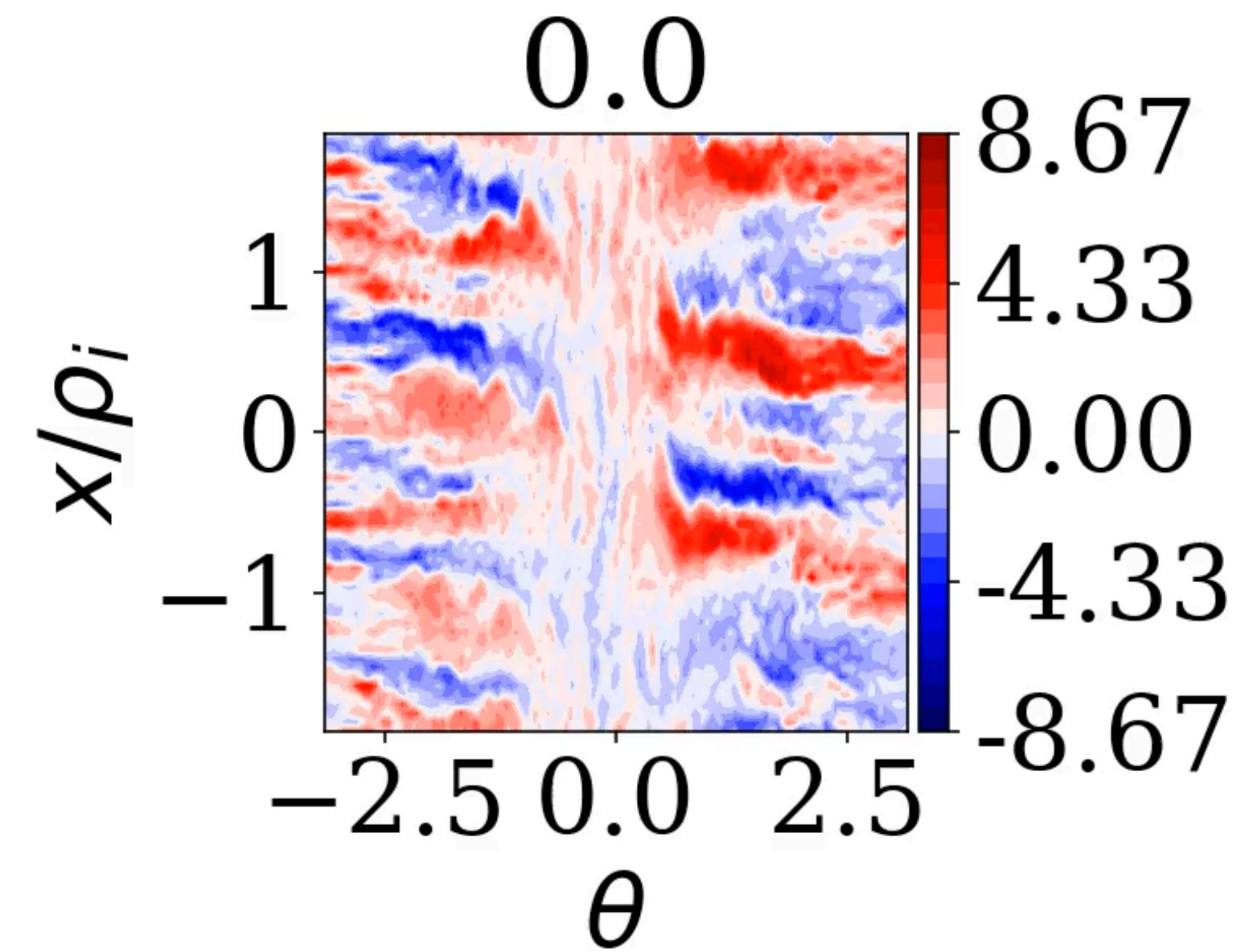
Intermediate

Toroidal modes still growing
Toroidal suppressing slab



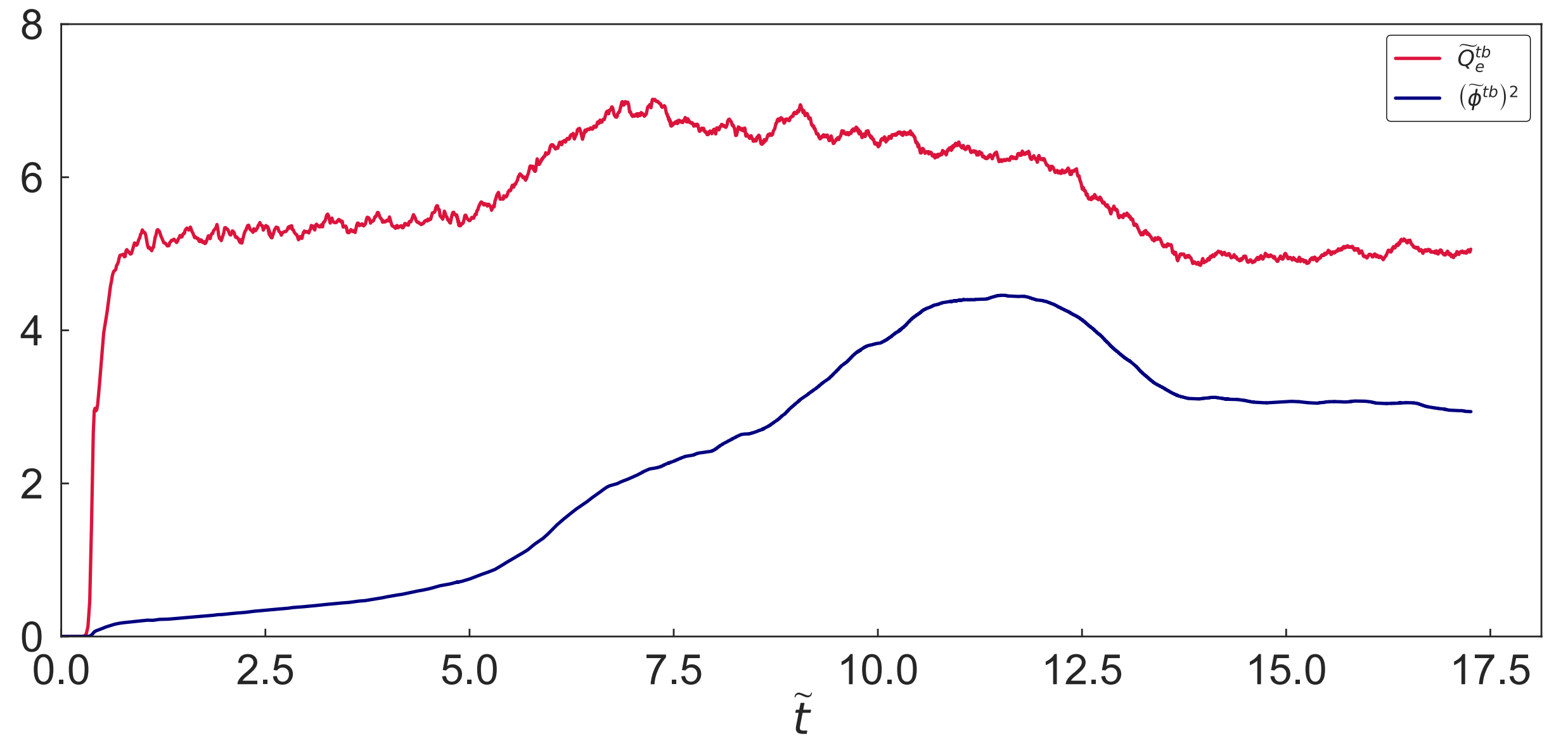
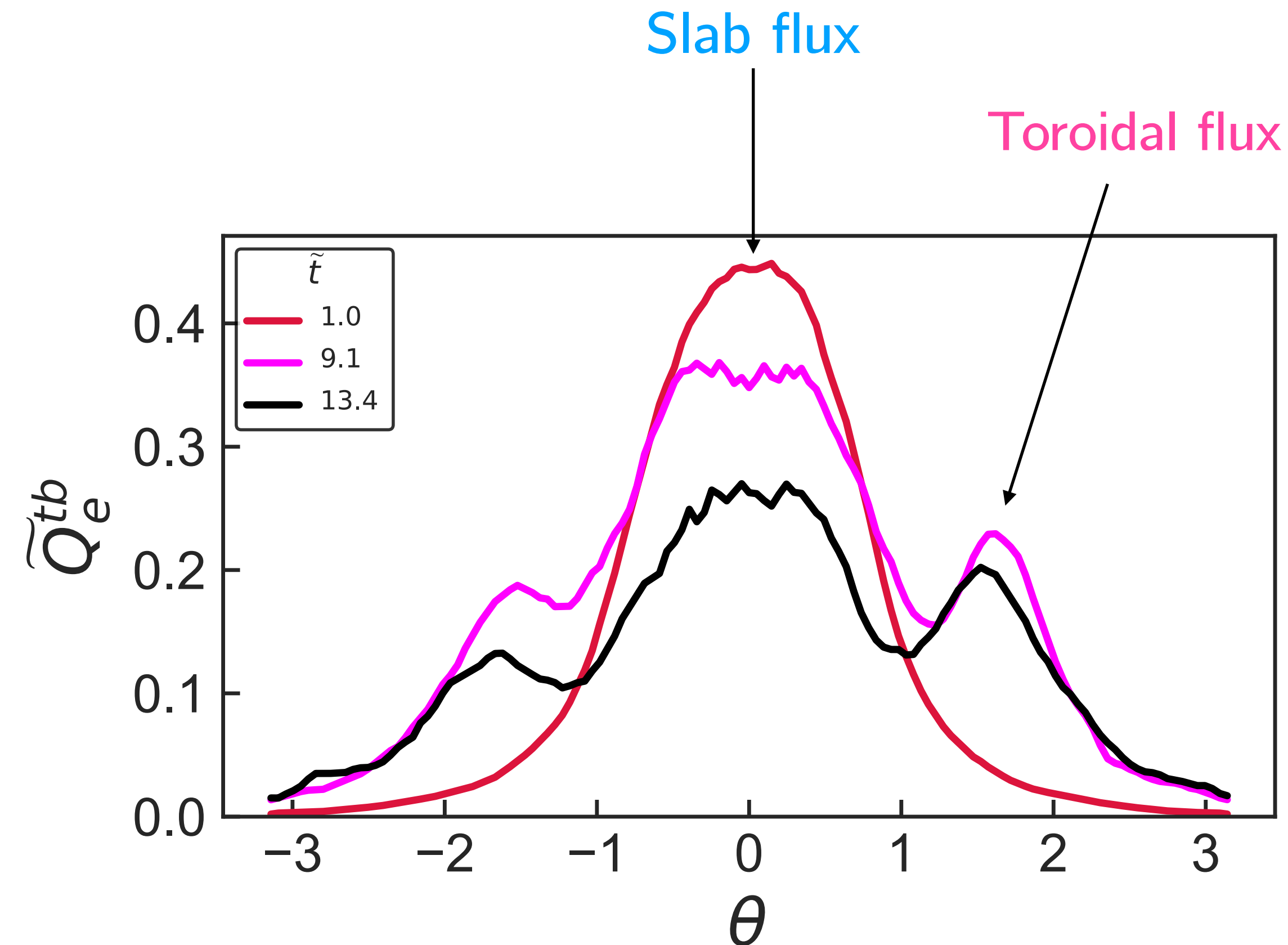
Late

Toroidal dominated state
Toroidal modes extend across θ



Nonlinear results

Over time, decrease in slab heat flux, increase in toroidal heat flux.

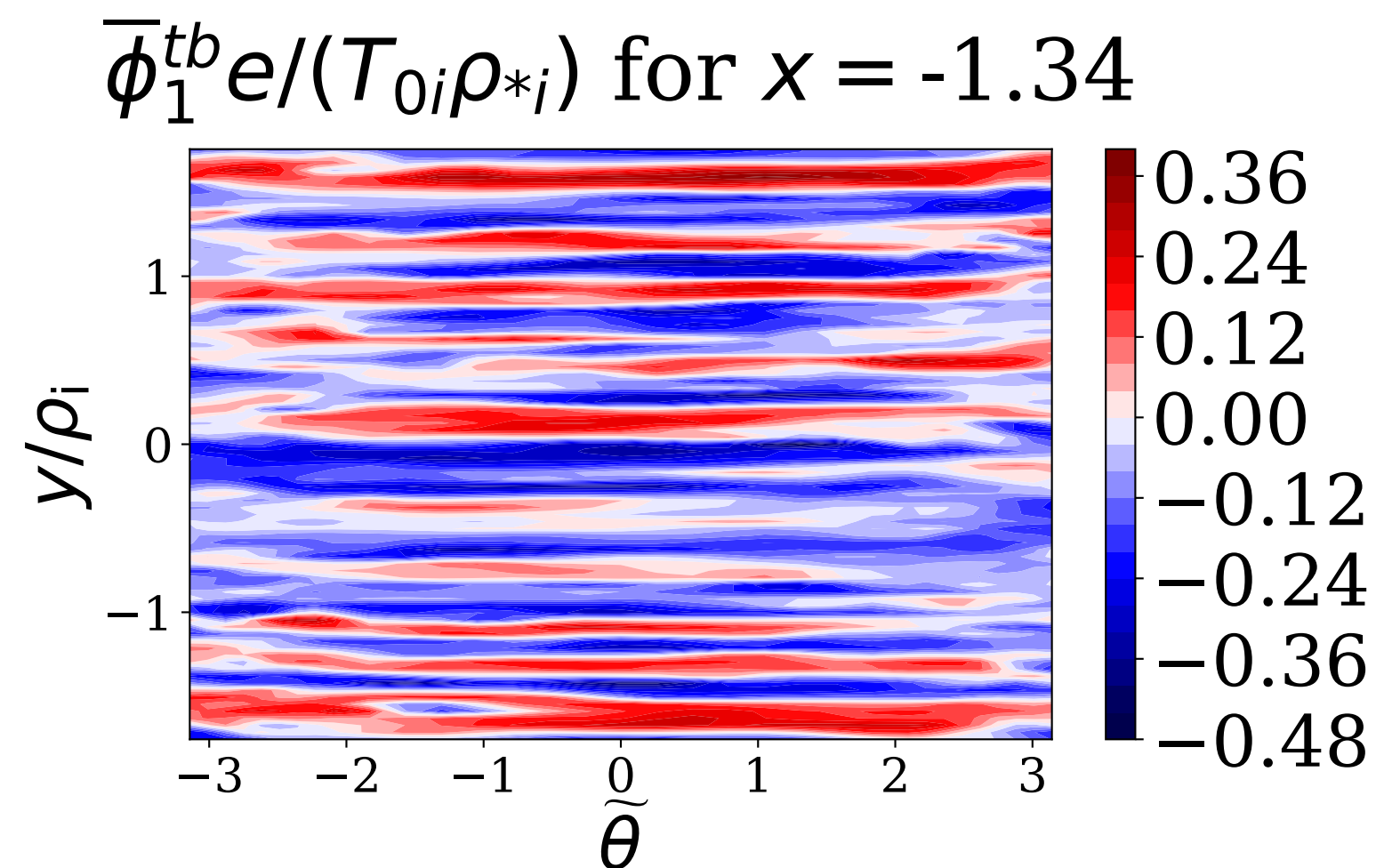
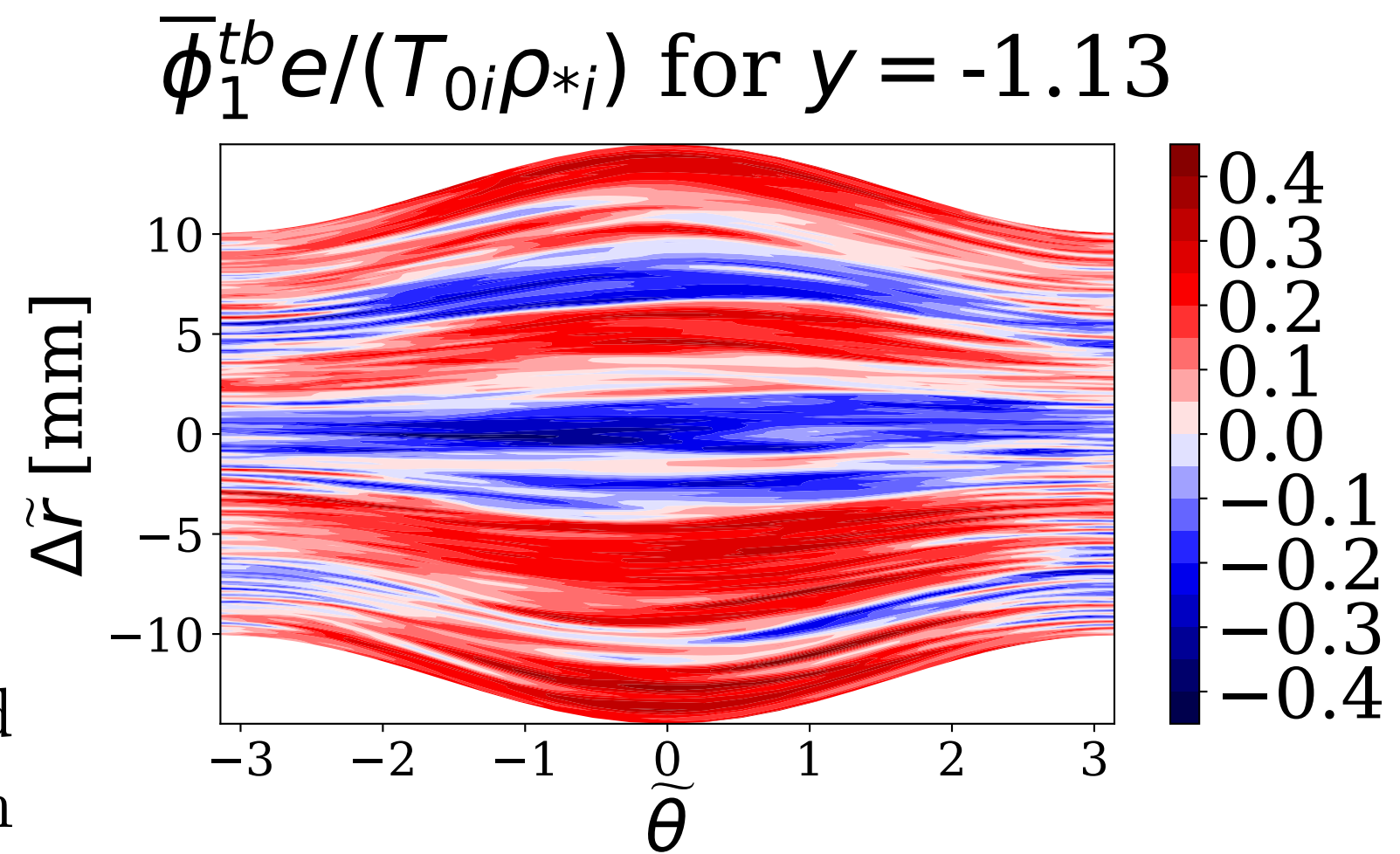


In this equilibrium, toroidal ETG modes appear to suppress more transport than they produce. Turning off magnetic drifts, heat flux doubles/quadruples.

Comparison of CBC and Pedestal ETG

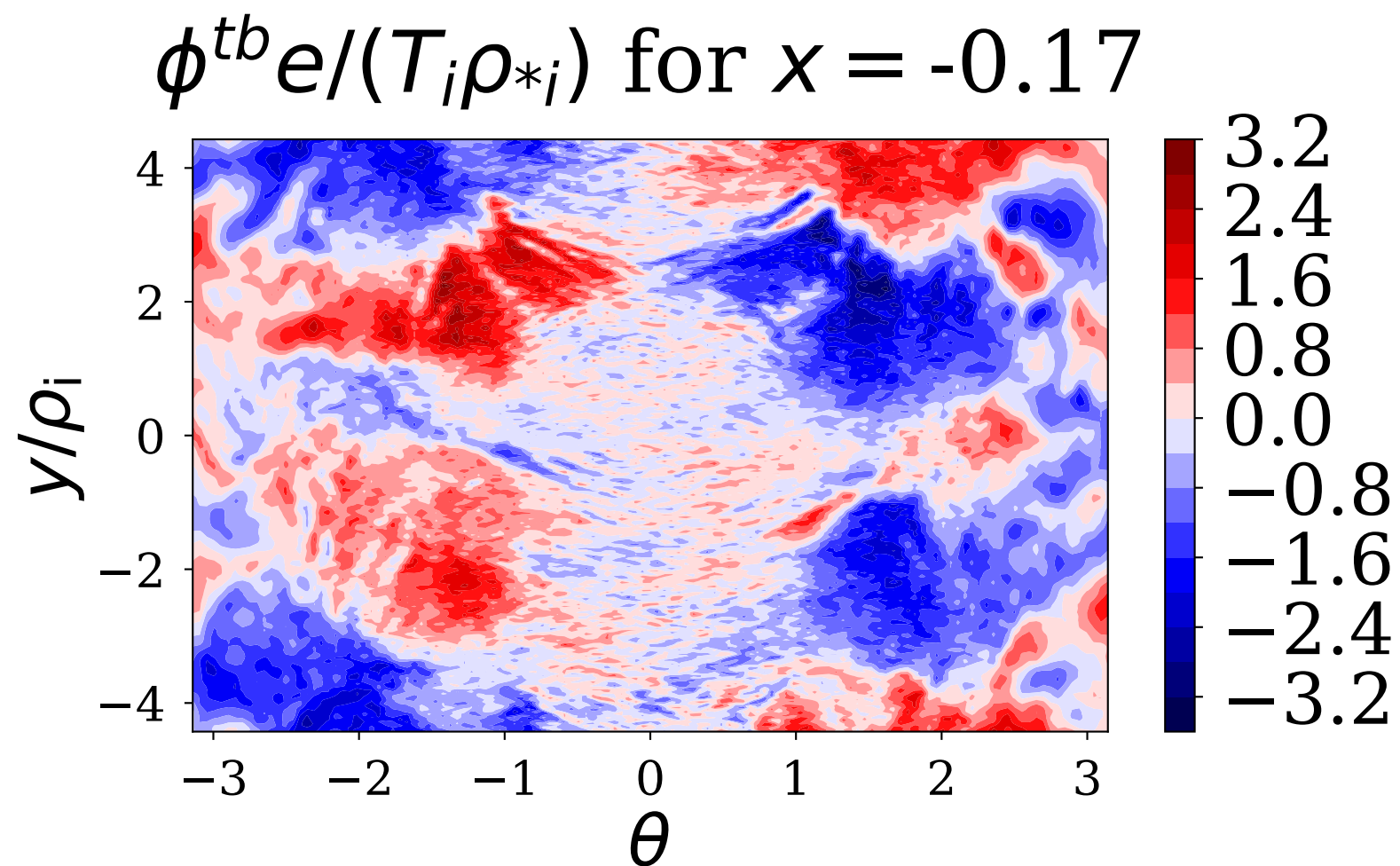
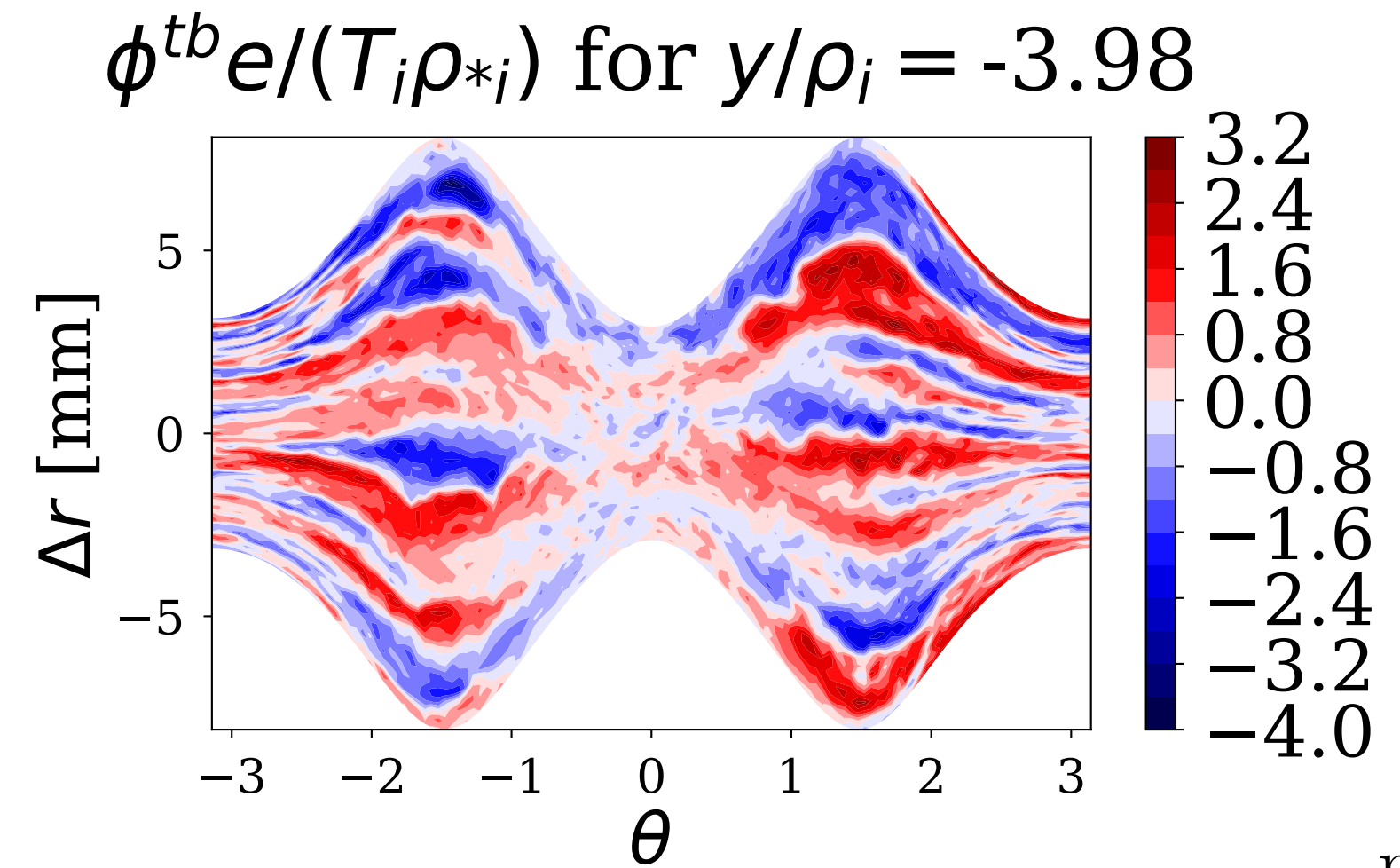
Pedestal turbulence is rather different to what we see in the core.

Cyclone Base Case-like ETG



Turbulence extended for a full connection length and highly ballooning

Pedestal ETG



Maximum amplitudes away from outboard midplane, and turbulent character depends on poloidal location.

Differentiating between slab and toroidal ETG turbulence

- In the messy, turbulent state of electrostatic pedestal turbulence, how do we differentiate between the different ETG modes?
- Answer: study the 'topography' of the magnetic drifts and FLR effects.

Differentiating between slab and toroidal ETG turbulence

FLR effects

- We can visualize FLR effects by plotting

$$\Gamma_0(b_e) = I_0(b_e)\exp(-b_e)$$

for a range of θ and θ_0 values,
where $2b_e = (k_{\perp}\rho_e)^2$.

- Γ_0 appears in dispersion relation.
- Plotting Γ_0 versus θ and θ_0 allows us to predict where the turbulence could exist.

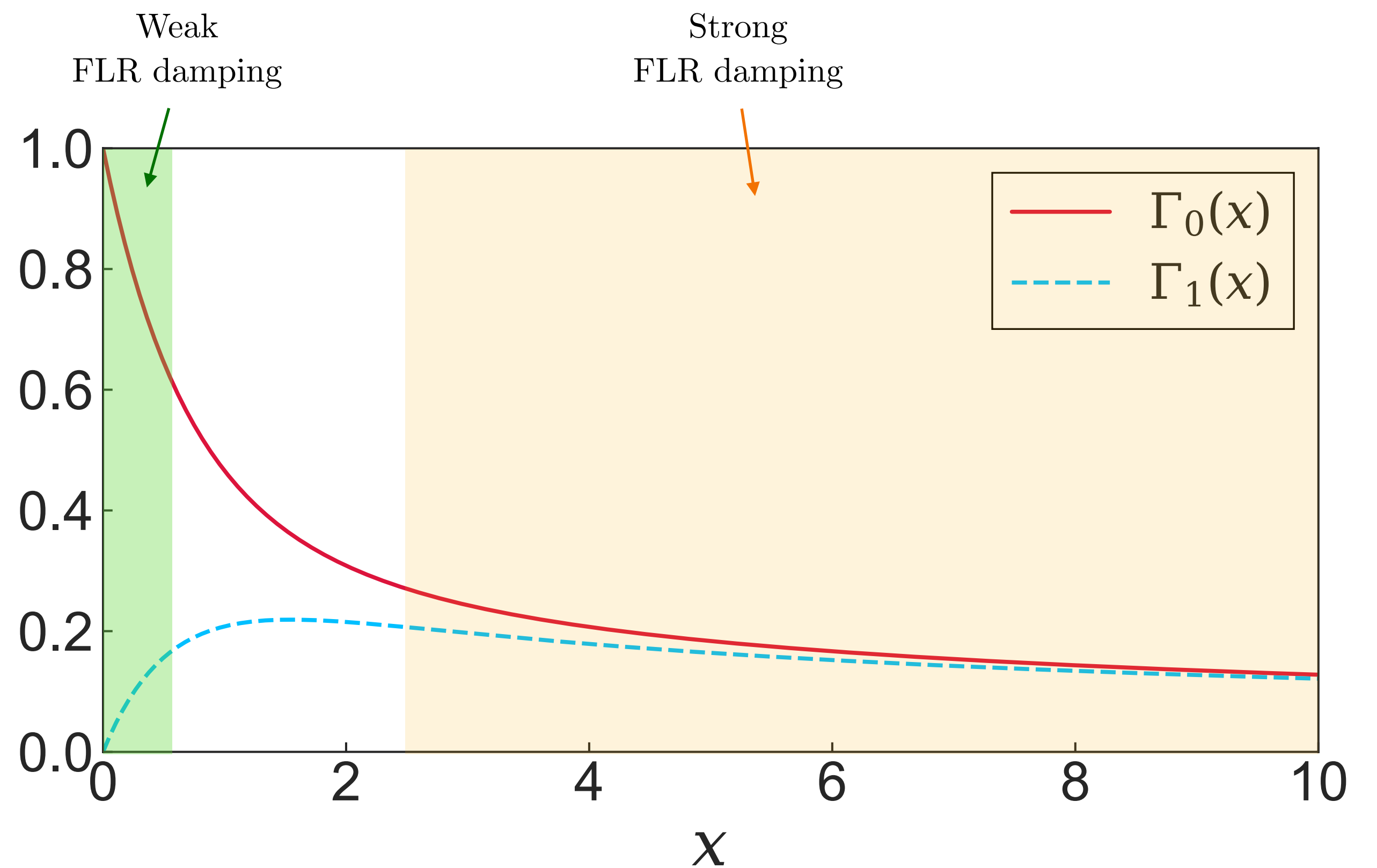


Figure: Functions $\Gamma_0(x)$ and $\Gamma_1(x)$.

Differentiating between slab and toroidal ETG turbulence

Hypothesis: we can predict where slab turbulence will be with plots of Γ_0 .

Weak FLR damping (expect stronger fluctuations here!)

$$k_y \rho_i = 21.2$$

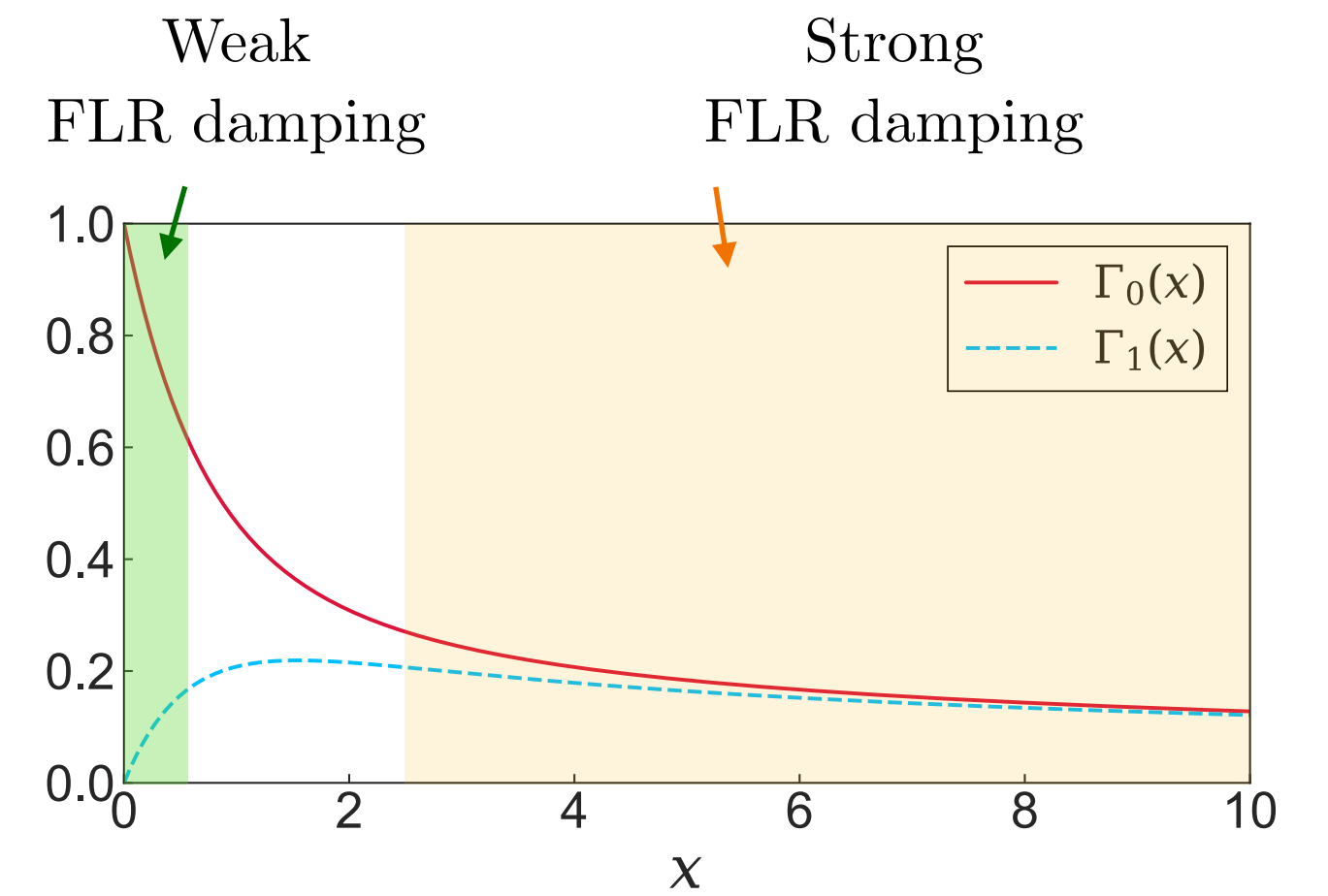
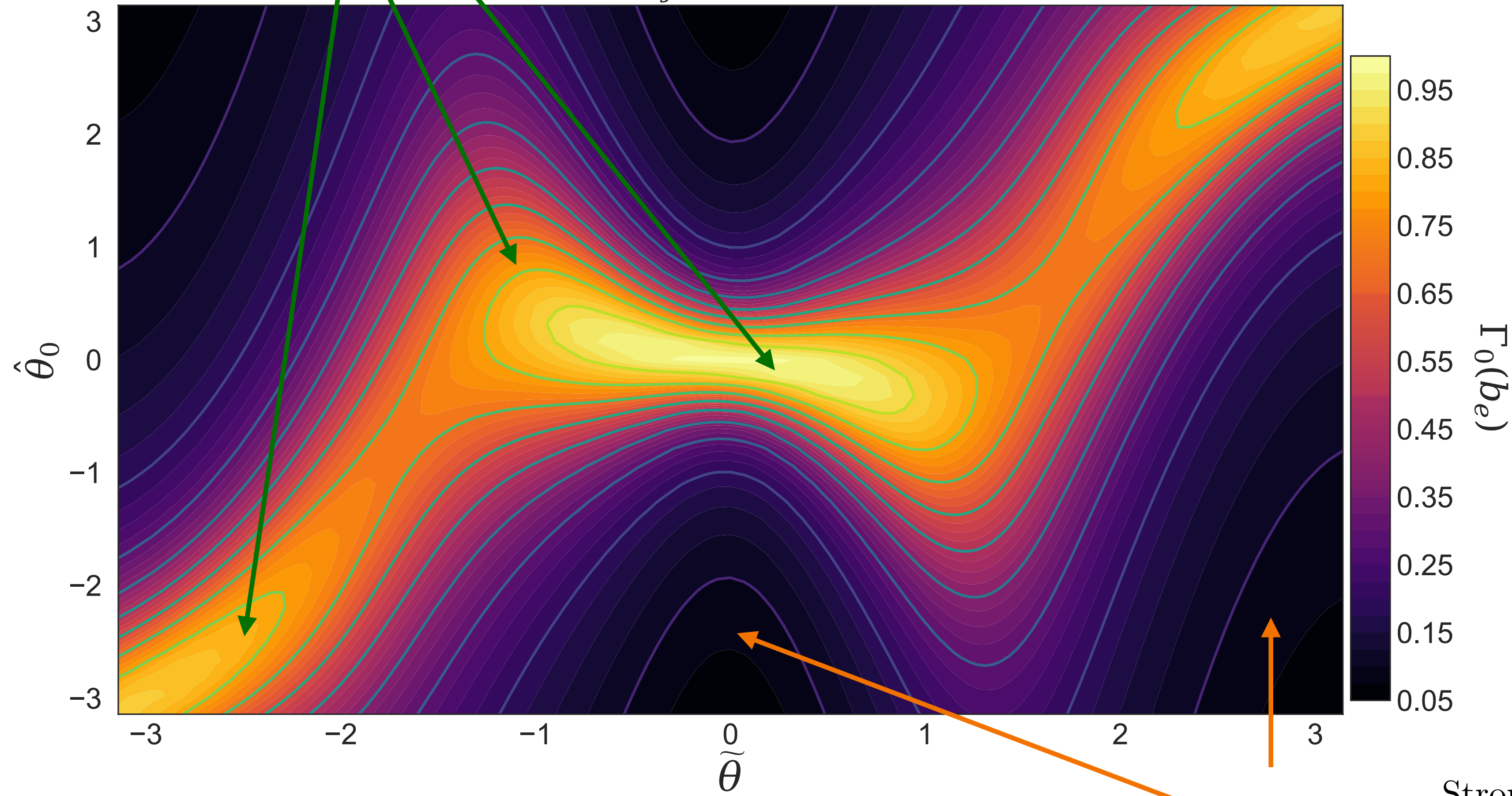


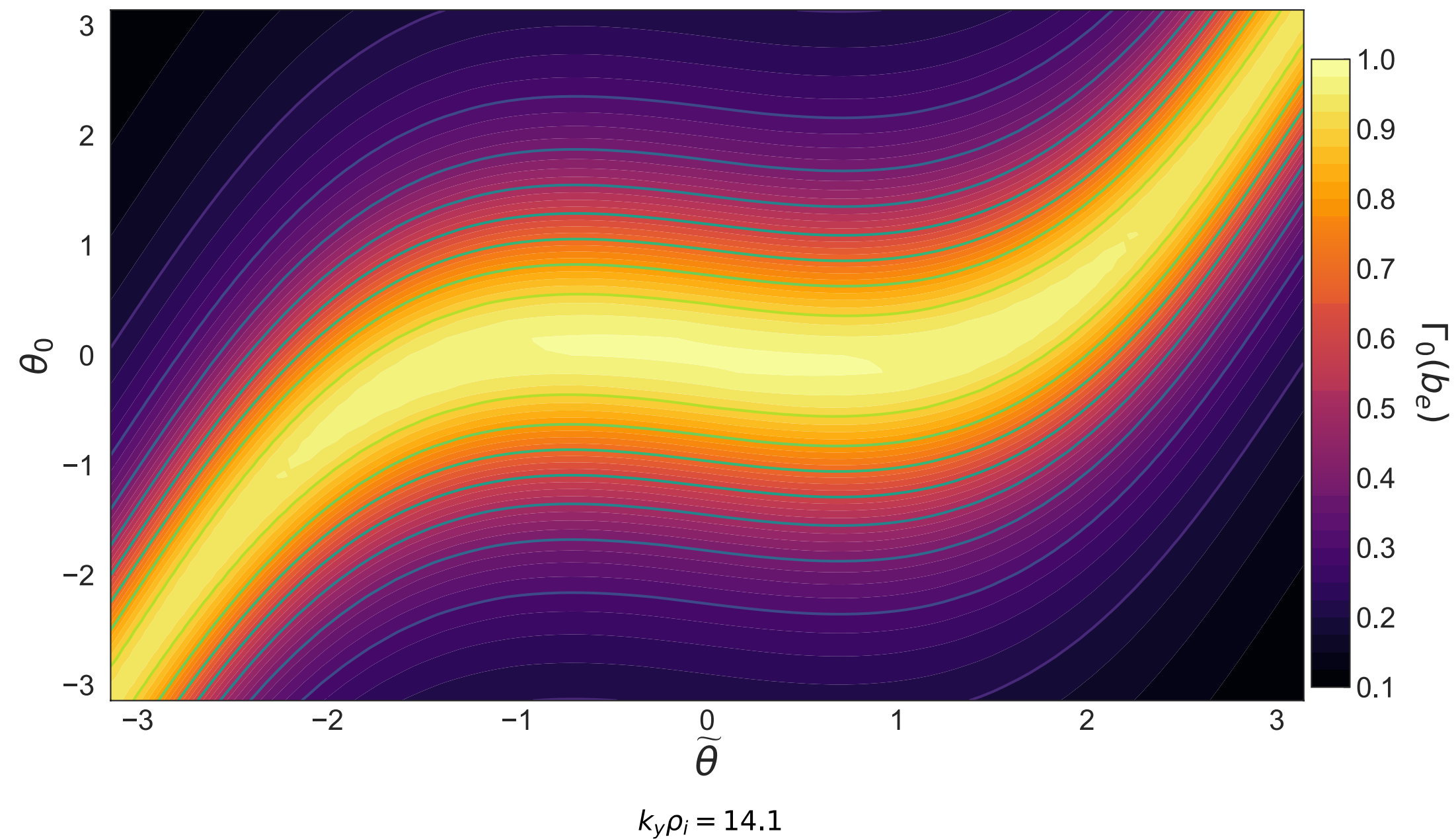
Figure: Functions $\Gamma_0(x)$ and $\Gamma_1(x)$.

Strong FLR damping
(expect weaker fluctuations here!)

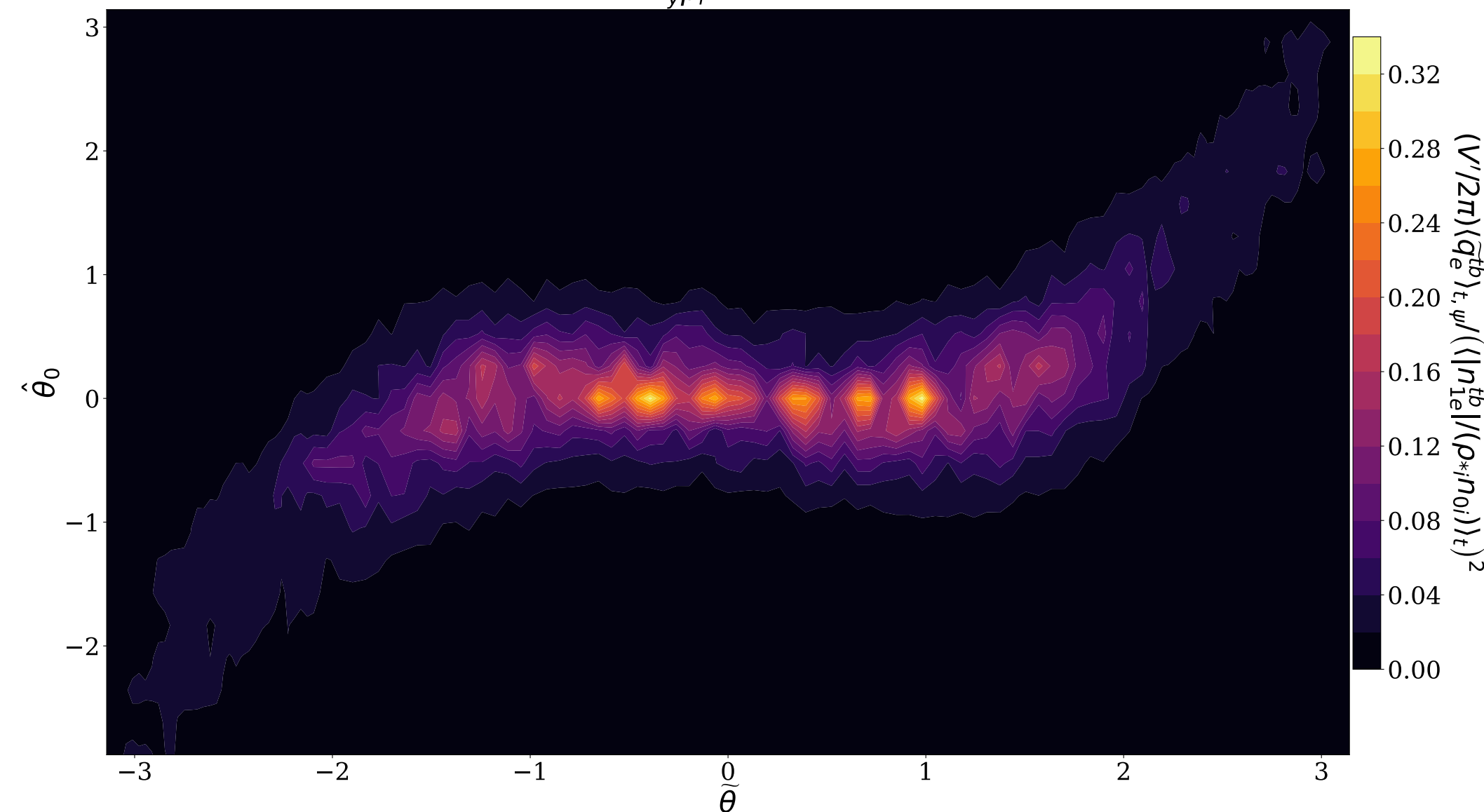
Slab ETG modes location

Experiment: run nonlinear slab ETG simulations in different geometries (ceteris paribus)

Geometry 1



Top row: Γ_0
 Bottom row: $Q_e^{tb} / (\phi^{tb})^2$.

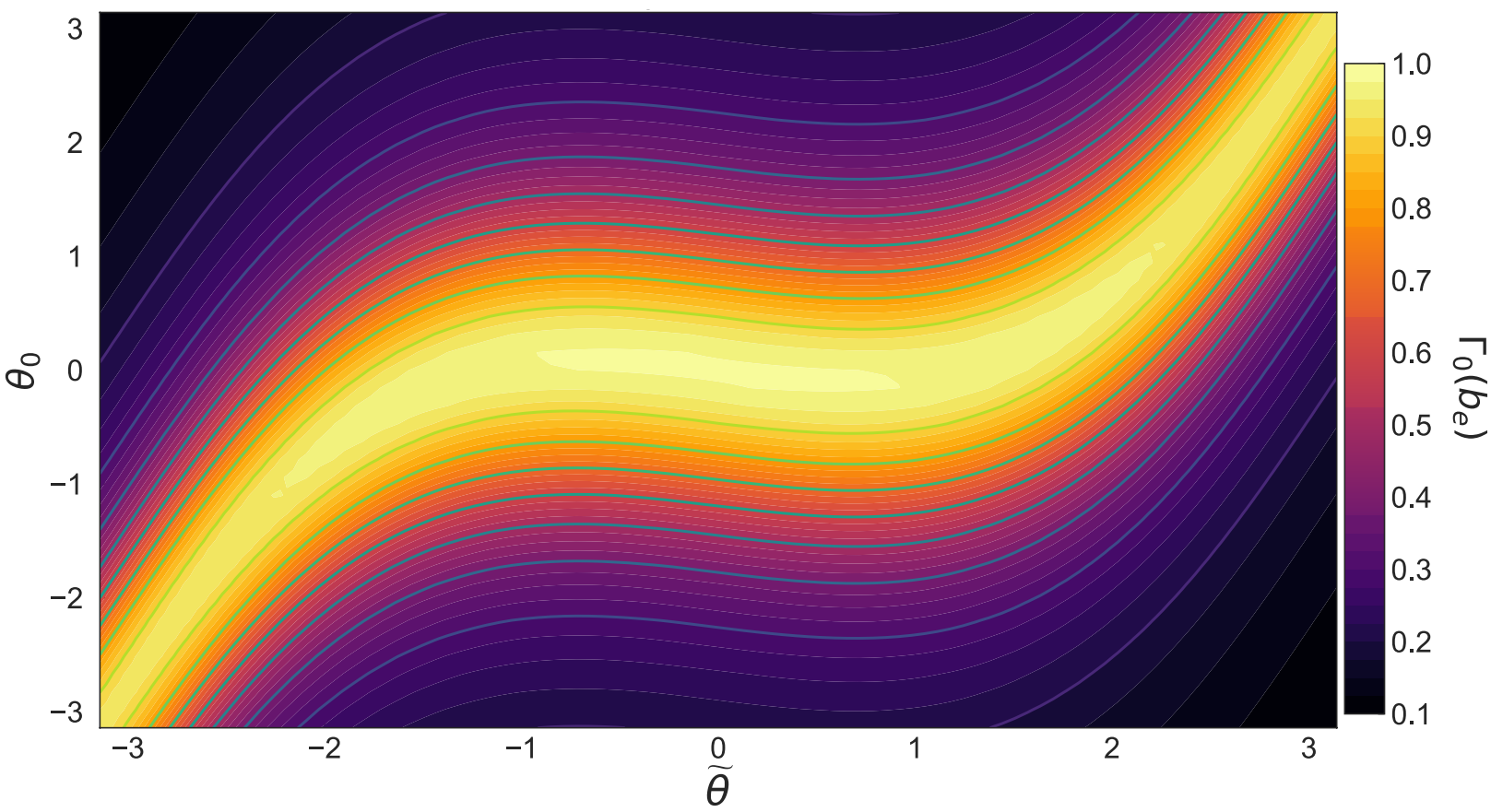


Slab ETG modes location

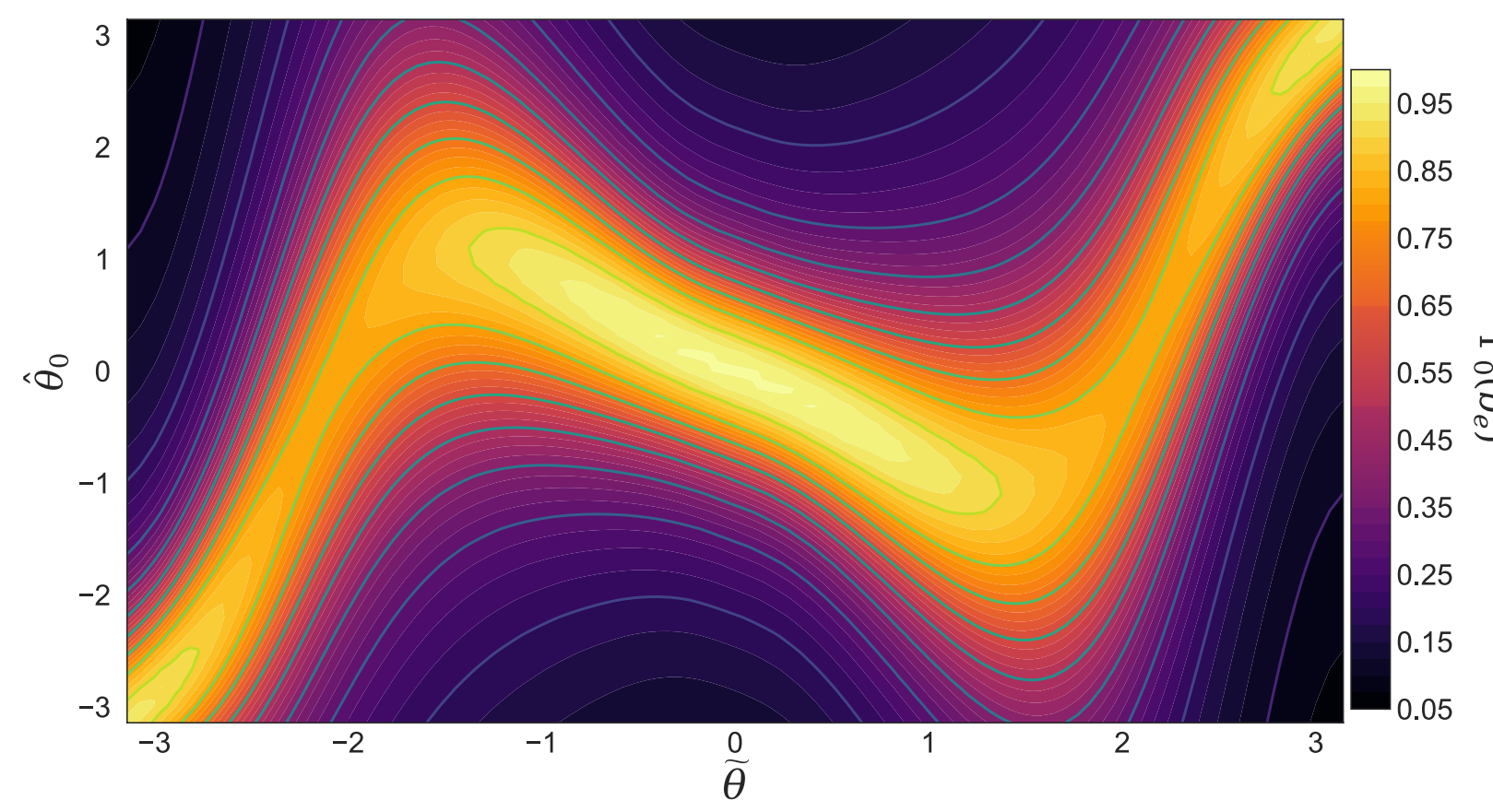
Experiment: run nonlinear slab ETG simulations in different geometries (ceteris paribus)

- Top row: Γ_0 , bottom row: $Q_e^{tb} / (\phi^{tb})^2$.

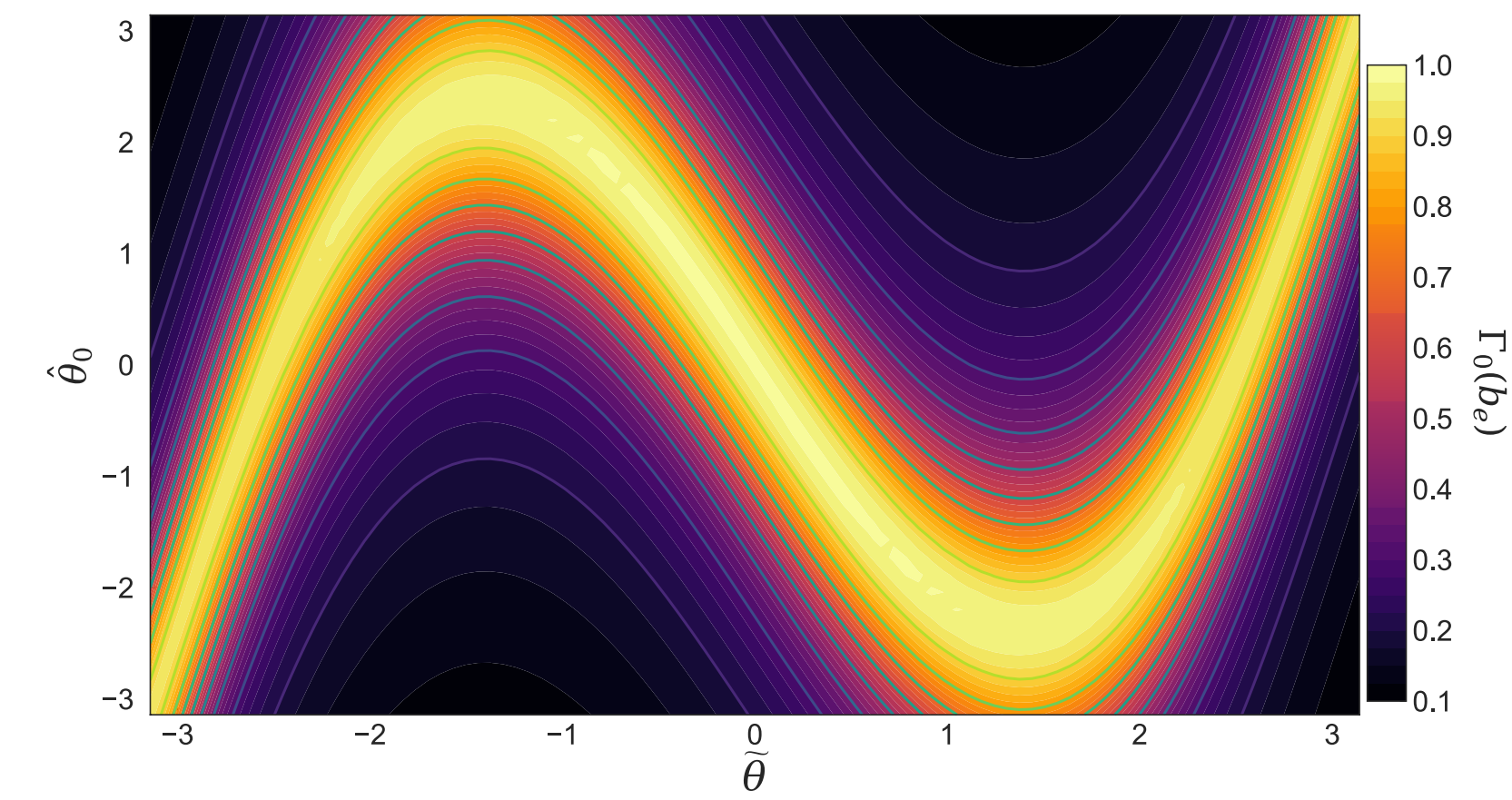
Geometry 1



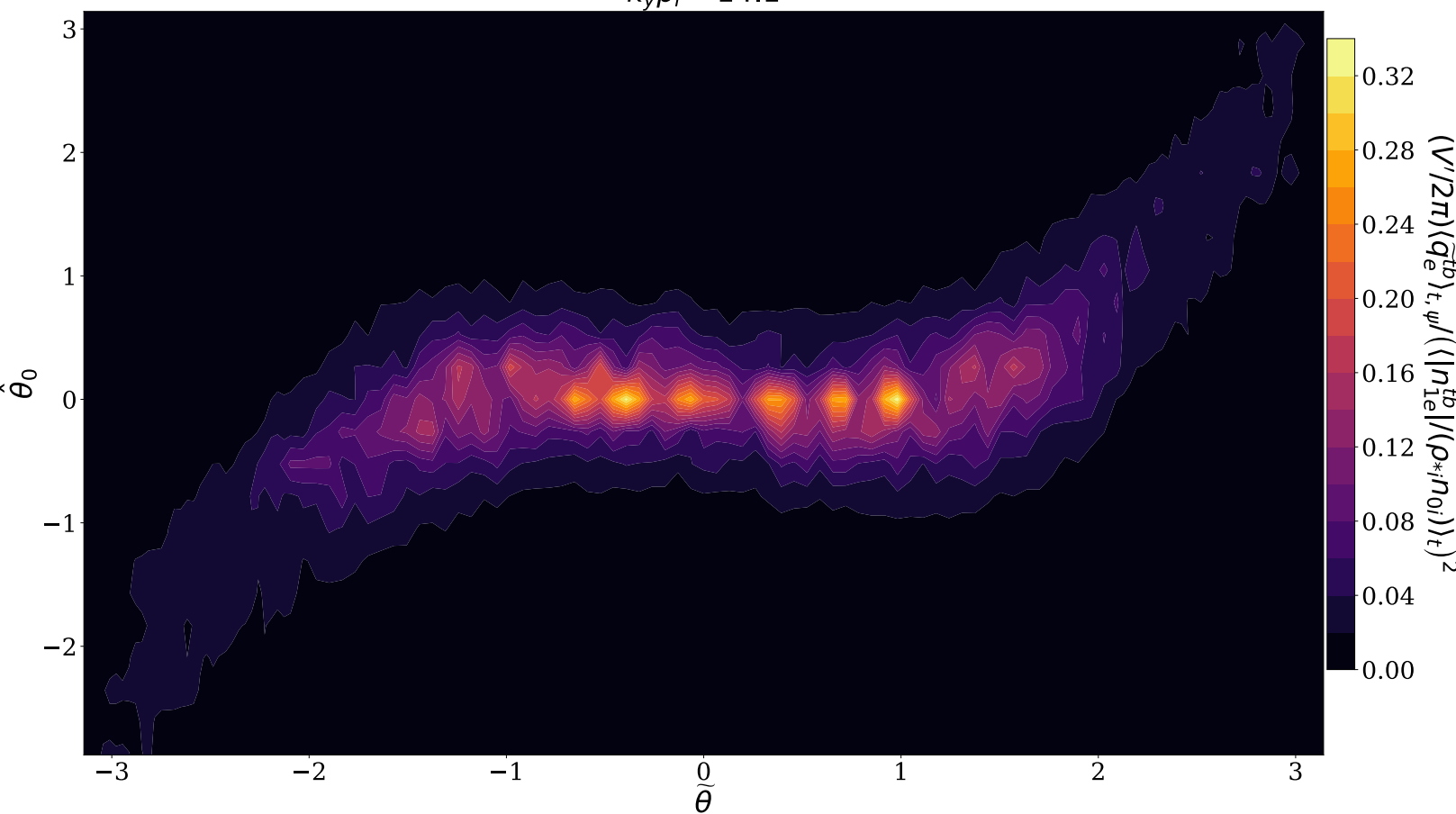
Geometry 2



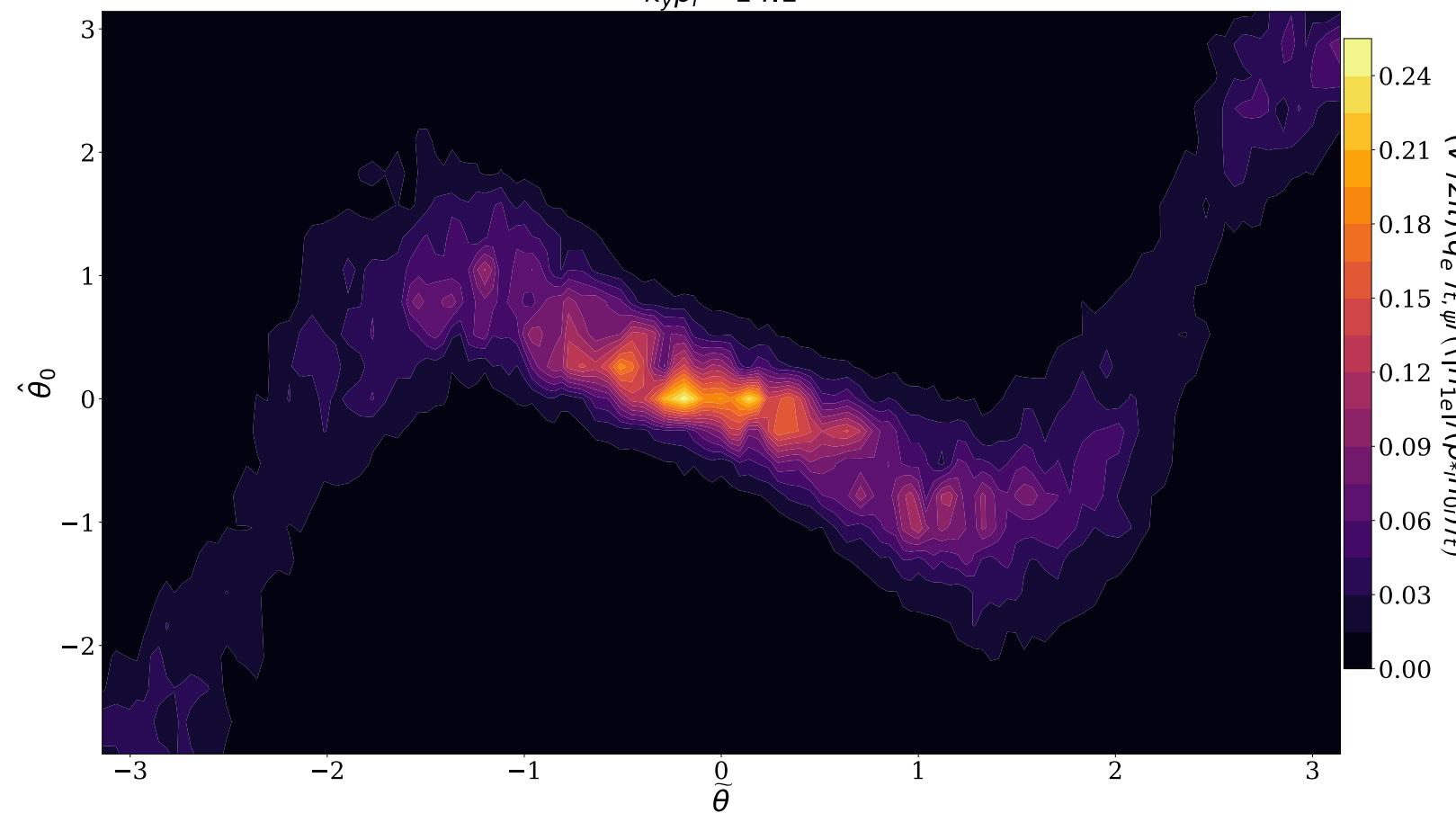
Geometry 3



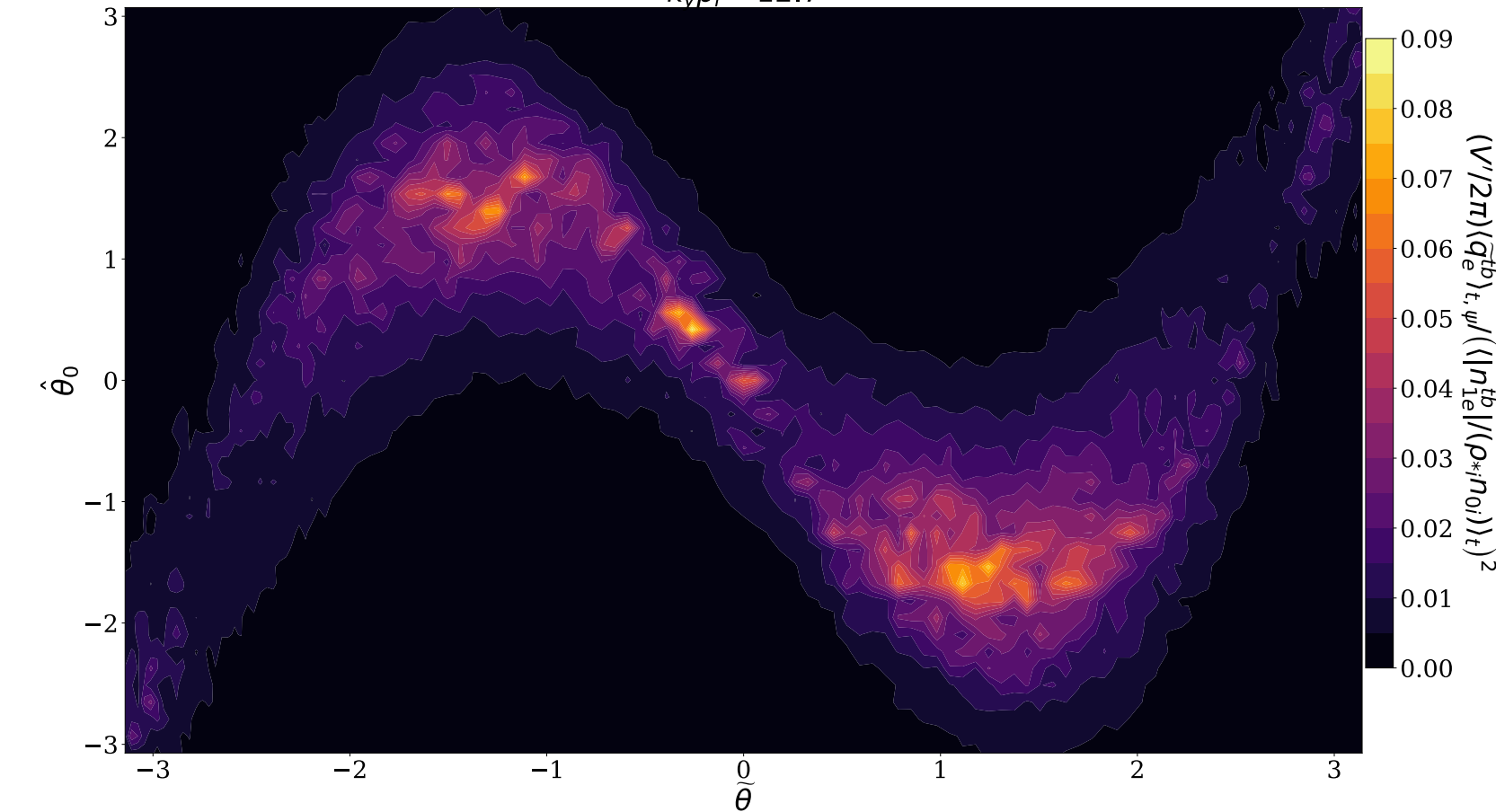
$k_y \rho_i = 14.1$



$k_y \rho_i = 14.1$



$k_y \rho_i = 12.7$



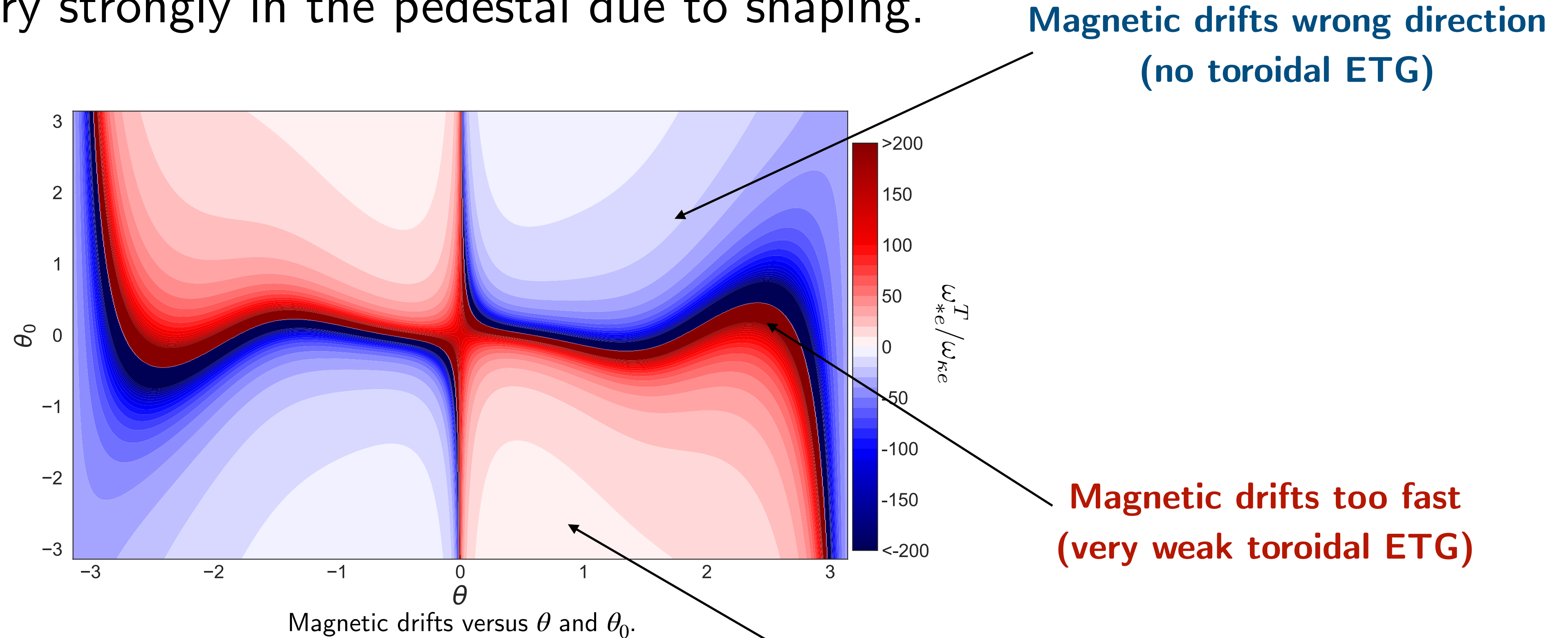
—> FLR effects determine slab ETG turbulence distribution.

(Parisi, 2020, thesis)

Toroidal ETG modes location

Magnetic drifts + FLR effects determine location of toroidal ETG turbulence

- Magnetic drifts vary strongly in the pedestal due to shaping.

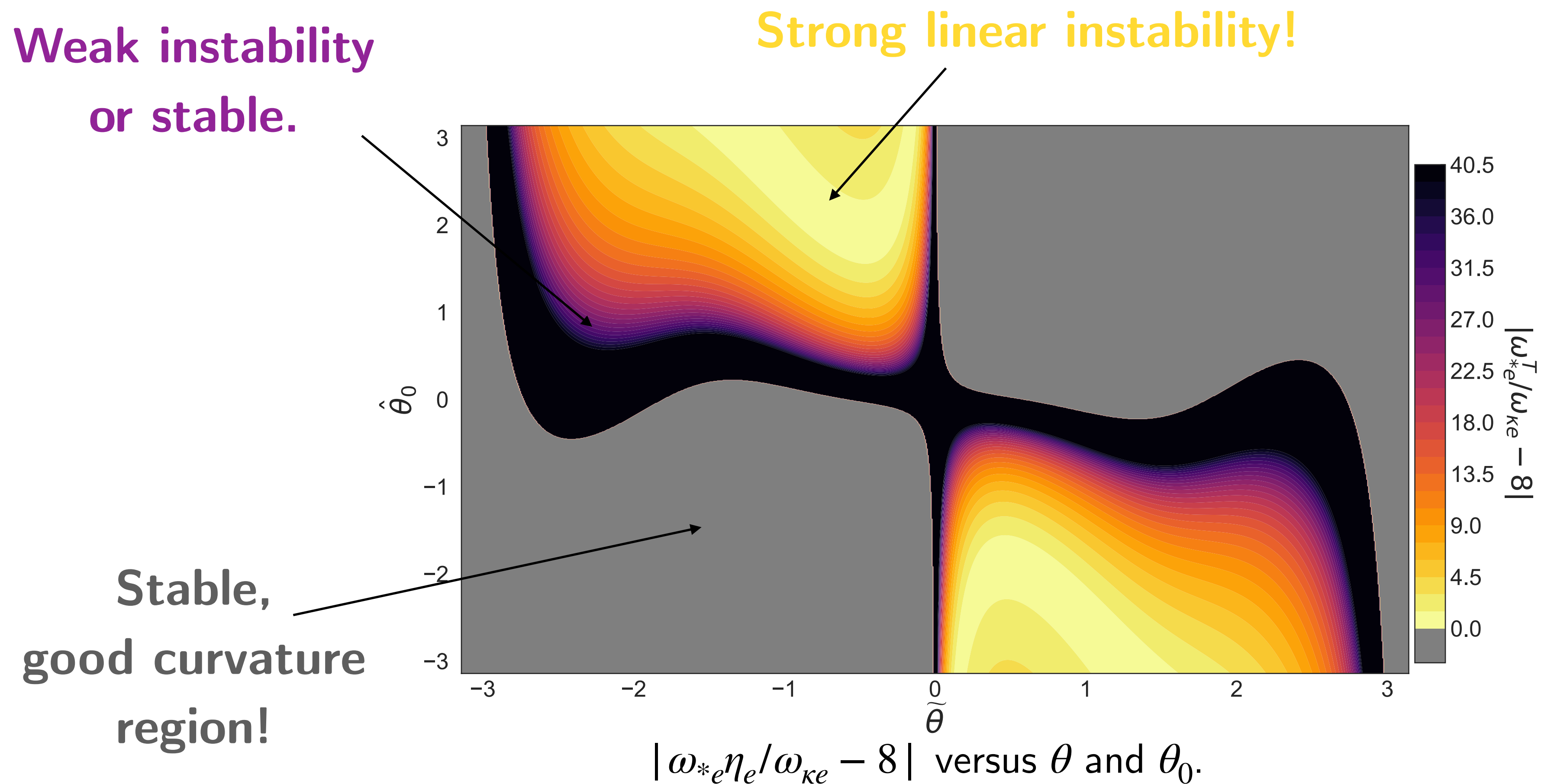


- Recall that for strong instability, $\frac{\omega_{*e}^T}{\omega_{Me}} \sim 1$.

Toroidal ETG modes location

Magnetic drifts + FLR effects determine location of toroidal ETG turbulence

- Regions where magnetic drifts satisfy $\omega_{*e}^T/\omega_{ke} \simeq 8$ have the highest growth rate for a wide range of parallel and perpendicular wavenumbers.

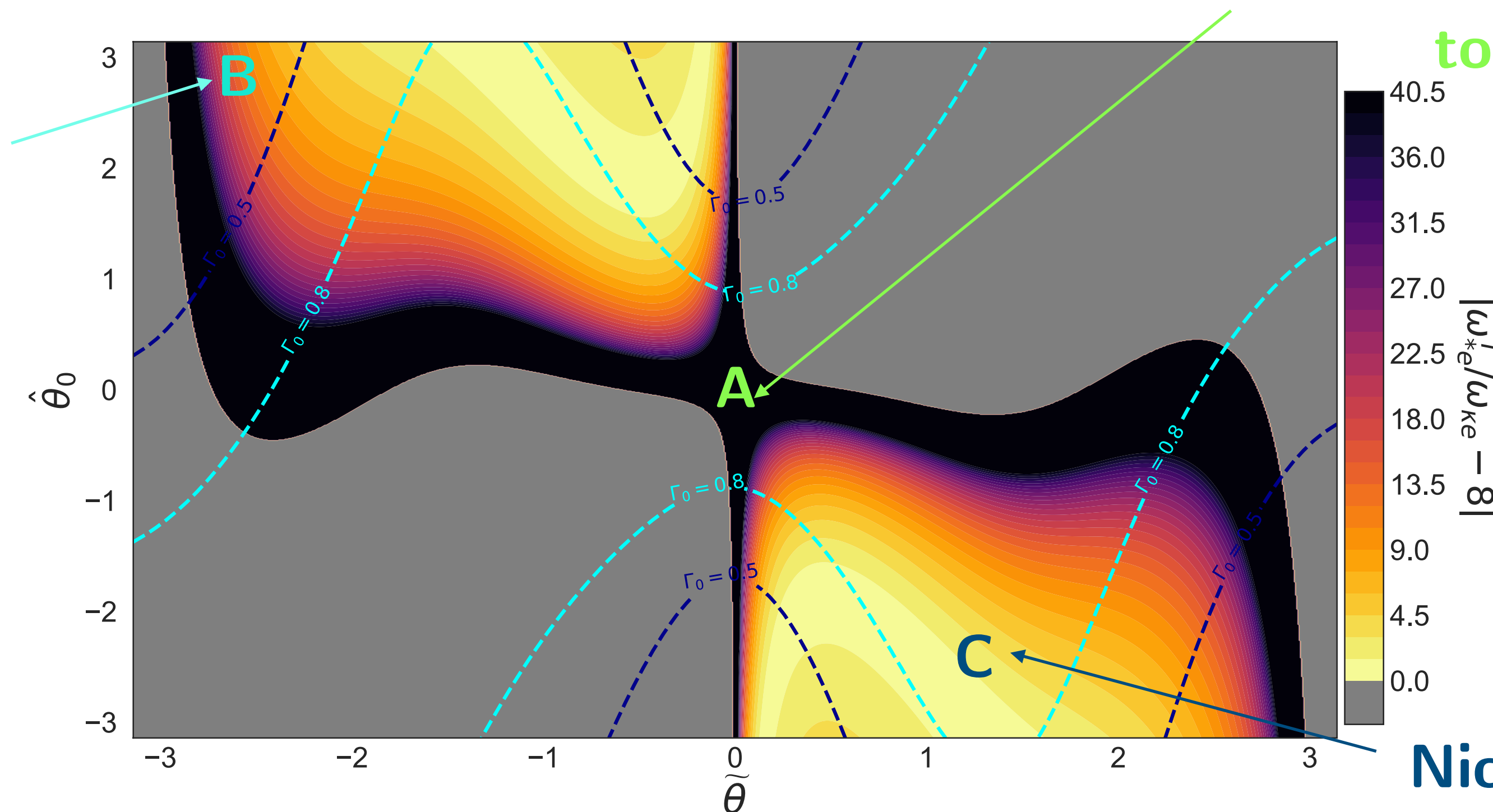


Nonlinear pedestal physics

Magnetic drifts + FLR effects determine location of toroidal ETG turbulence

- Regions where magnetic drifts satisfy $\omega_{*e}^T/\omega_{ke} \simeq 8$ have the highest growth rate.
- $|\partial_\theta(\omega_{*e}^T/\omega_{ke})|$ cannot be too large, otherwise k_{\parallel} too large and kills instability.
- FLR effects cannot be too strong.

FLR unfavorable,
and magnetic drifts
too slow + steep.



FLR favorable, but magnetic drifts
too slow + steep.

$|\omega_{*e}^T/\omega_{ke} - 8|$ versus θ and $\hat{\theta}_0$ with Γ_0 contours with $k_y \rho_i$ fixed.

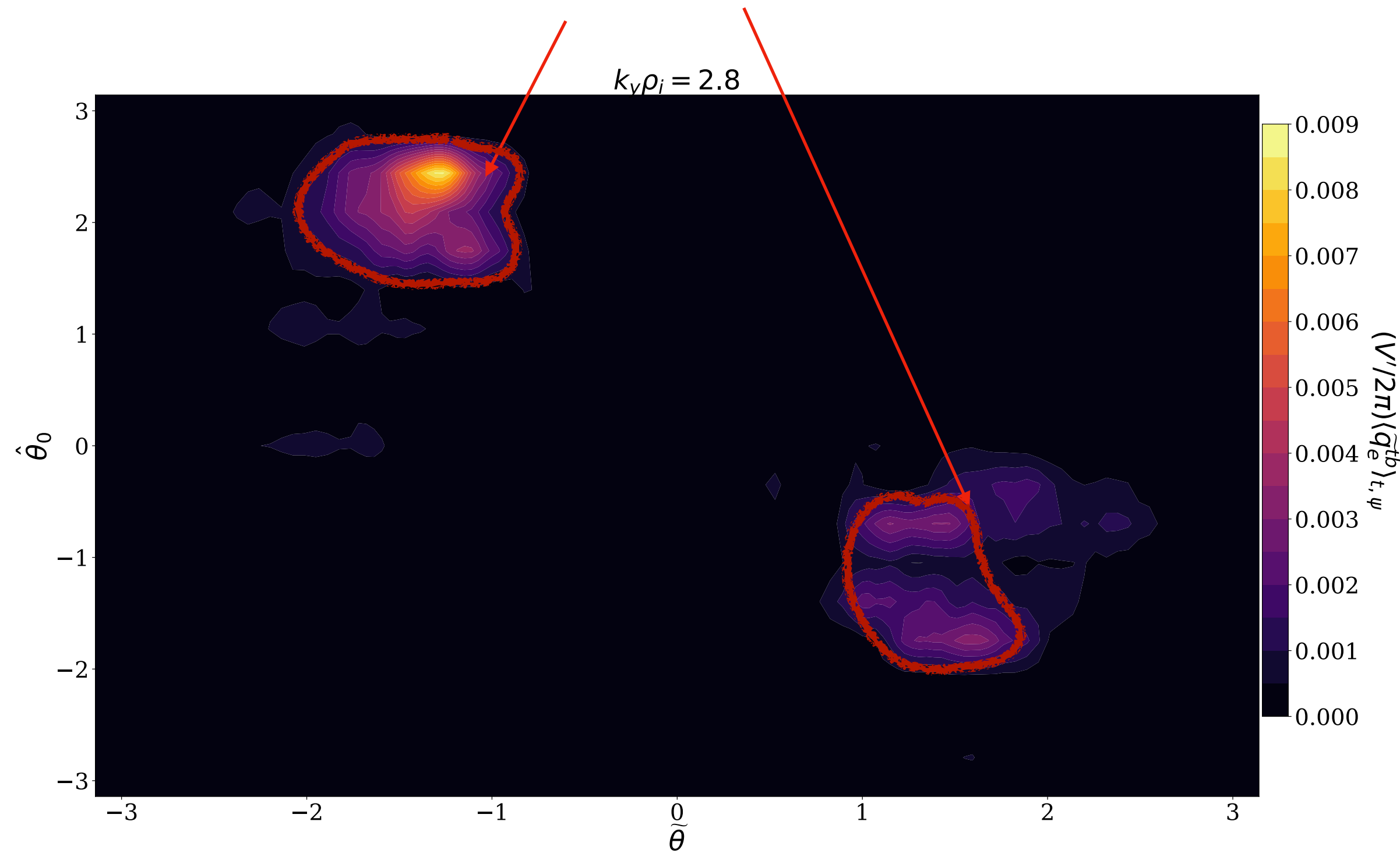
Nice region for toroidal
ETG turbulence!

Nonlinear pedestal physics

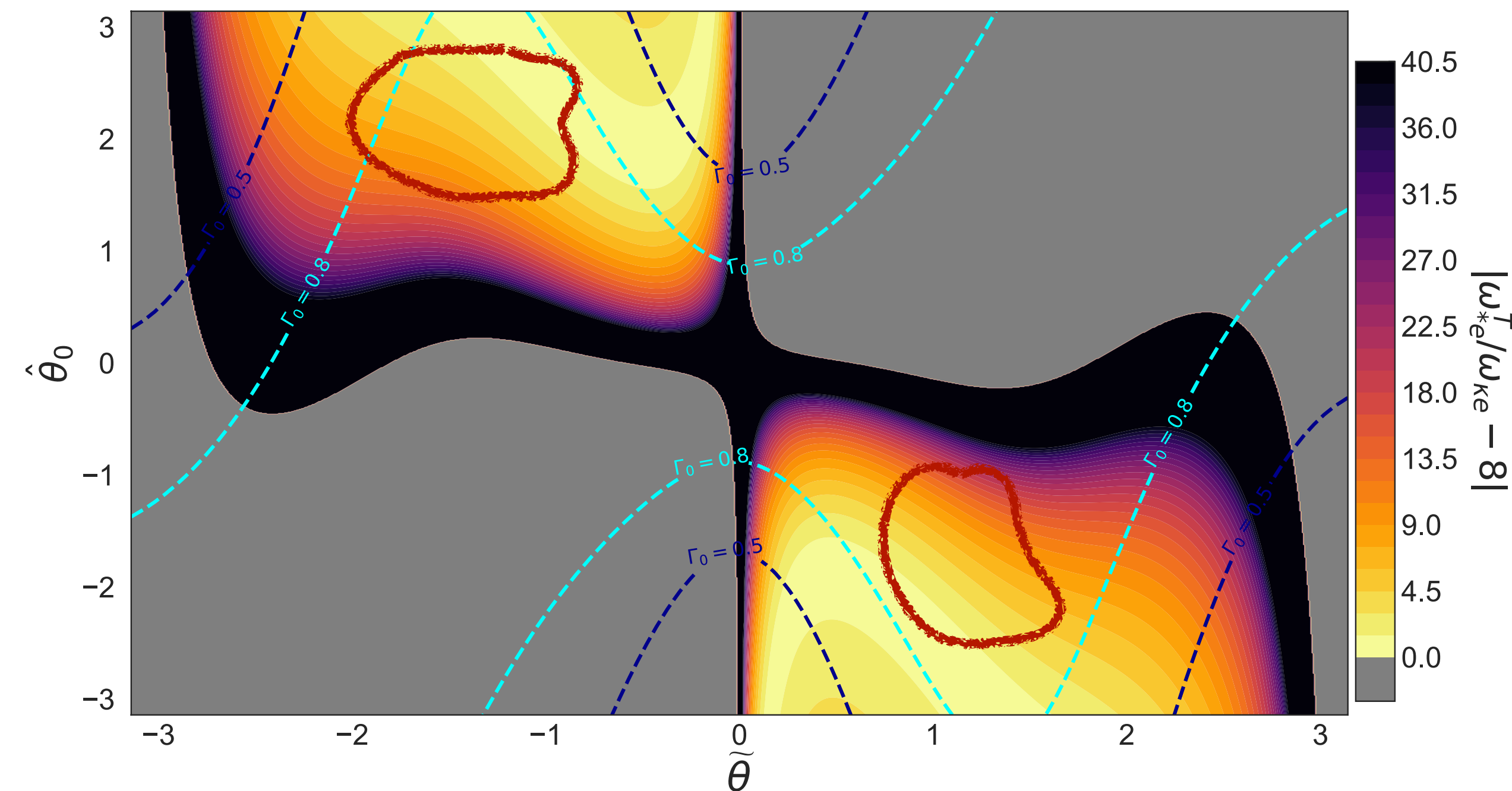
Magnetic drifts + FLR effects determine location of toroidal ETG turbulence

- Predictions supported by simulations.

Toroidal ETG modes



Heat flux versus θ and θ_0 .



$|\omega_{*e} n_e / \omega_{ke} - 8|$ versus θ and θ_0 with Γ_0 contours.

Section Summary

- Nonlinear simulations in steep temperature gradient regions are hard.
- One has to wait long enough to allow the slower modes to saturate.
- One can distinguish between toroidal and slab ETG modes by comparing the fluctuations with the topography of $\omega_{*e}^T/\omega_{ke}$ and Γ_0 .

Stellarator physics

Stellarator Physics

Toroidal ETG at $a/R \ll 1$

- Application of toroidal ETG modes to low aspect ratio devices such as stellarators.
- Recall that toroidal ETG modes in tokamak pedestal required $R/L_{Te} \gg 1$. In stellarator, we can make R/L_{Te} large by having R relatively large because $a/R \ll 1$, even if $a/L_{Te} \sim 1$:

$$\frac{\omega_{*e}^T}{\omega_{ke}} \sim \frac{k_y R}{k_{\perp} L_{Te}} \sim \frac{k_y a}{k_{\perp} L_{Te}} \frac{1}{\epsilon} \sim 1,$$

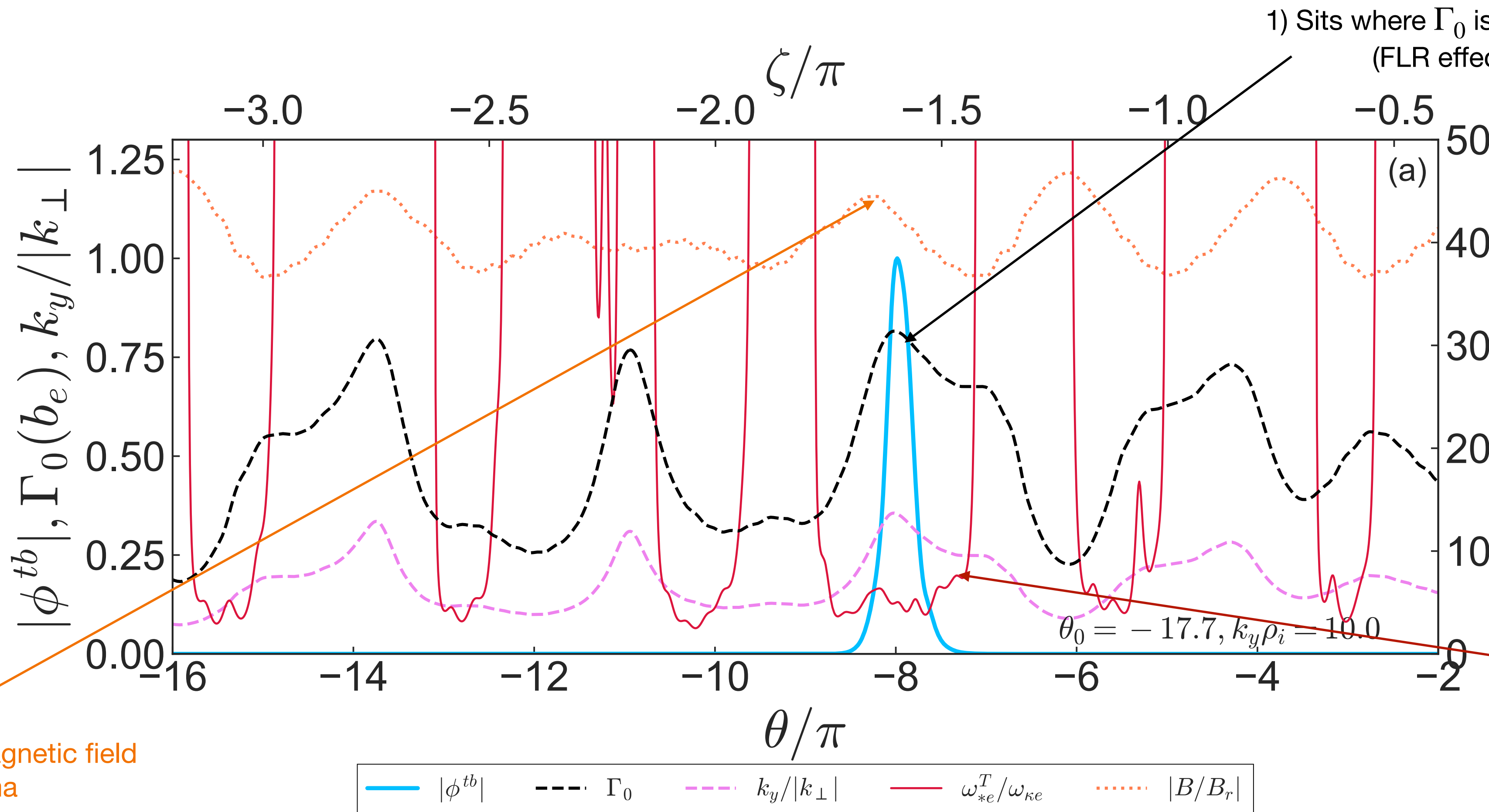
and hence we find the toroidal ETG modes with $k_{\perp} \gg k_y$.

5) Kinetic and adiabatic ions makes no difference (which it would for TEM).

Linear simulations

Toroidal ETG modes in W7-X

- How do we know these are toroidal ETG modes?



1) Sites where Γ_0 is close to a local maximum (FLR effects not too strong)

2) Mode location not magnetic field strength minima

3) the quantity $\omega_{*e}^T/\omega_{ke} \simeq 5$.

AND

4) the region $\omega_{*e}^T/\omega_{ke}$ is sufficiently wide such that $k_{||}$ is not too big (otherwise the mode is damped!)

Discussion

Discussion

- Steep temperature gradients cause ITG and ETG to span a wider range of perpendicular and parallel scales.
- Makes nonlinear gyrokinetic simulations much more challenging than in the core.
- Nonlinear gyrokinetic simulations need to be run for sufficiently long to capture slowest growing modes in box, which modify transport at long times.
- Pedestal toroidal ETG is not ballooning; tends to reside at poloidal cross section top/bottom.

Future Work

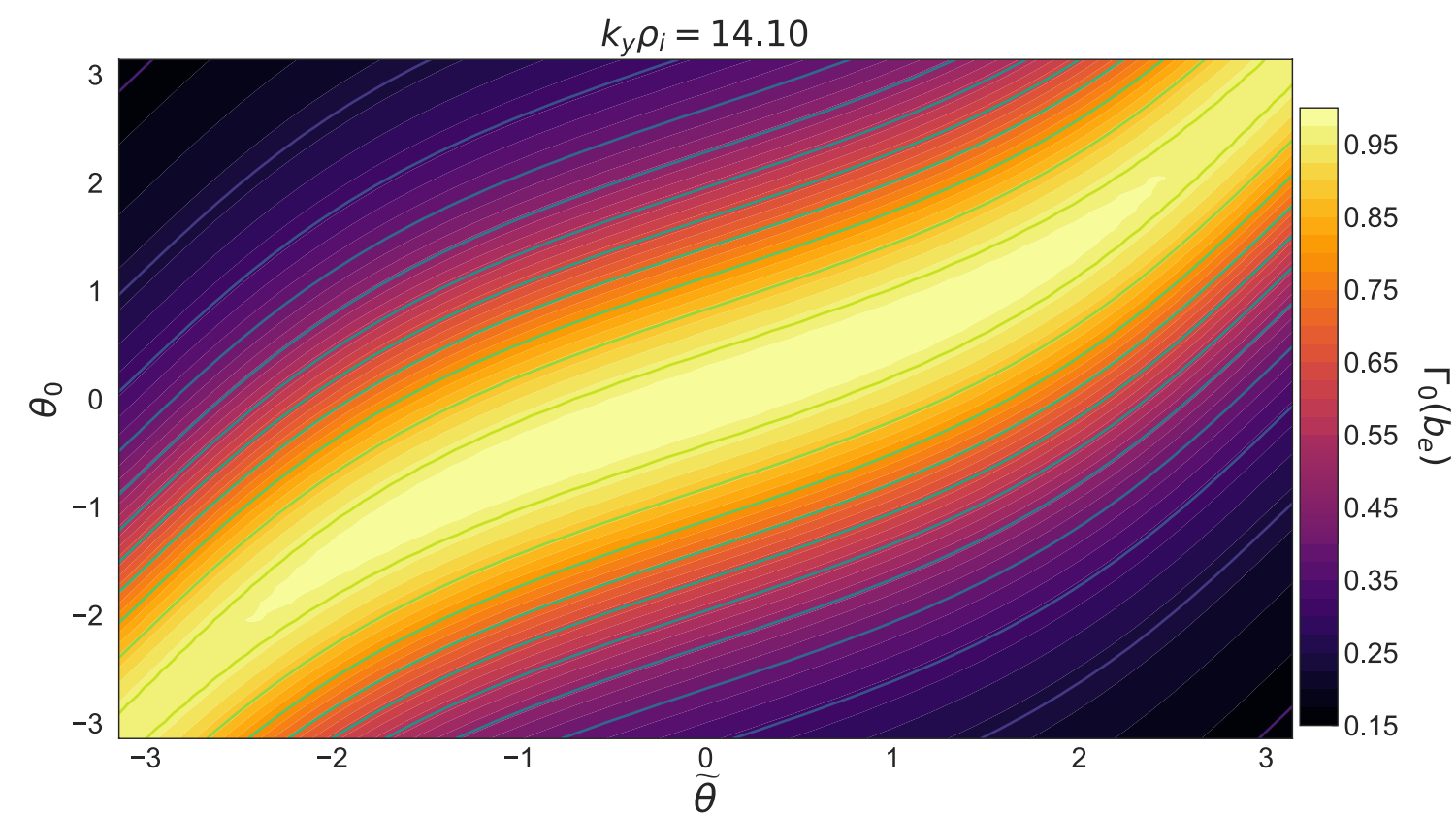
Some future research directions

- Investigate role of shaping in pedestal transport:
Can we use different magnetic geometries to optimize turbulent transport in the pedestal? (from the perspective of magnetic drifts and FLR effects)
- Experimentally, search for fluctuation amplitudes at pedestal cross section top/bottom.
- Scrape off layer / divertor physics: is non-ballooning pedestal turbulence problematic?
- How much do electromagnetic effects change the picture?

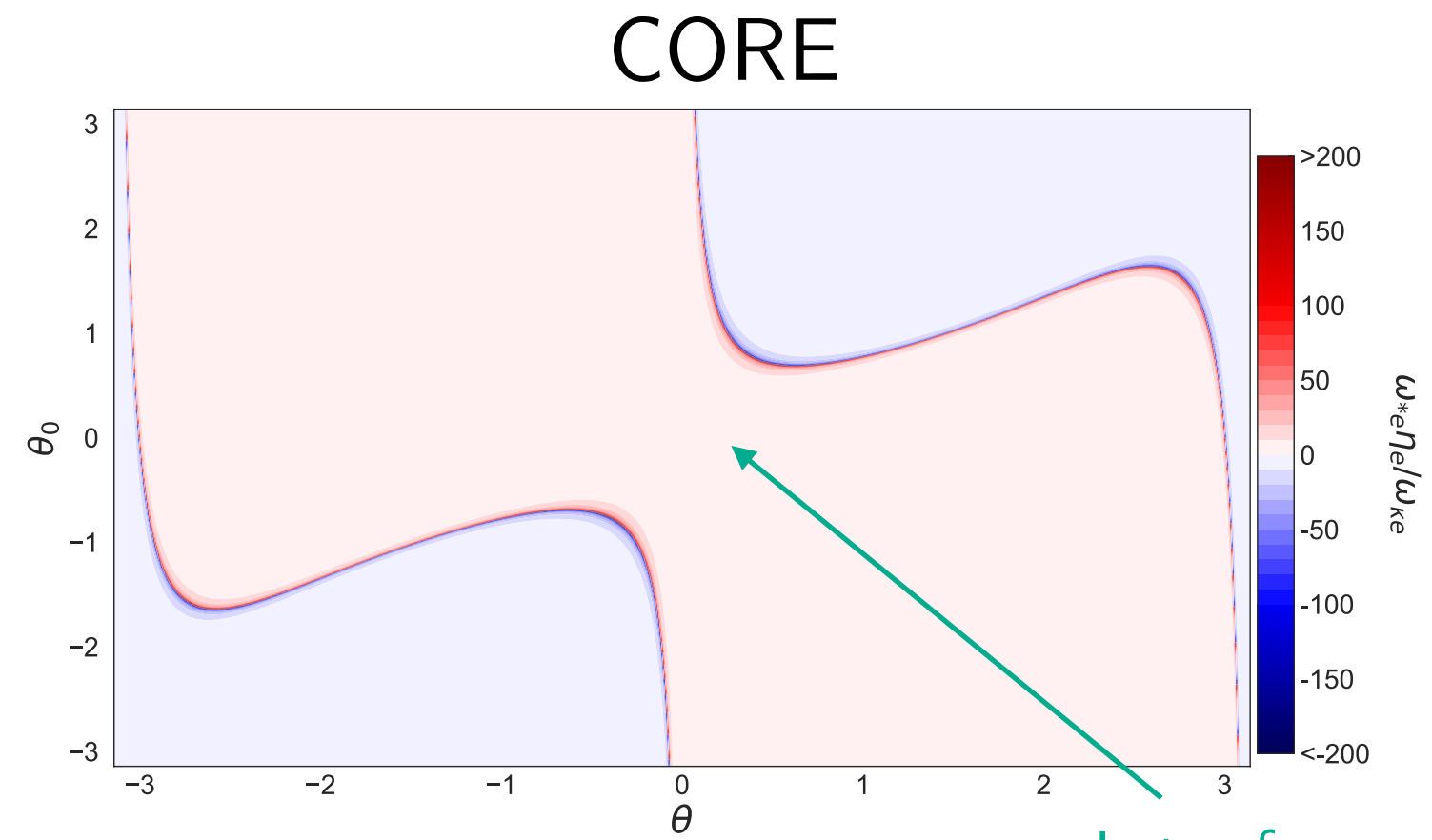
Backup slides

Nonlinear pedestal physics

What's new? Why don't we see this turbulence in the core?

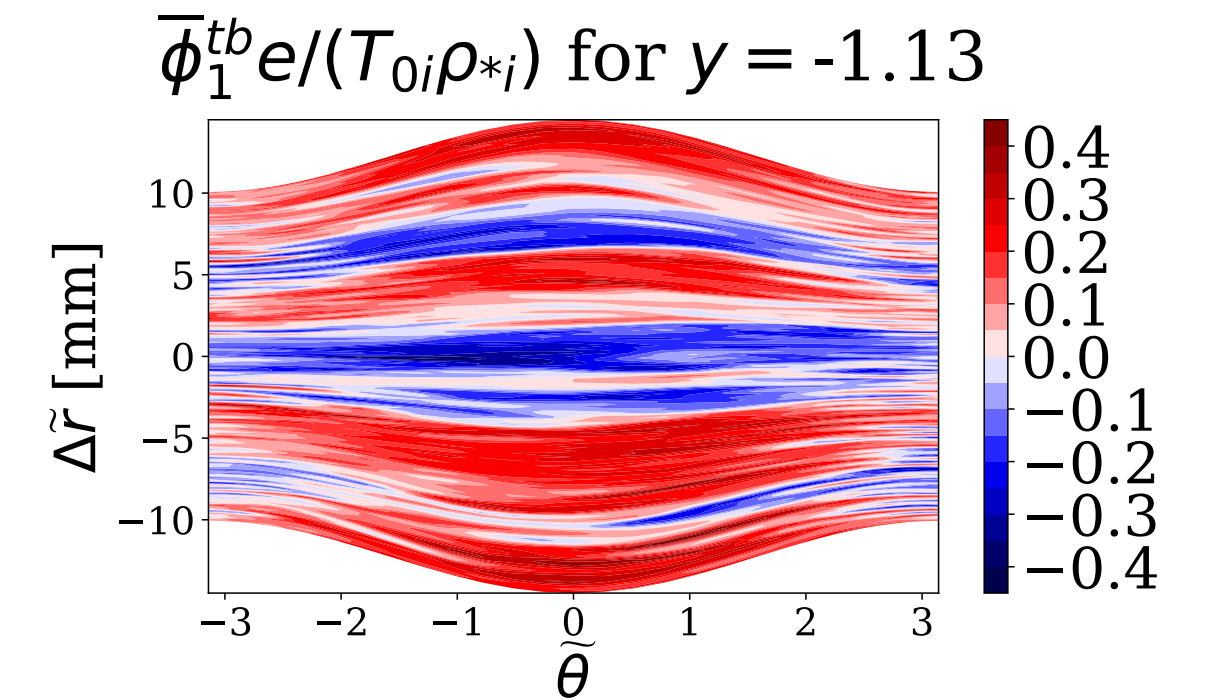


a) FLR Effects

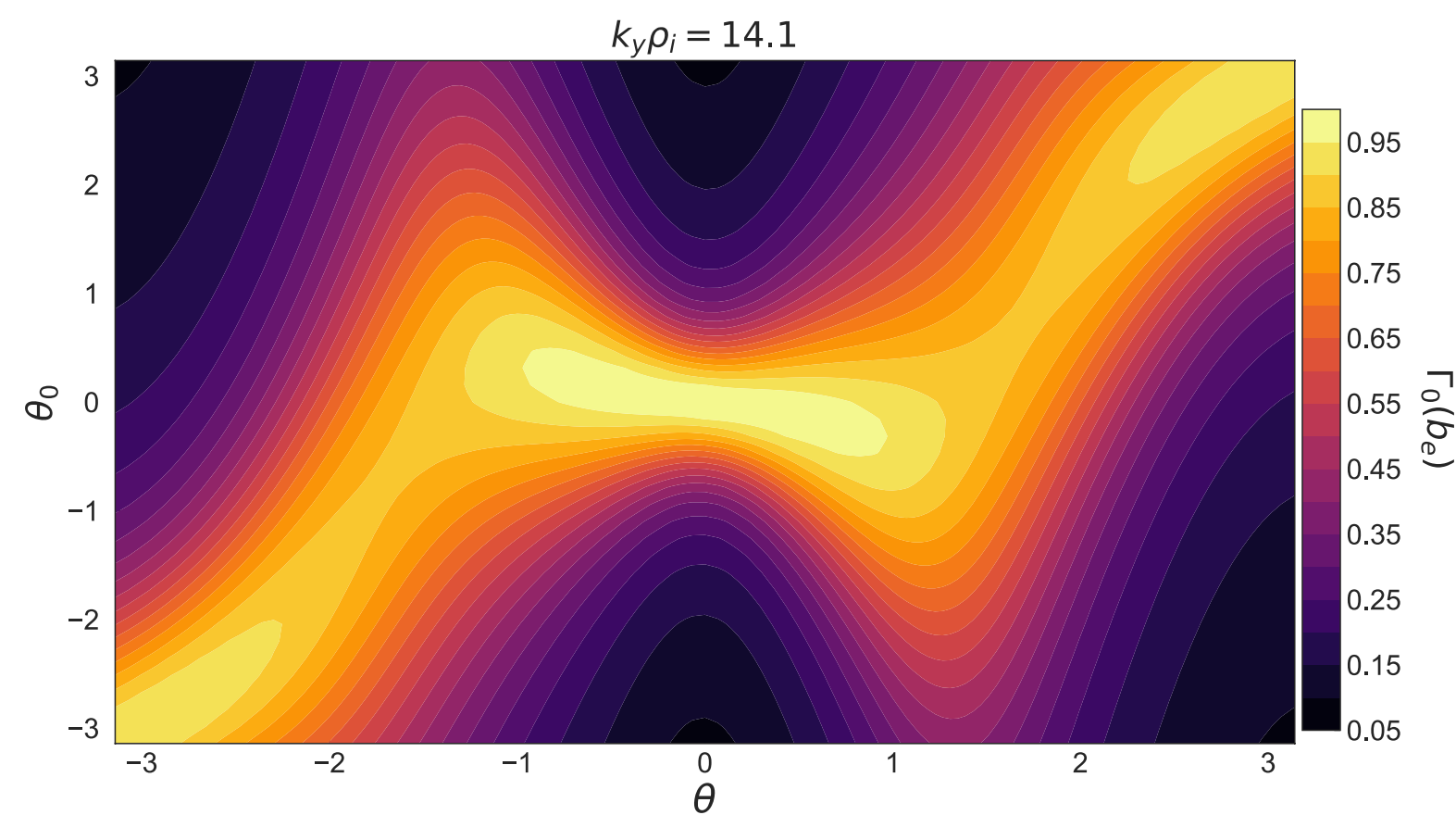


b) Magnetic drifts

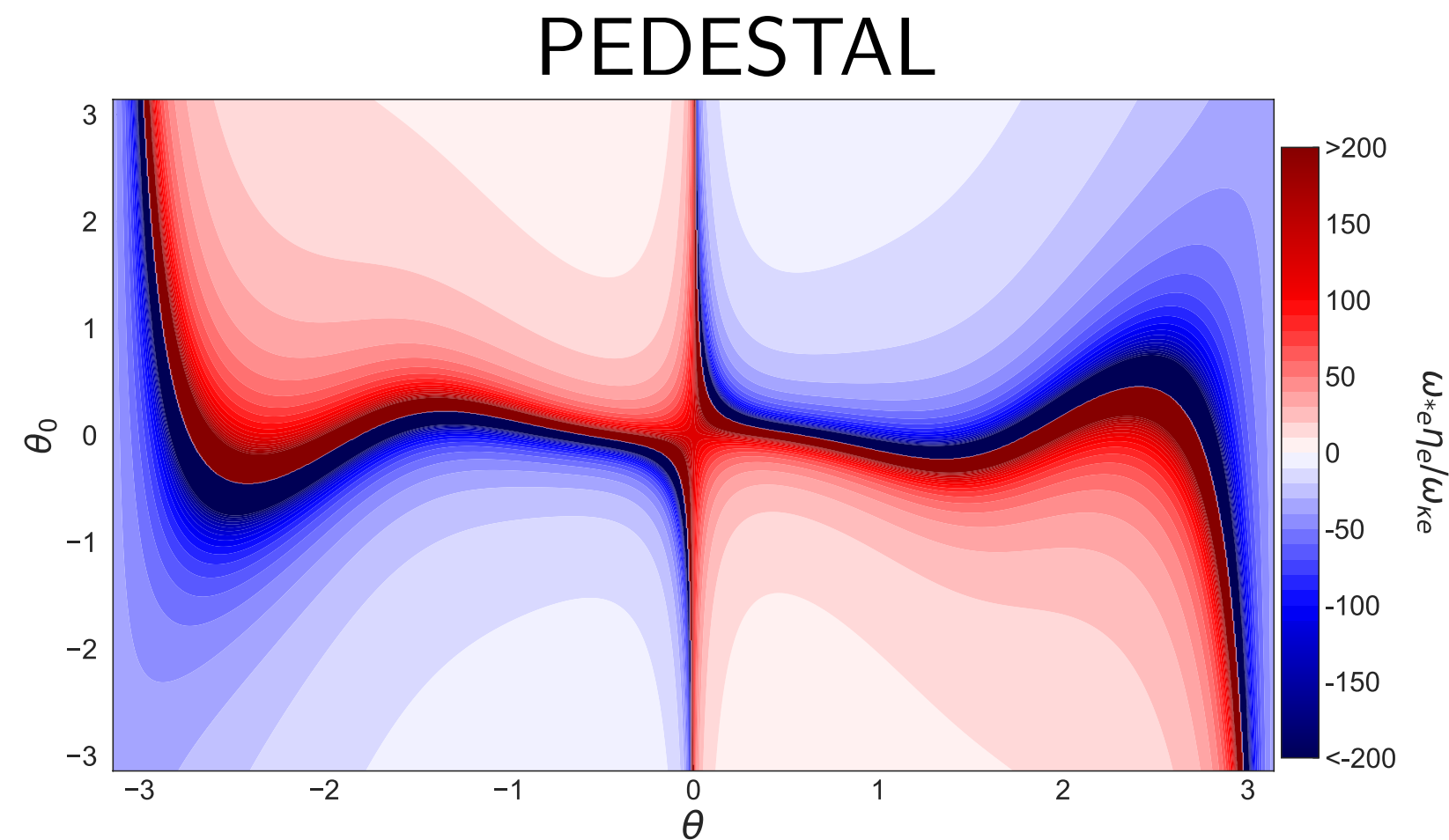
Lots of space for toroidal
ETG instability



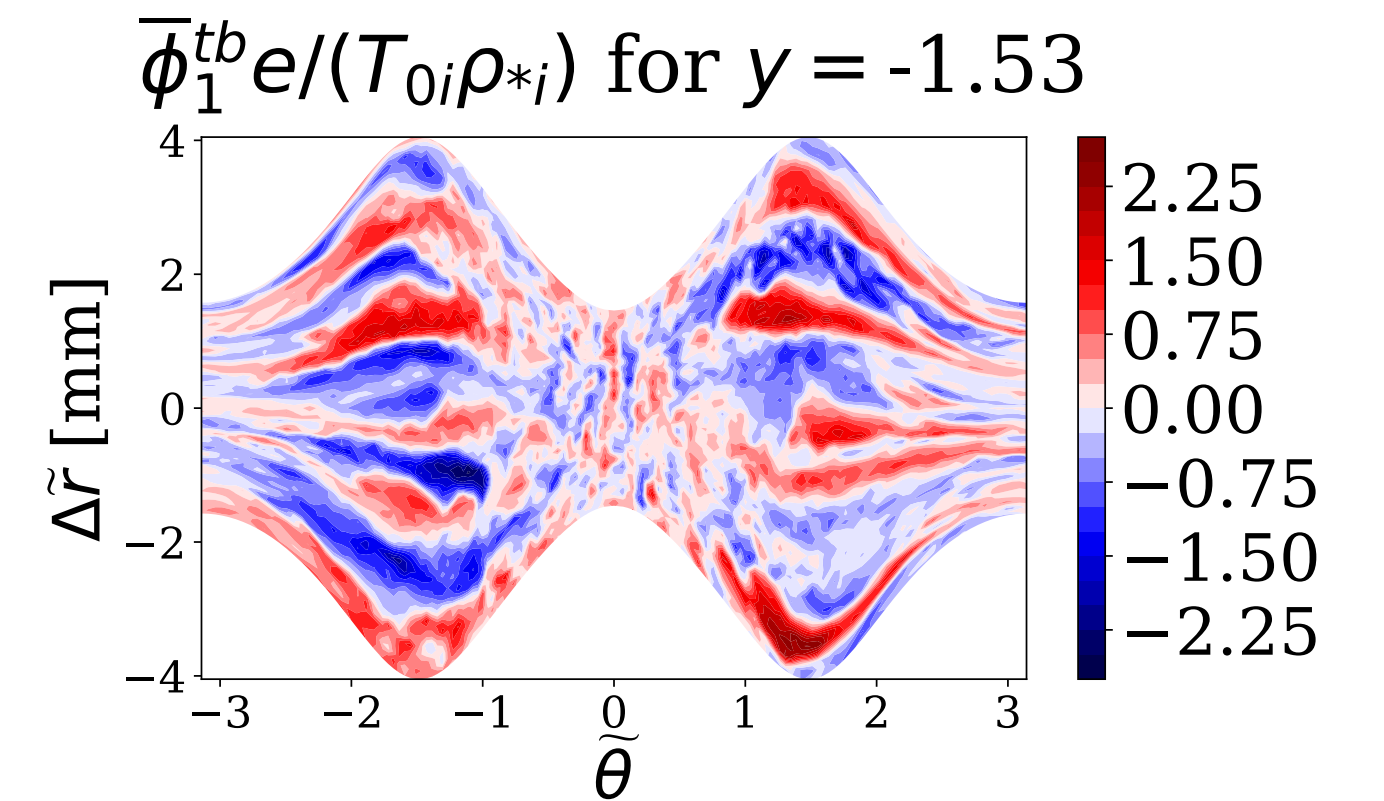
c) Radial and poloidal turbulence



d) FLR Effects



e) Magnetic drifts



f) Radial and poloidal turbulence

- Core: favorable Γ_0 and $\omega_{*e} \eta_e / \omega_{ke}$ align. Pedestal: separated!

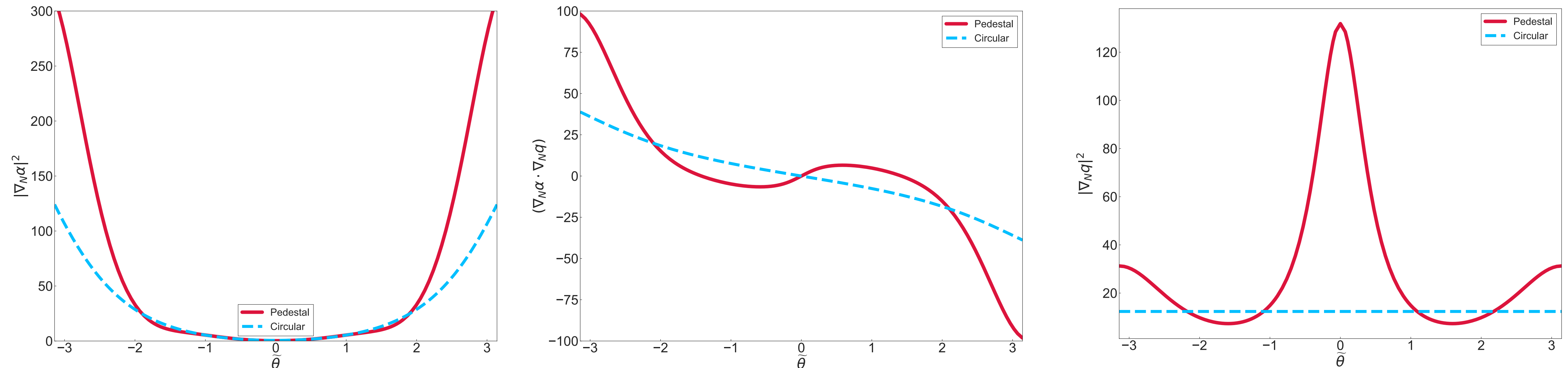
Nonlinear pedestal physics

Flux expansion and local magnetic shear mostly responsible for turbulent ‘confinement’

- The local magnetic shear and flux surface expansion localize turbulence in the pedestal. The perpendicular wavenumber can be written as

$$|k_{\perp}|^2 = k_y^2 \left| g_2 + 2\hat{\theta}_0 g_{21} + \hat{\theta}_0^2 g_{22} \right|,$$

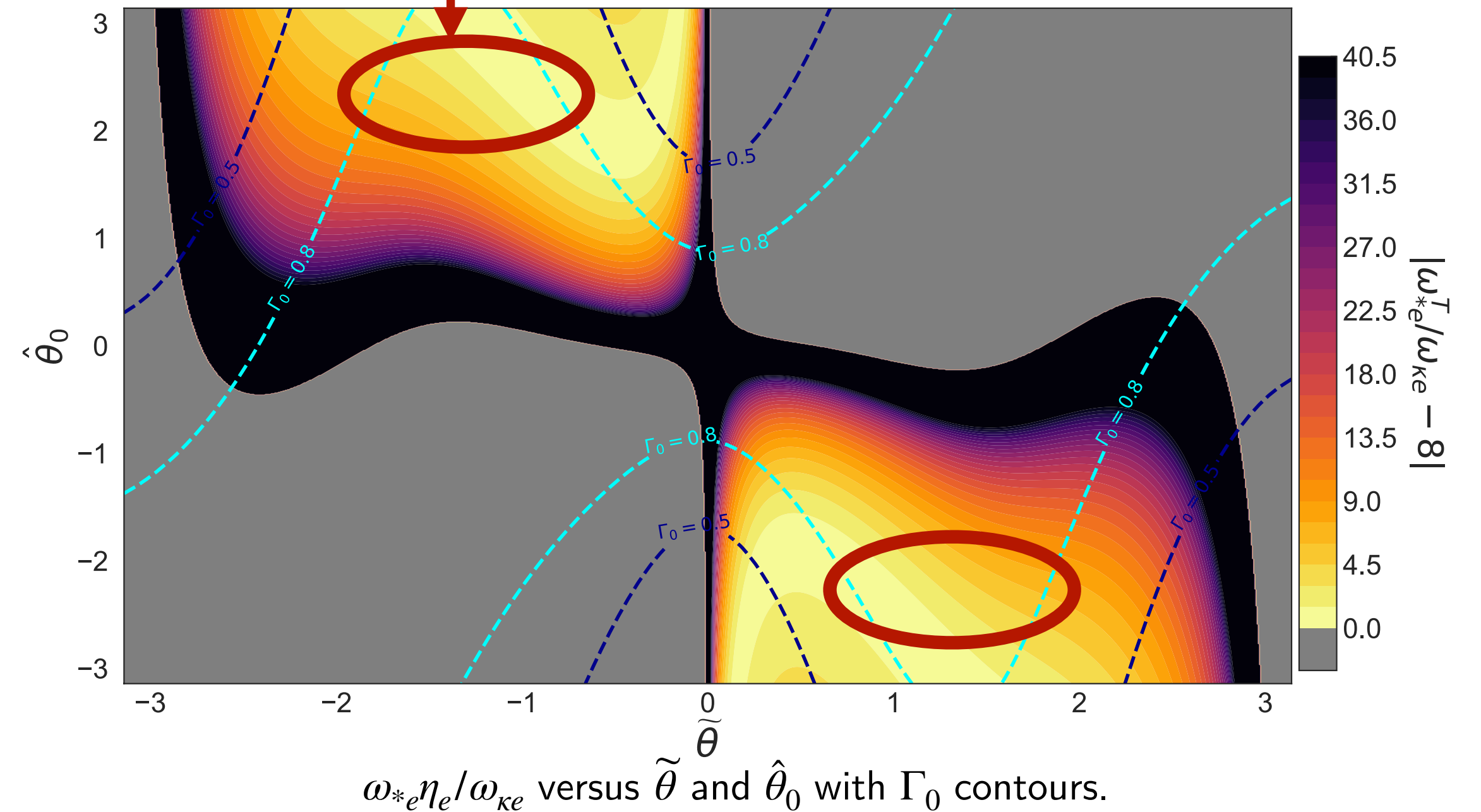
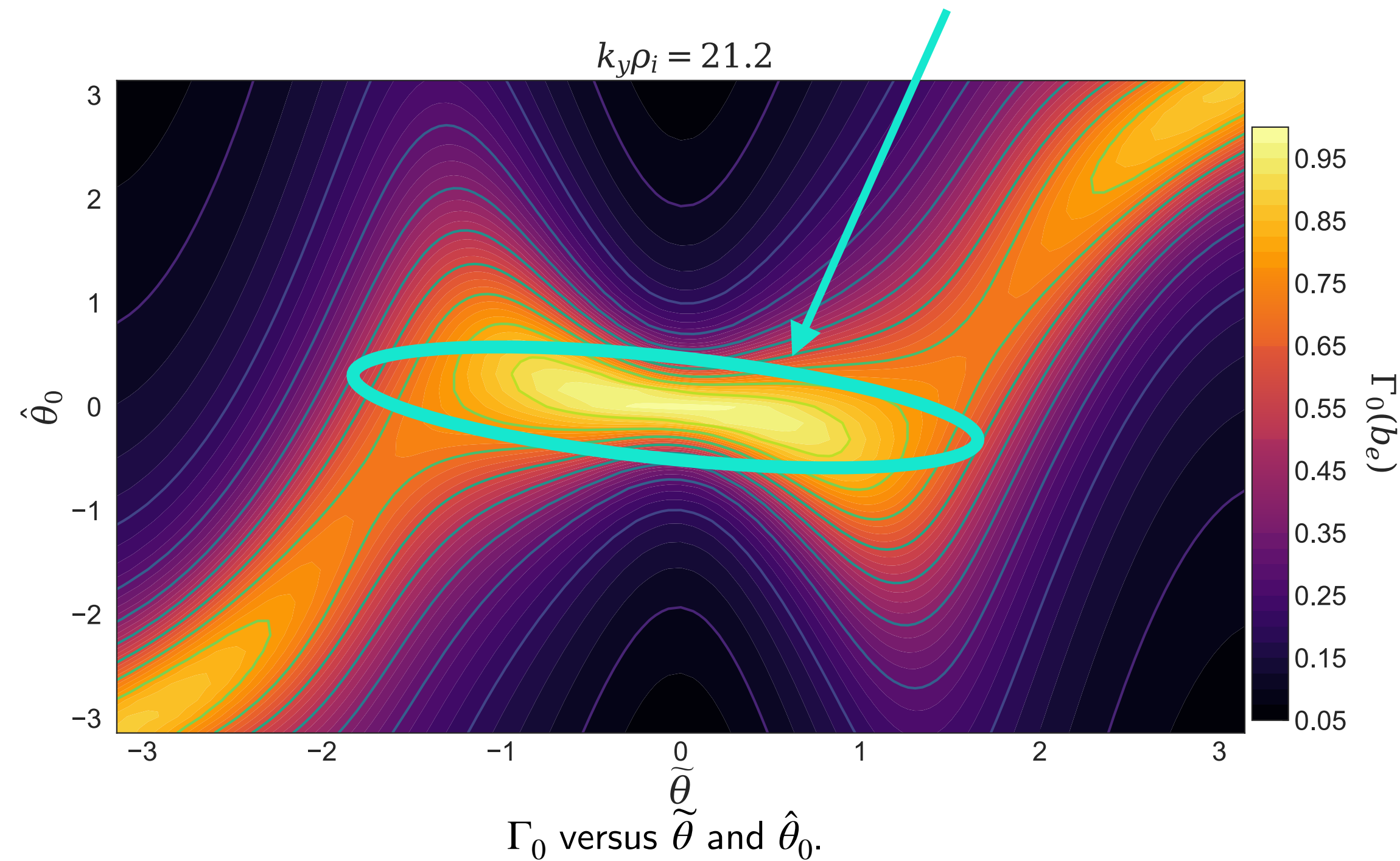
where $g_2 = |\nabla_N \alpha|^2$ (field line distance), $g_{21} = \nabla_N \alpha \cdot \nabla_N q$ (\sim local magnetic shear), $g_{22} = |\nabla_N q|^2$ (flux surface expansion).



Nonlinear pedestal physics

Summary: slab and toroidal modes live in different poloidal locations.

- Magnetic drifts too slow at $\theta = \theta_0 = 0$, so **toroidal ETG modes** move away from $\theta = \theta_0 = 0$, whereas **slab ETG modes** tend to abhor k_{\perp} so live where k_{\perp} is smallest.

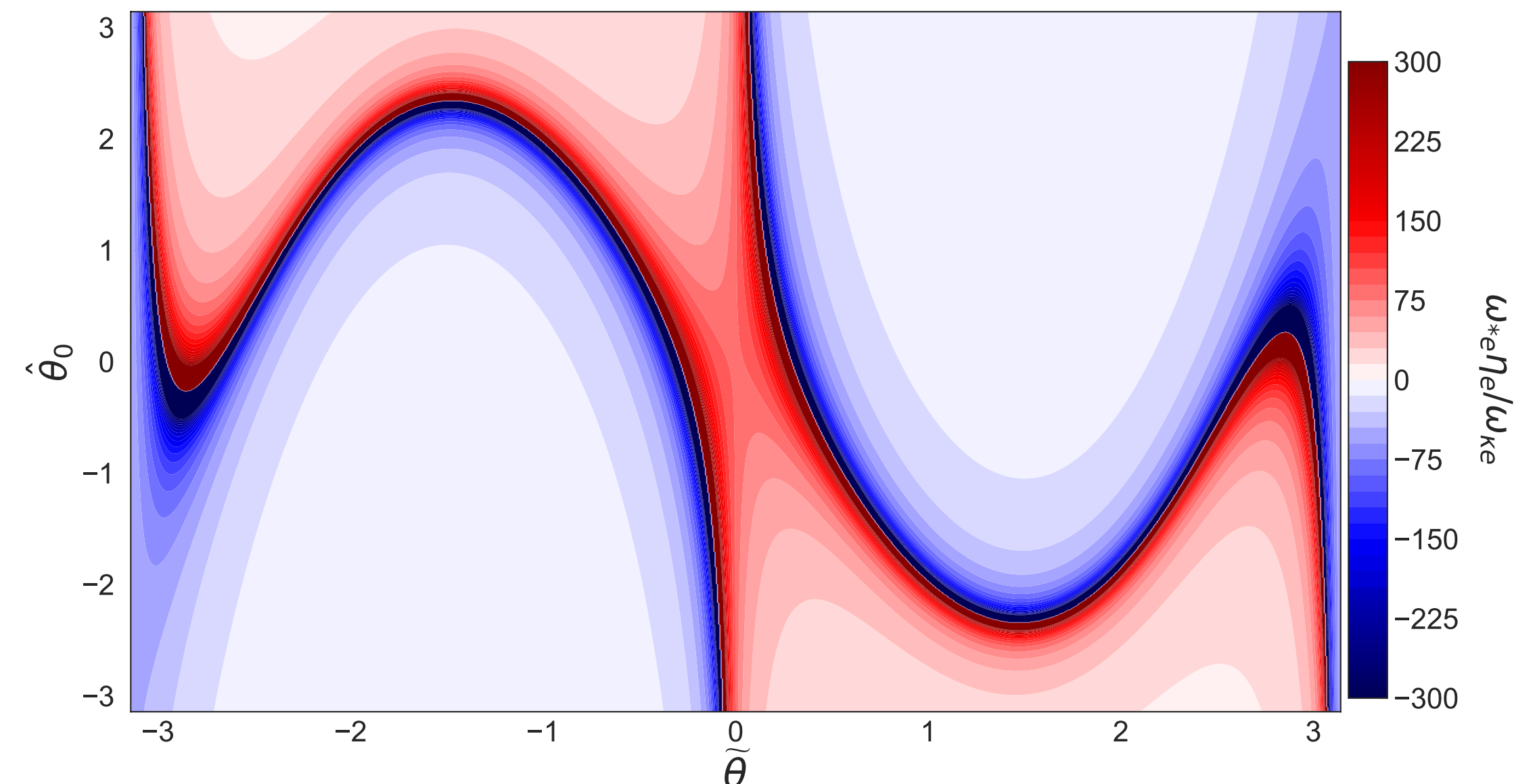
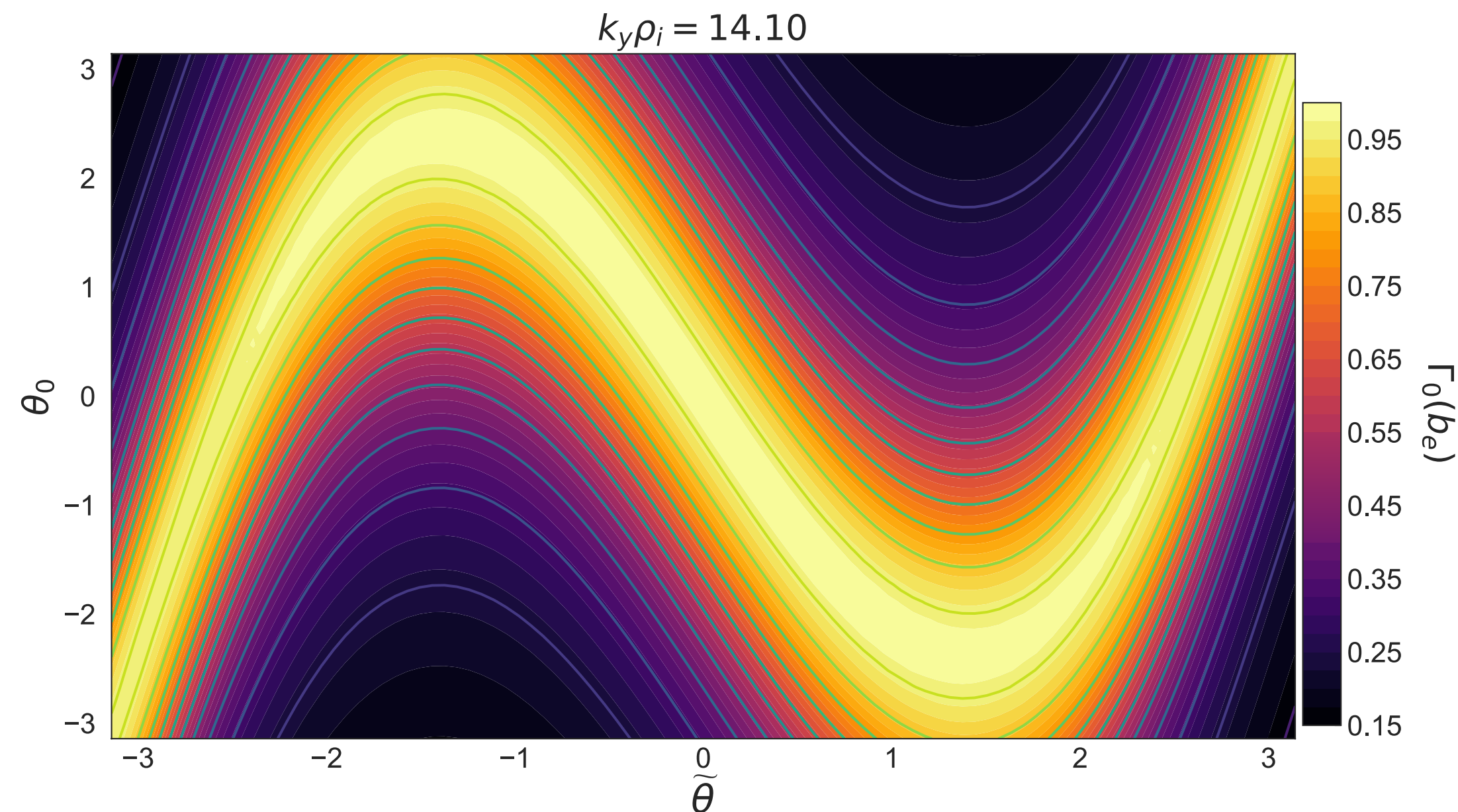


- Flux surface expansion and local magnetic shear responsible the shaping that keeps slab ETG turbulence at the outboard midplane.

Nonlinear pedestal physics

Changing the $\tilde{\theta}$ location of slab and toroidal modes (pedestal-scaping)

- Using our understanding of the geometry, can we move toroidal and slab ETG modes to different locations?
- For example, what would the turbulence look like if we had the following geometry (circle plus betaprim)?



Main idea explored in this talk

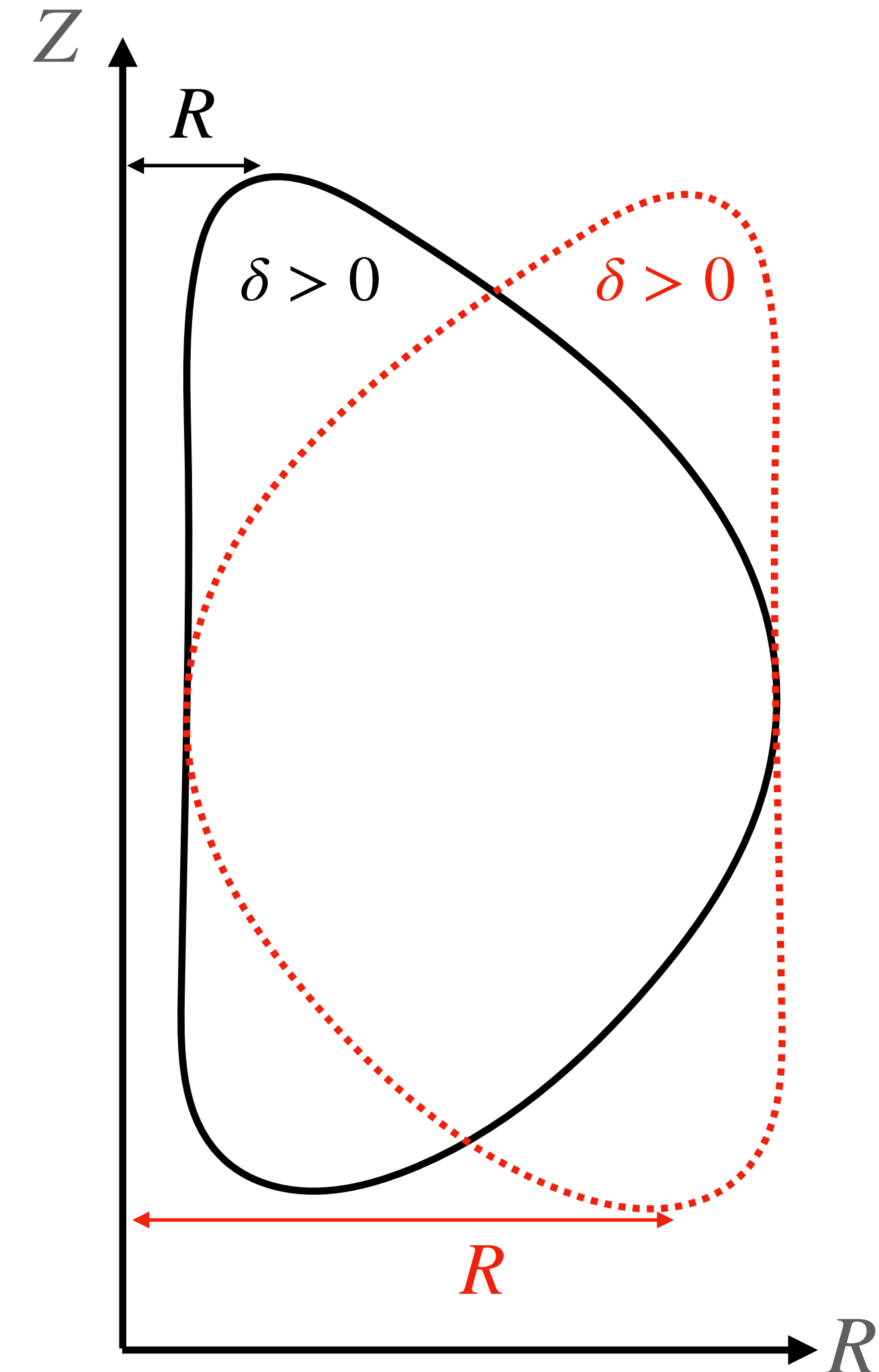
Shaping significantly changes the character of toroidal ETG mode in pedestal

- Because we require

$$\frac{\omega_{*e}^T}{\omega_{ke}} \sim \frac{k_y R}{k_{\perp} L_{Te}} \sim \frac{1}{\hat{s}\theta} \frac{R}{L_{Te}} \sim 1,$$

the distance to the mode R can significantly change the toroidal ETG physics, especially the **critical gradient** (more on this later).

- Consider a **positive triangularity** surface being deformed to a **negative triangularity** surface at tight aspect ratio (see figure). This changes R significantly!

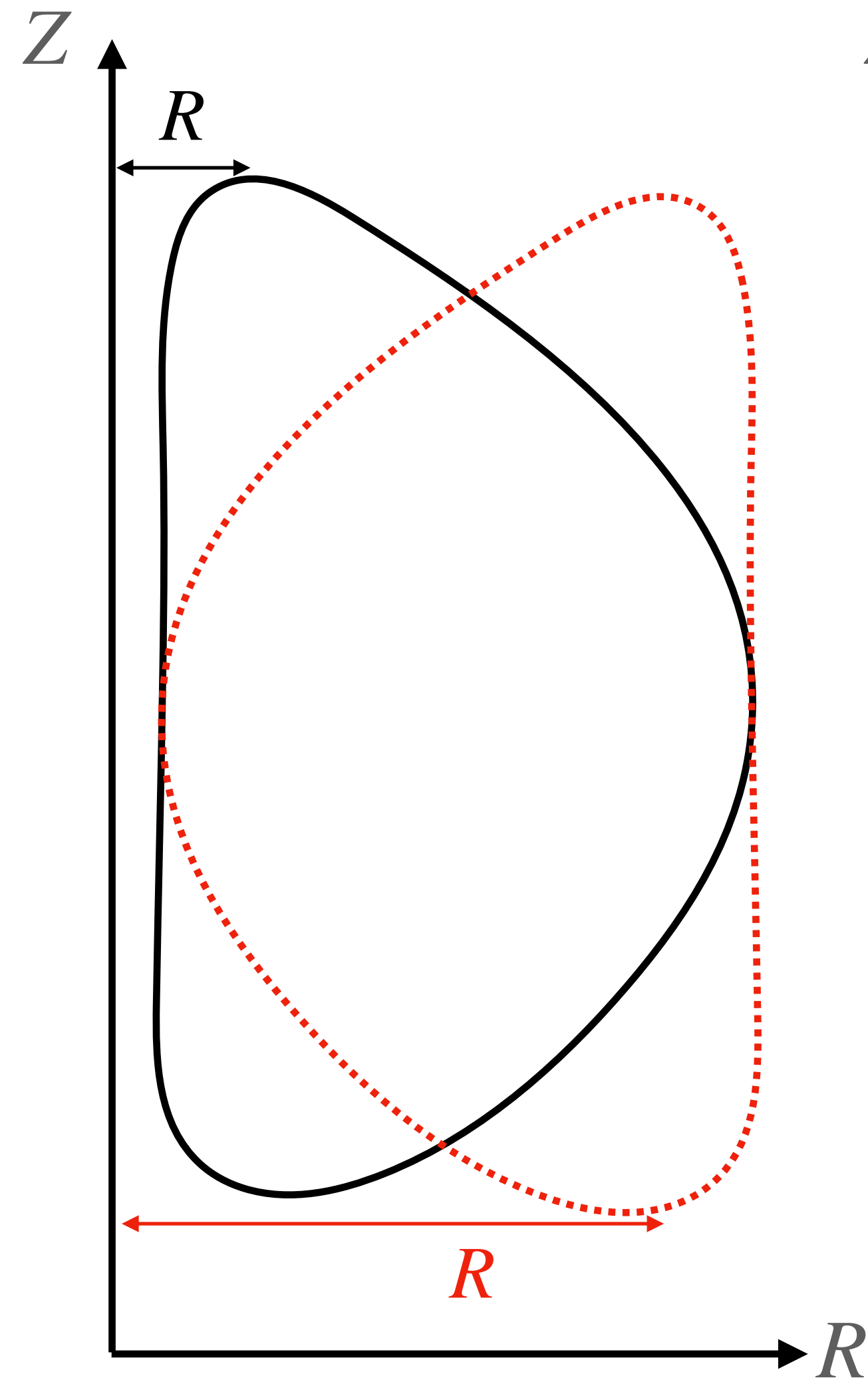


Effect of shaping on R

Shaping parameters that change R :

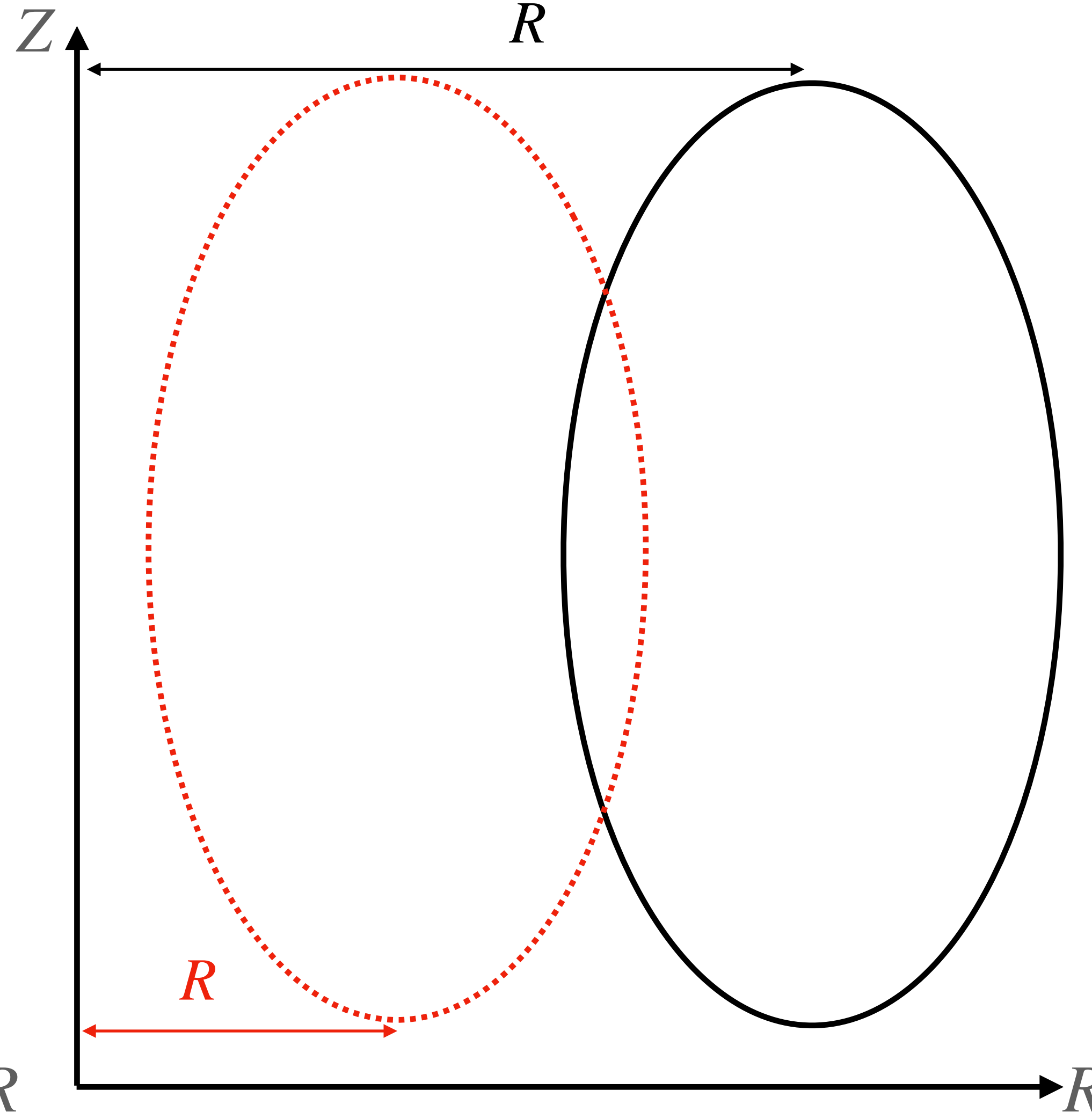
Triangularity

$$\delta \rightarrow -\delta$$



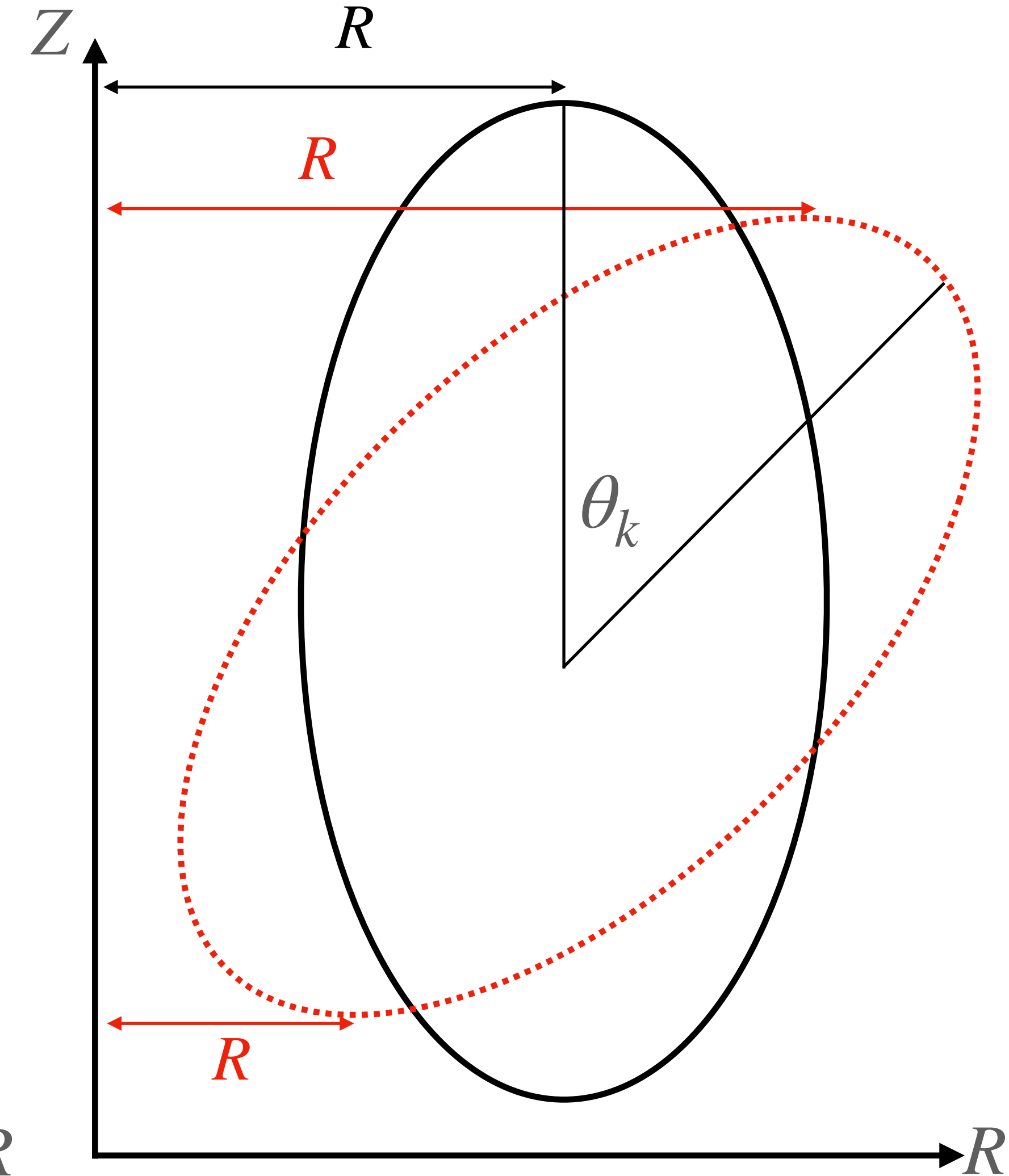
Aspect Ratio

$$\epsilon \rightarrow 3\epsilon$$



Tilt Angle

$$\theta_k = 0 \rightarrow \theta_k = \pi/4$$



Critical gradients How to stabilize toroidal ETG modes in the pedestal?

- For instability, we require $C < \frac{\omega_{*e}^T}{\omega_{ke}} < D$, where C and D are real numbers.

- Using $k_{\perp} \simeq k_y \hat{s} \theta$, we find $\frac{\omega_{*e}^T}{\omega_{ke}} \sim \frac{k_y R}{k_{\perp} L_{Te}} \sim \frac{1 R}{\hat{s} \theta L_{Te}}$ and so for instability,

$$\frac{1 R}{D L_{Te}} \frac{1}{\hat{s}} \lesssim \theta \lesssim \theta_{\max} \equiv \frac{1 R}{C L_{Te}} \frac{1}{\hat{s}} \quad (1).$$

- There might not be values of θ in an equilibrium that satisfy (1)! When this happens, the mode is stable, which is when $\theta_{\min} \simeq \theta_{\max}$, where θ_{\min} is given by the geometry. Thus, the critical gradient is given by

$$\frac{a}{L_{Te,crit}} = C \theta_{\min} \frac{a}{R} \hat{s}.$$

Critical gradients

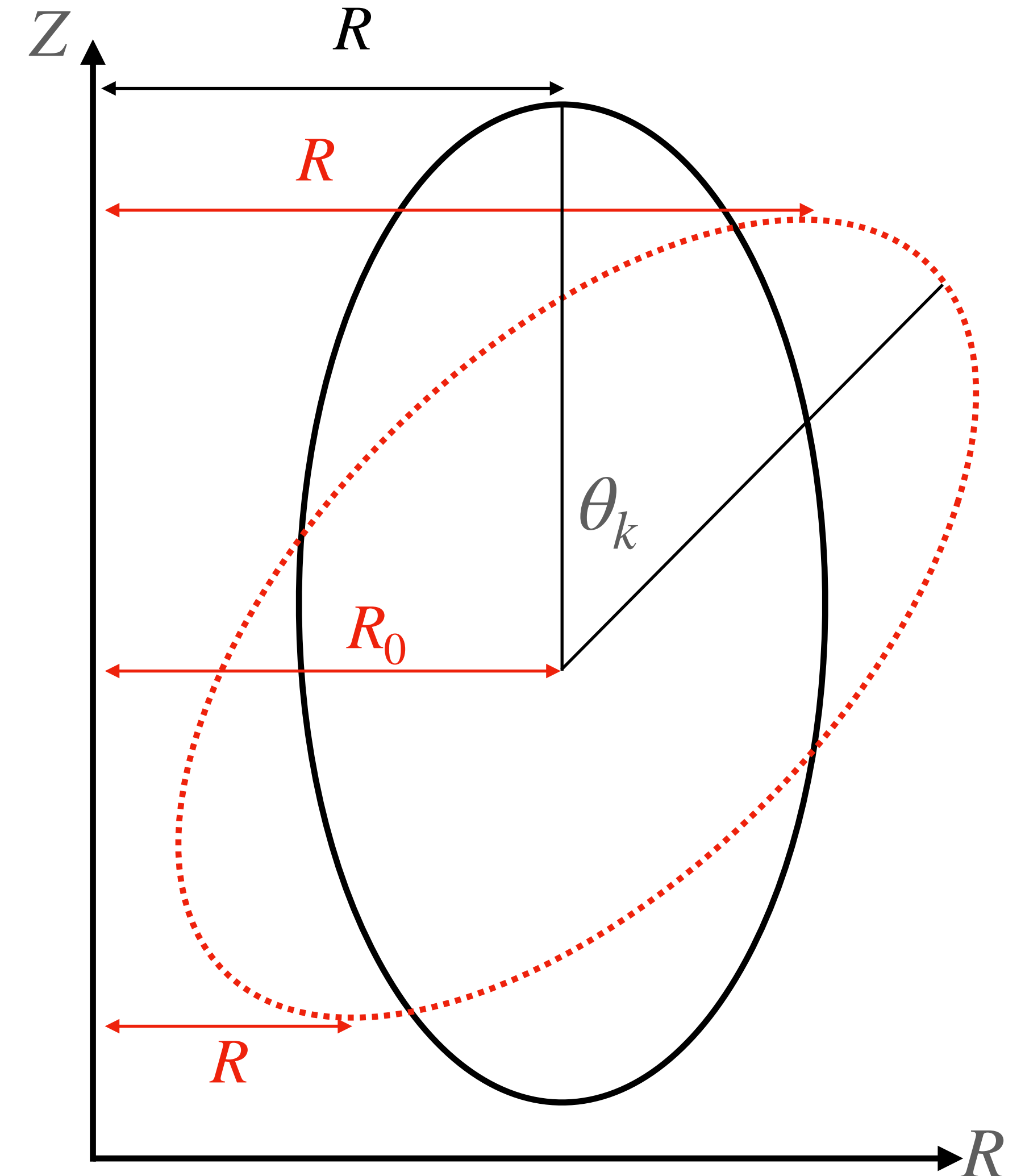
- Can play with the scaling

$$\frac{a}{L_{Te,crit}} = C\theta_{\min} \frac{a}{R} \hat{s}$$

to give scalings with triangularity, aspect ratio, tilt angle, etc. For example, with tilt angle, can write

$$R \simeq R_0 \pm \kappa a \sin \theta_k$$

Effect of tilt angle.

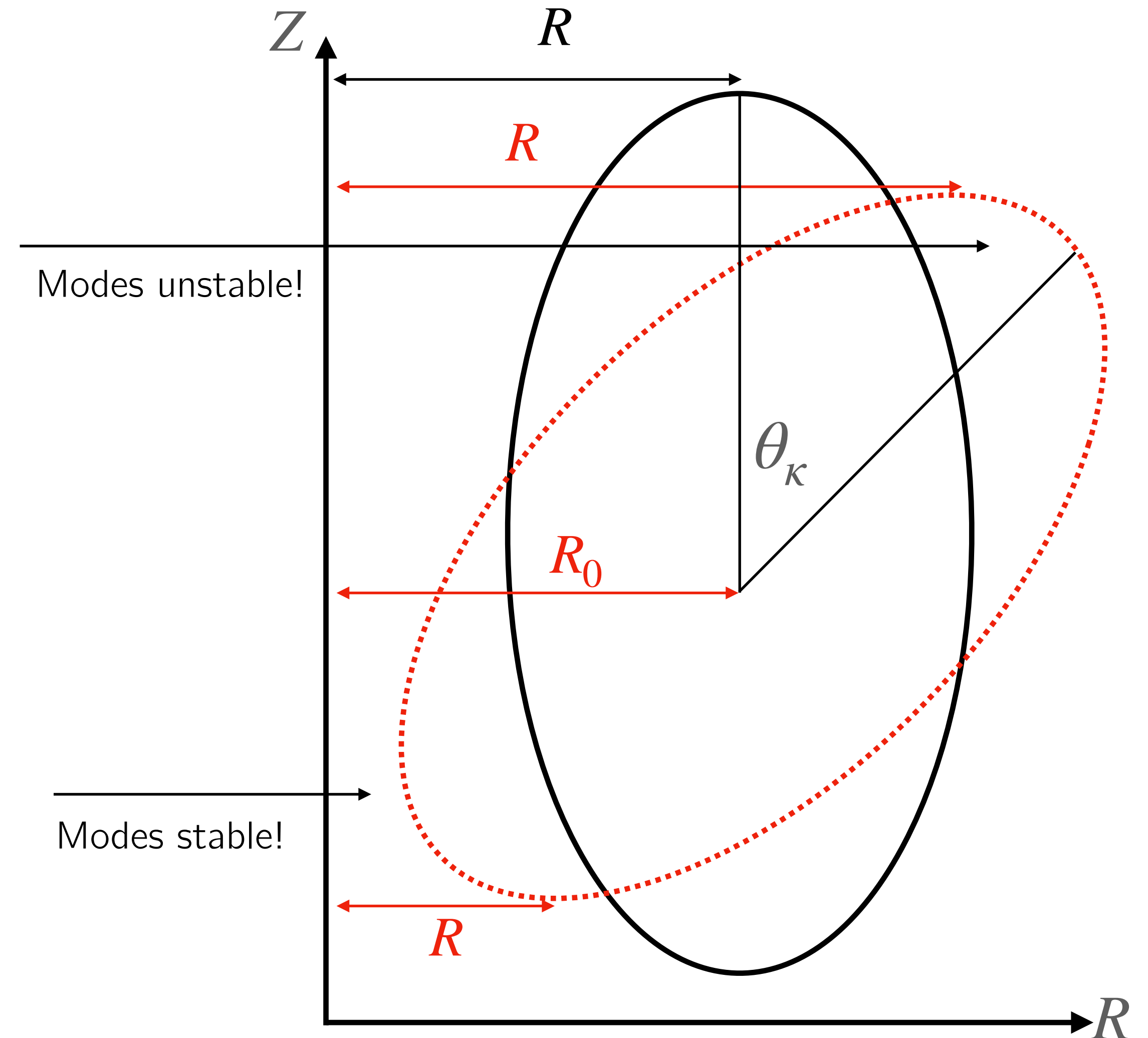


Critical gradients

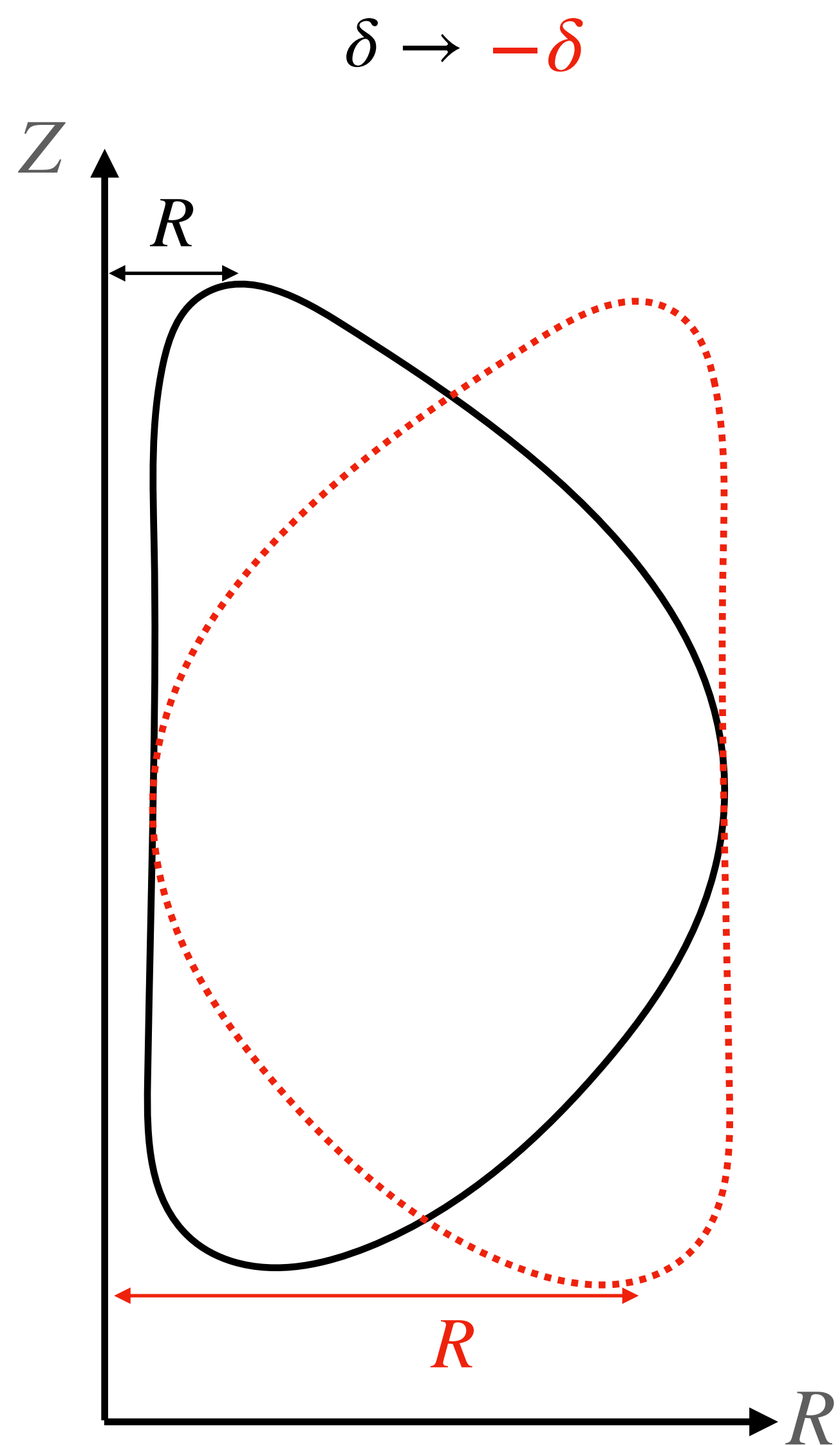
- After algebra, find

$$\frac{a}{L_{Te, \text{crit}}} \sim C \hat{s} \theta_{\min} \left(\frac{R_0}{a} \pm \kappa \sin \theta_{\kappa} \right)^{-1}$$

Effect of tilt angle.



Effect of shaping on L_B : triangularity



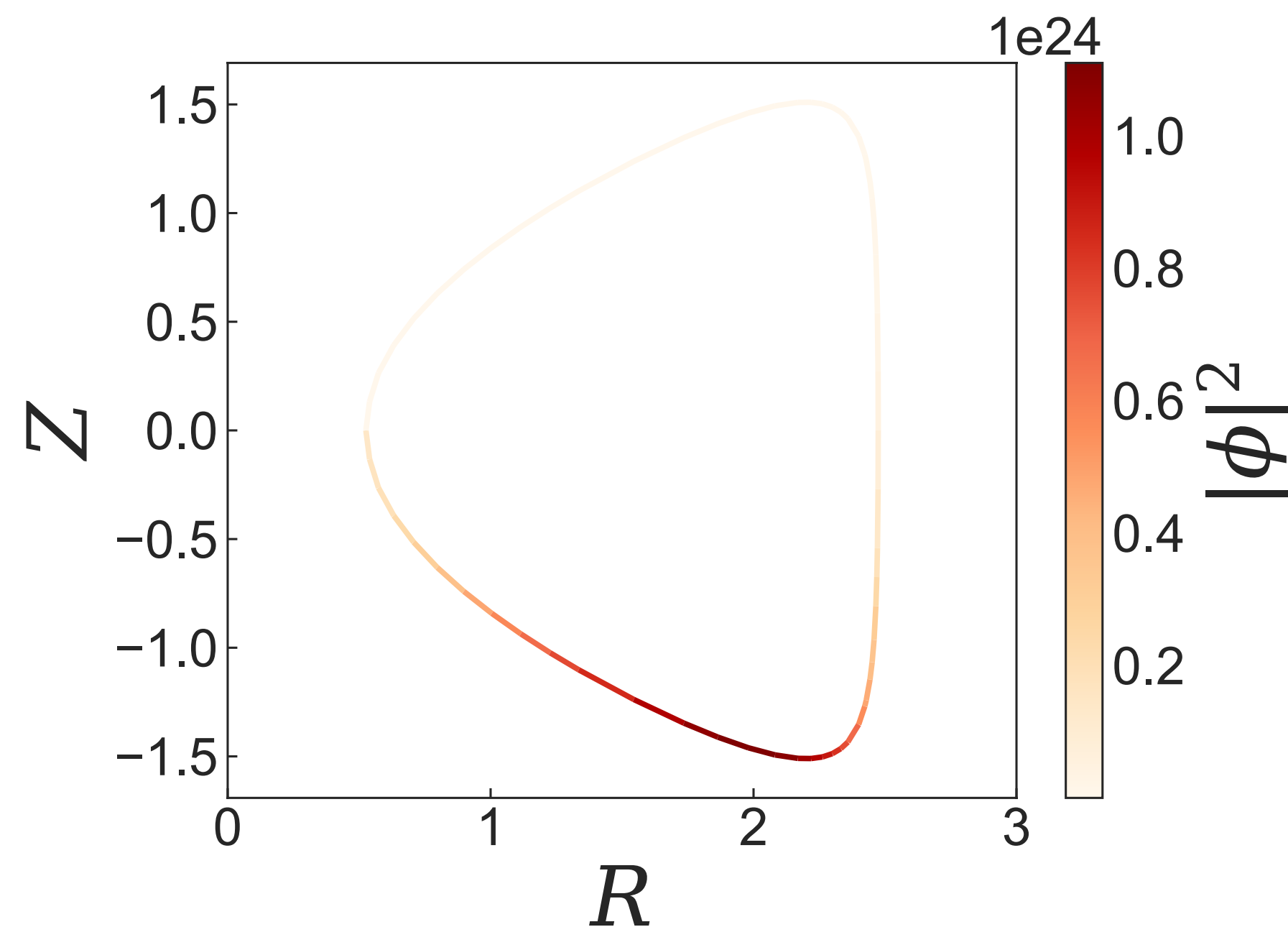
Write

$$R \simeq R_0 - a\delta \simeq a \left(\frac{1}{\epsilon} - \delta \right)$$

$$\frac{\omega_{*e}^T}{\omega_{ke}} \sim \frac{1}{\hat{s}\theta} \frac{R}{L_{Te}}$$

Why top/bottom of flux surface?

Answer: local flux expansion



- Perpendicular wavenumber can be written as

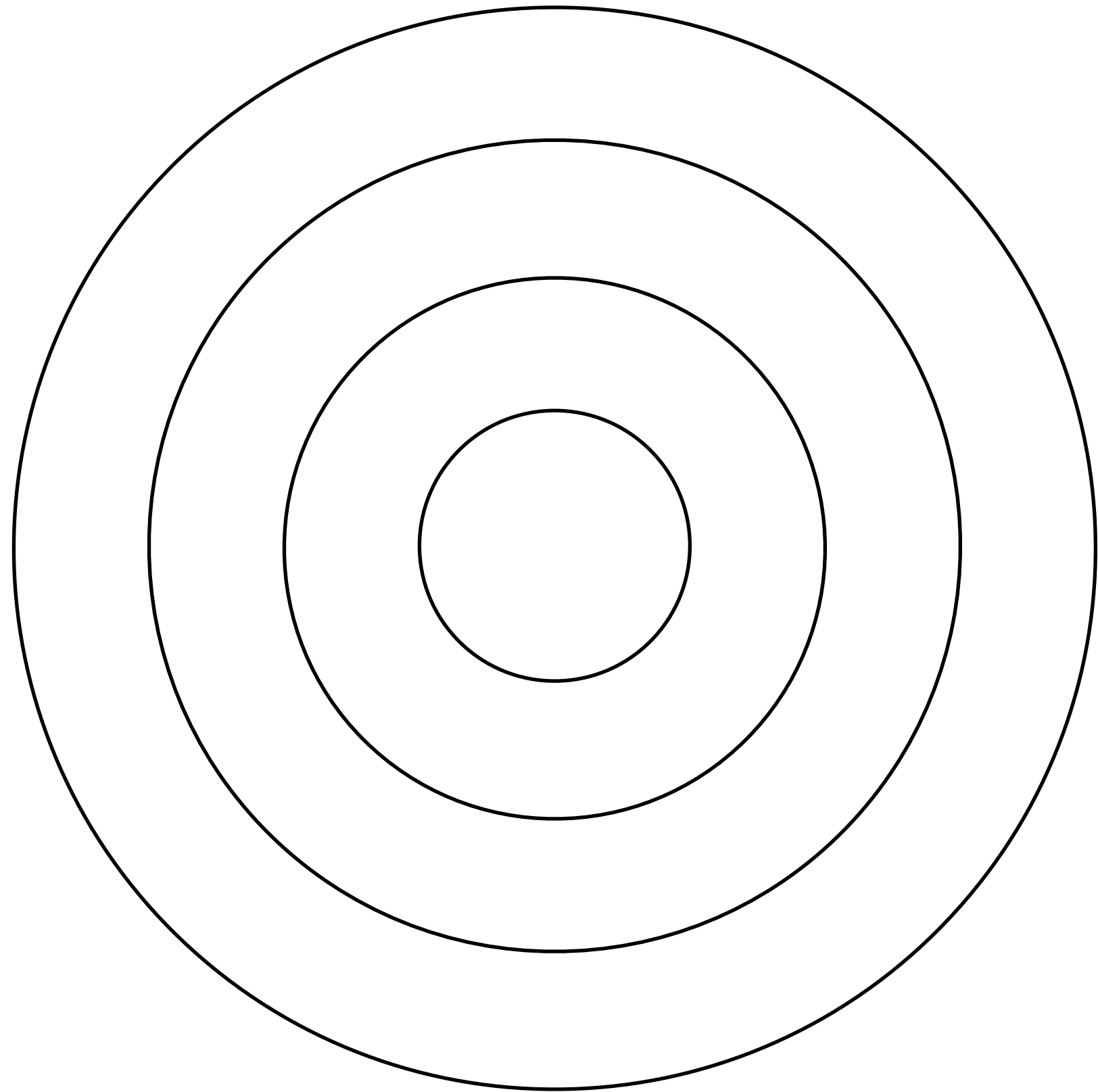
$$k_{\perp}^2 = k_y^2 \left(|\nabla y|^2 + \theta_0 \nabla x \cdot \nabla y + \theta_0^2 |\nabla x|^2 \right).$$

- The quantity $\nabla x \cdot \nabla y$ is roughly the local magnetic shear and $|\nabla x|^2$ is the **local flux expansion**.
- When $|k_{\perp} \rho_s|$ is smaller, **finite Larmor radius (FLR)** effects are weaker, and so the growth rate is typically higher for $|k_{\perp} \rho_s|$ smaller.

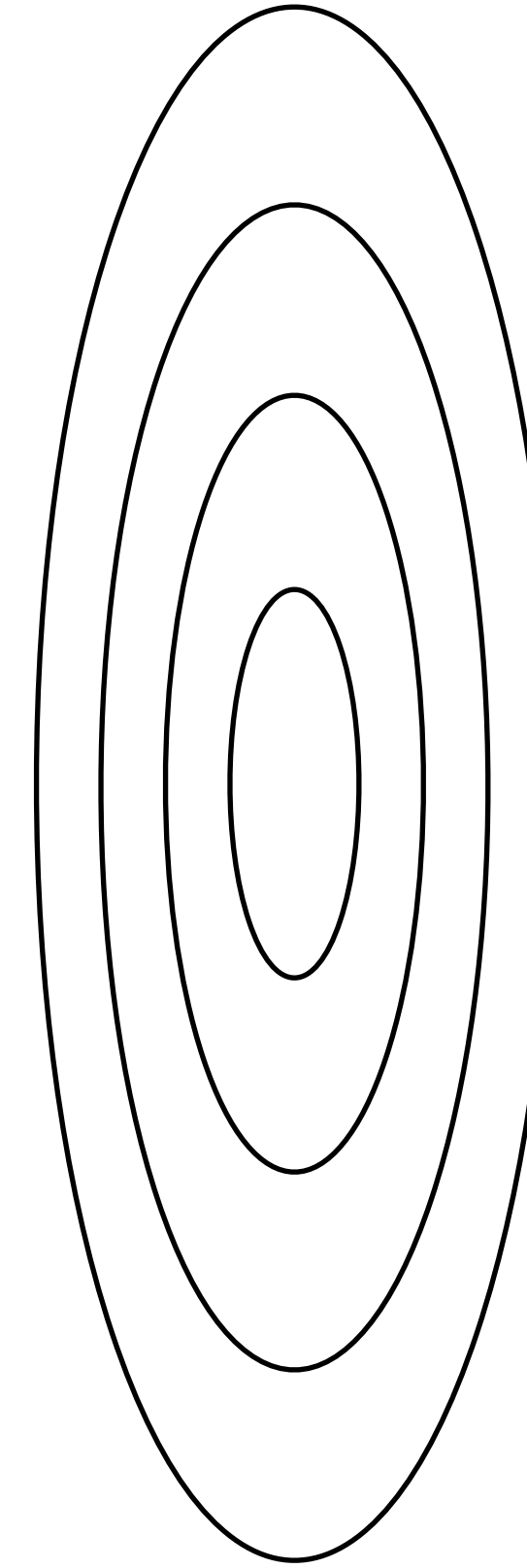
Flux expansion cartoon

Consider flux surfaces for two different shapes

Circular



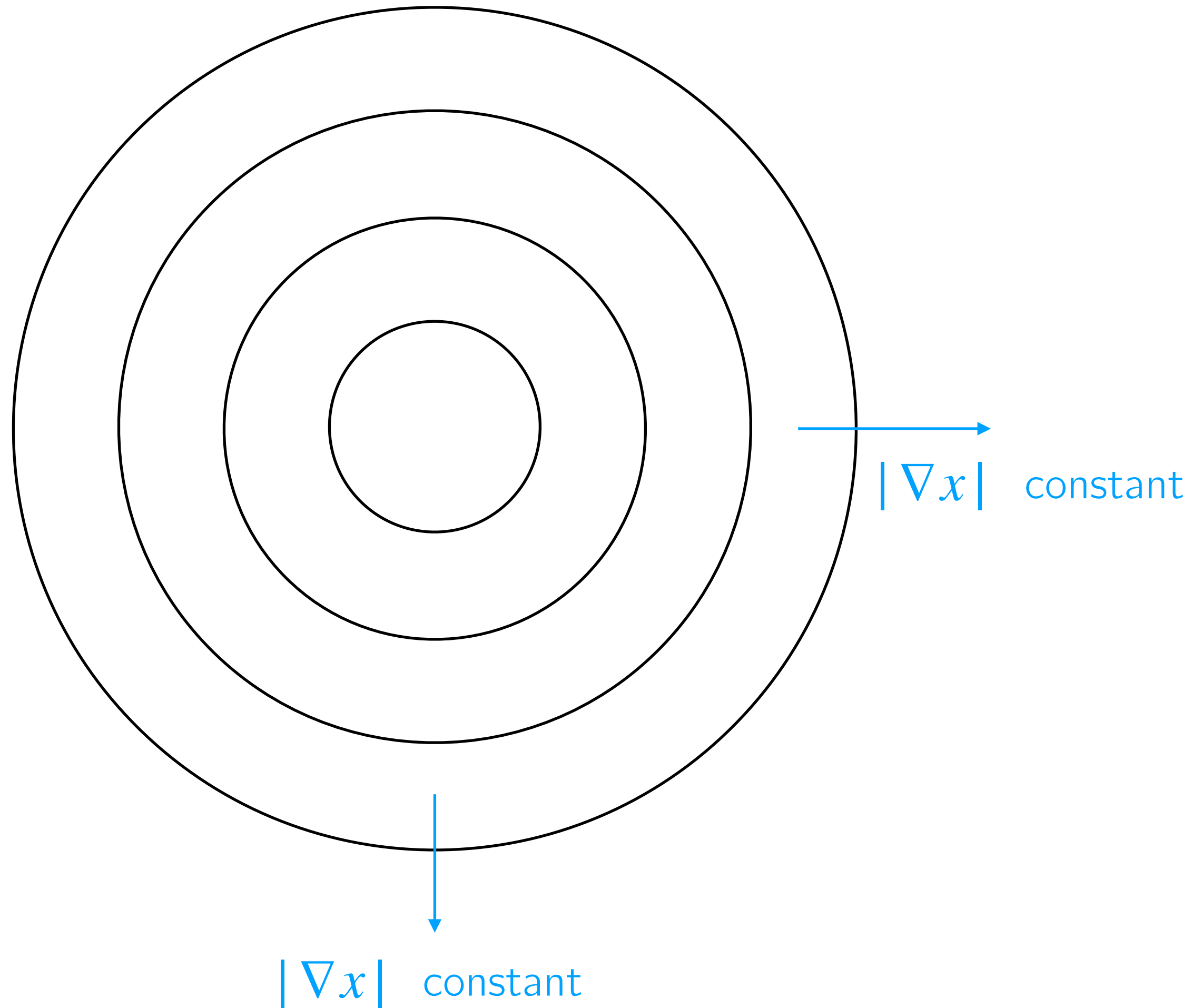
Elongated



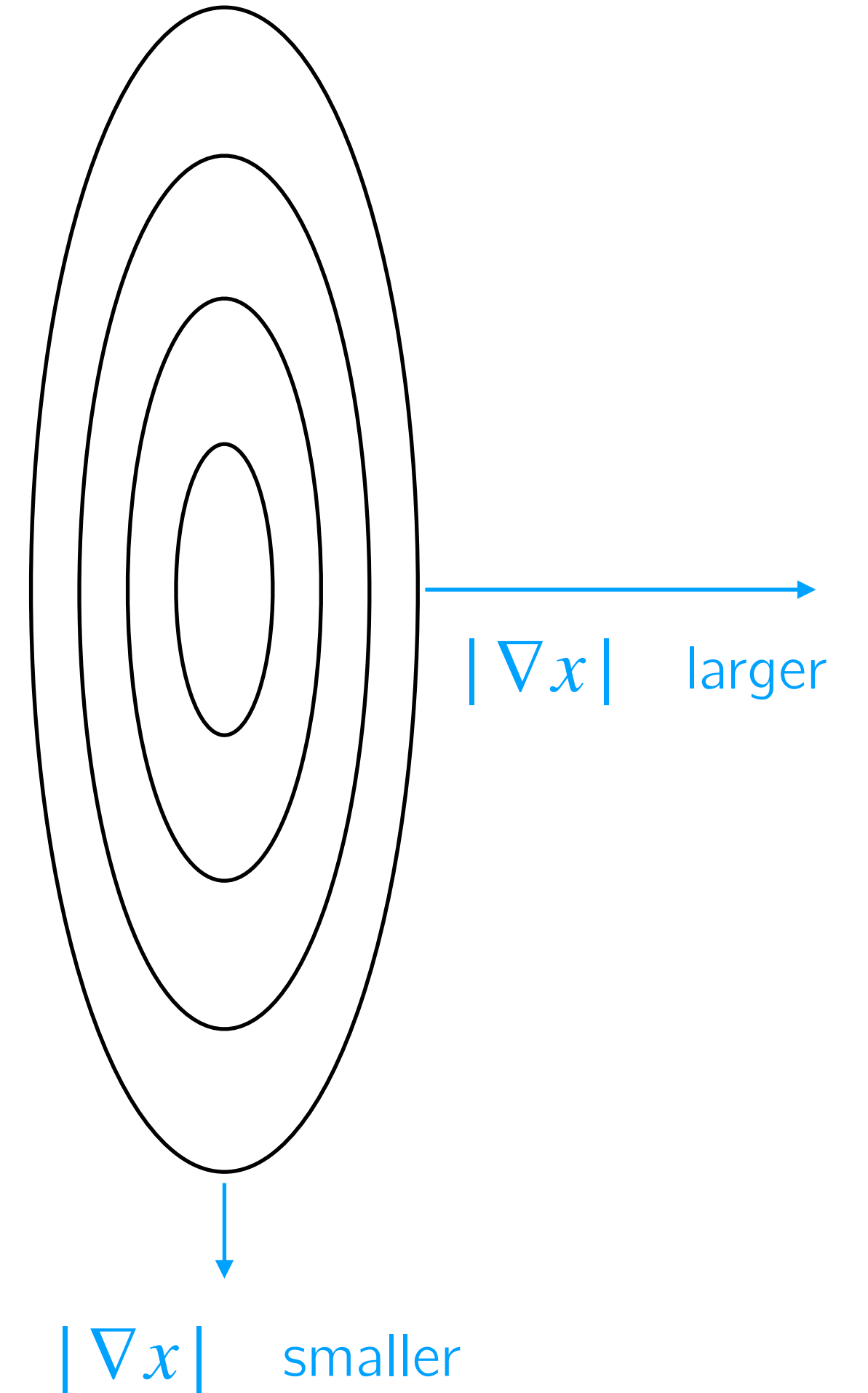
Flux expansion cartoon

Consider flux surfaces for two different shapes

Circular



Elongated

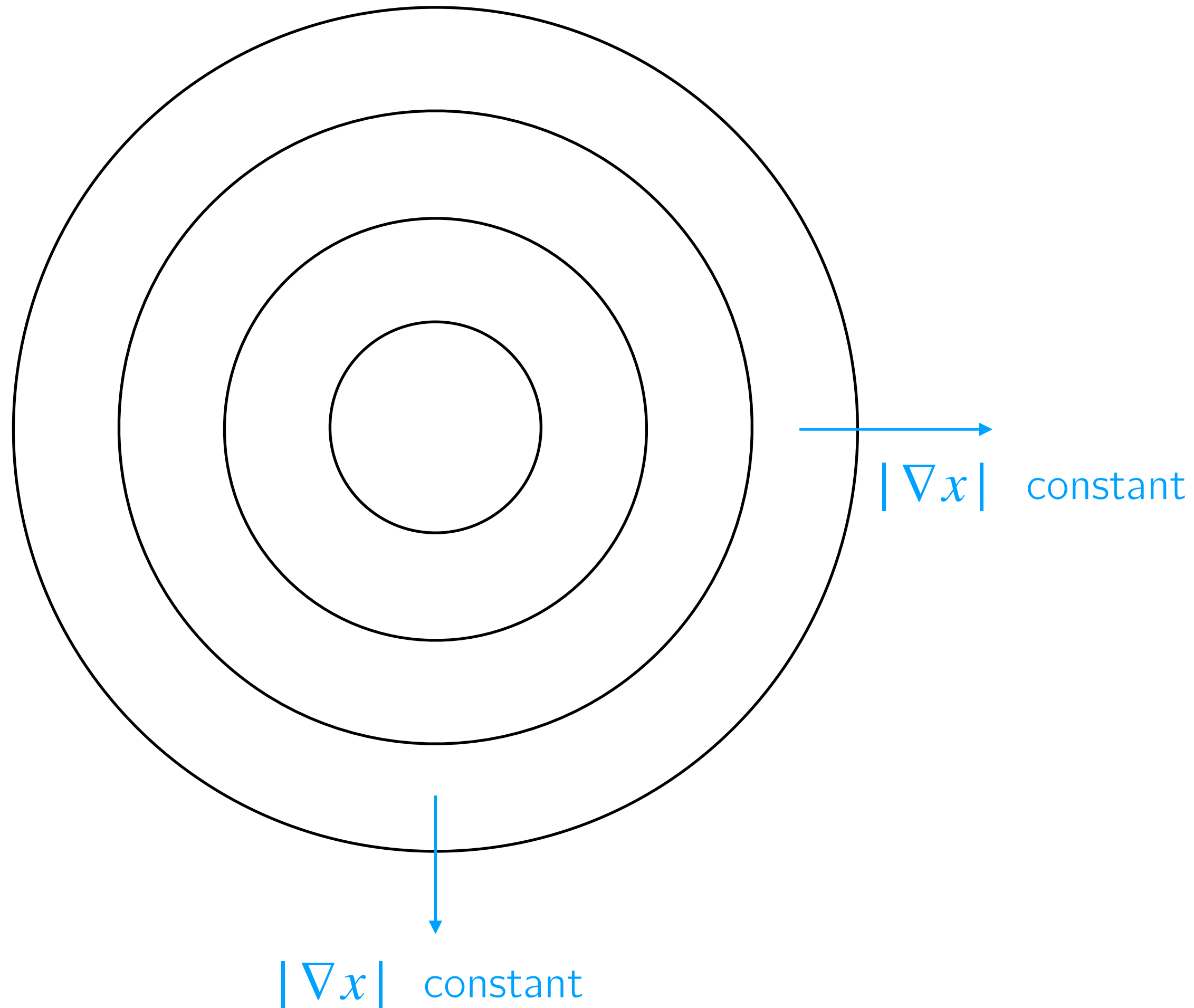


Flux expansion cartoon

Consider flux surfaces for two different shapes

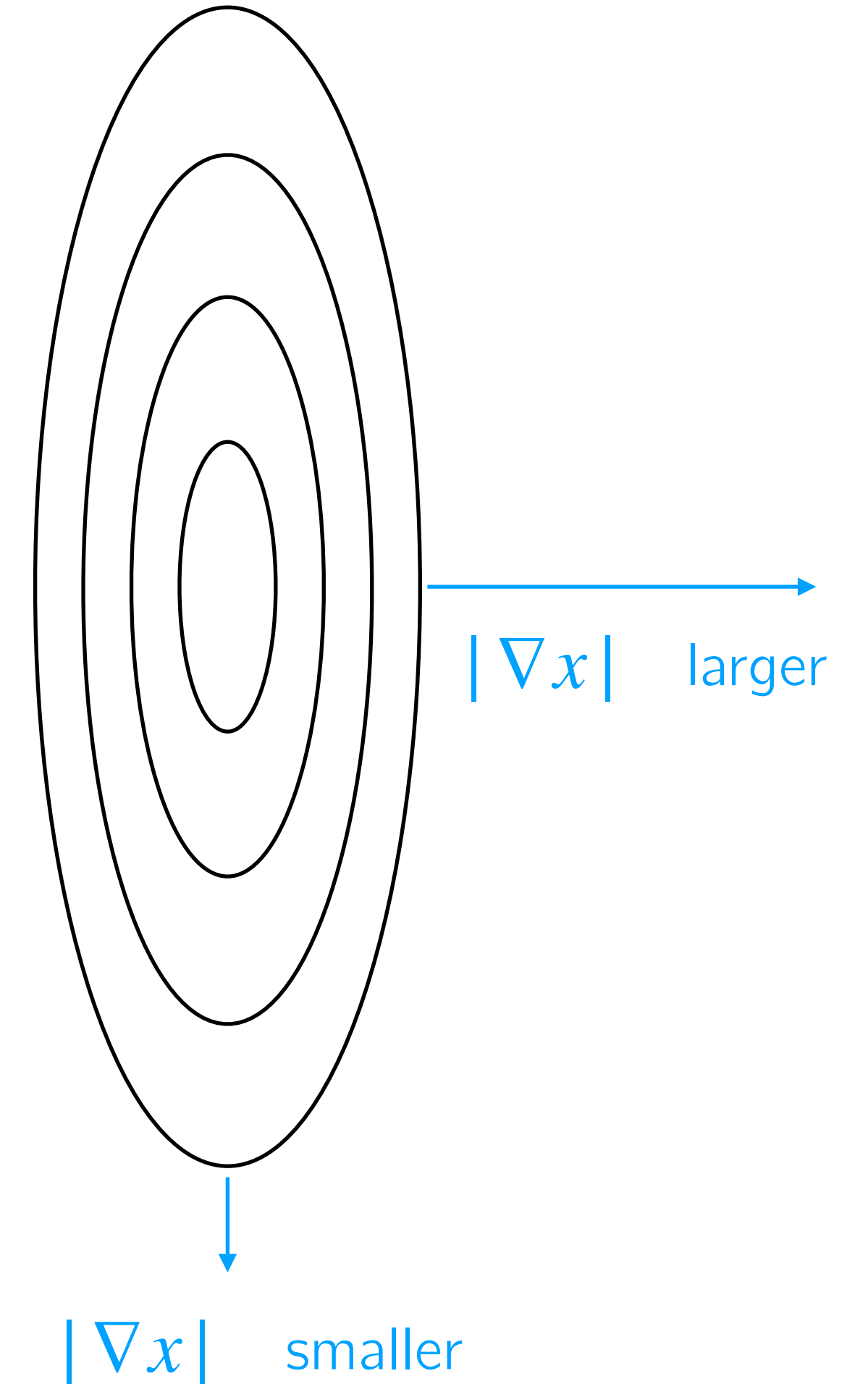
Circular

Flux expansion
constant



Elongated

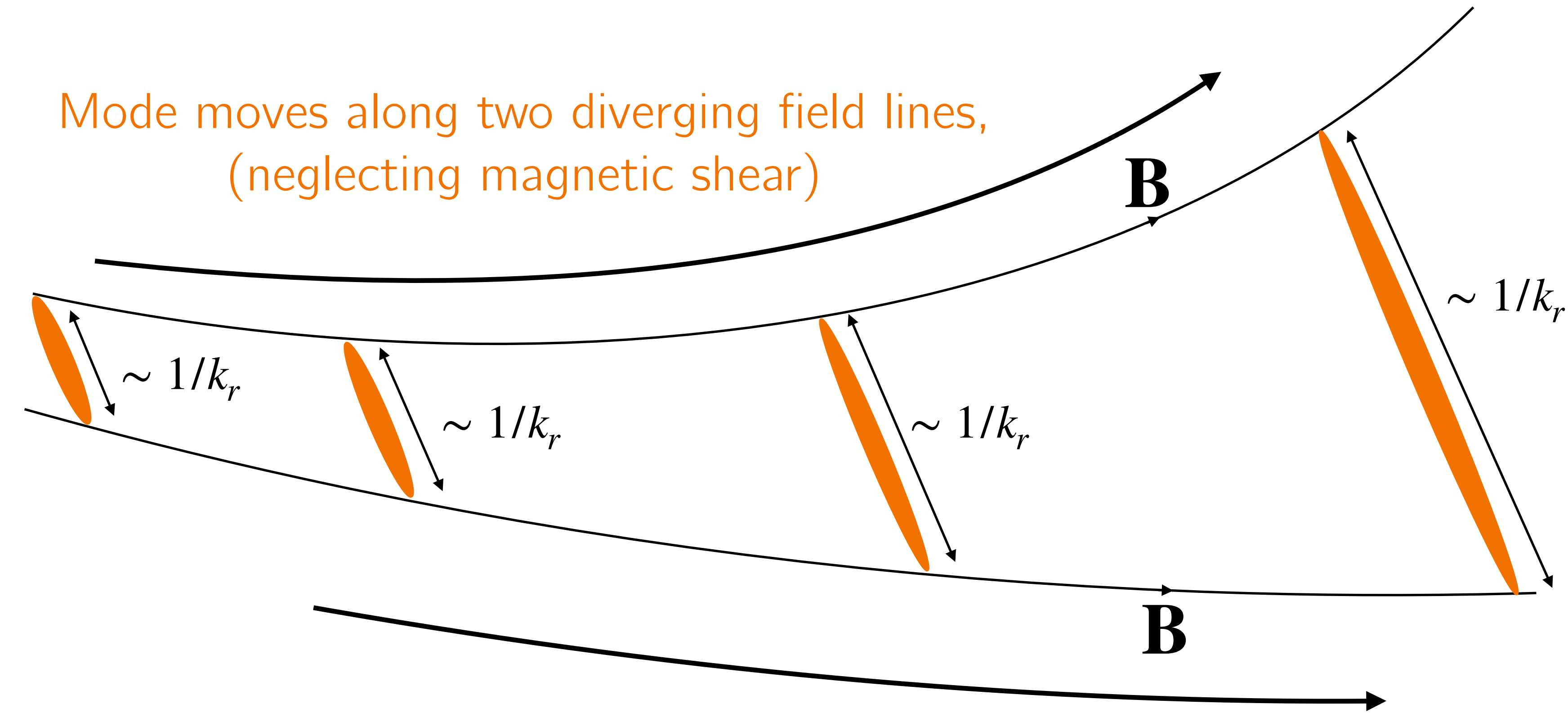
Flux expansion
varies with θ



Flux expansion cartoon

How flux expansion affects the radial wavenumber

Mode moves along two diverging field lines,
(neglecting magnetic shear)



$|\nabla x|$ decreasing

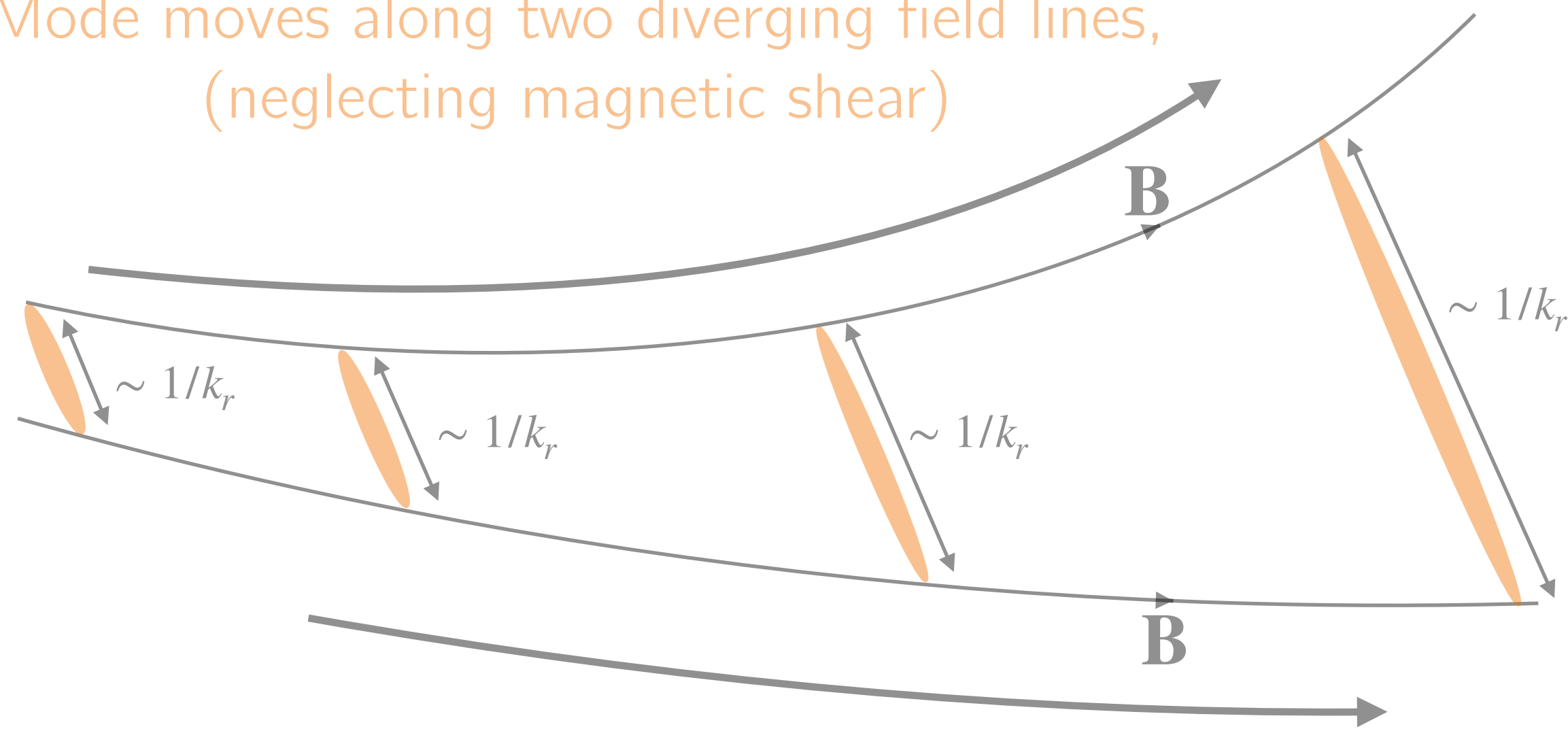
$|k_r|$ decreasing

$|\nabla x|$

Flux expansion cartoon

How flux expansion affects the radial wavenumber

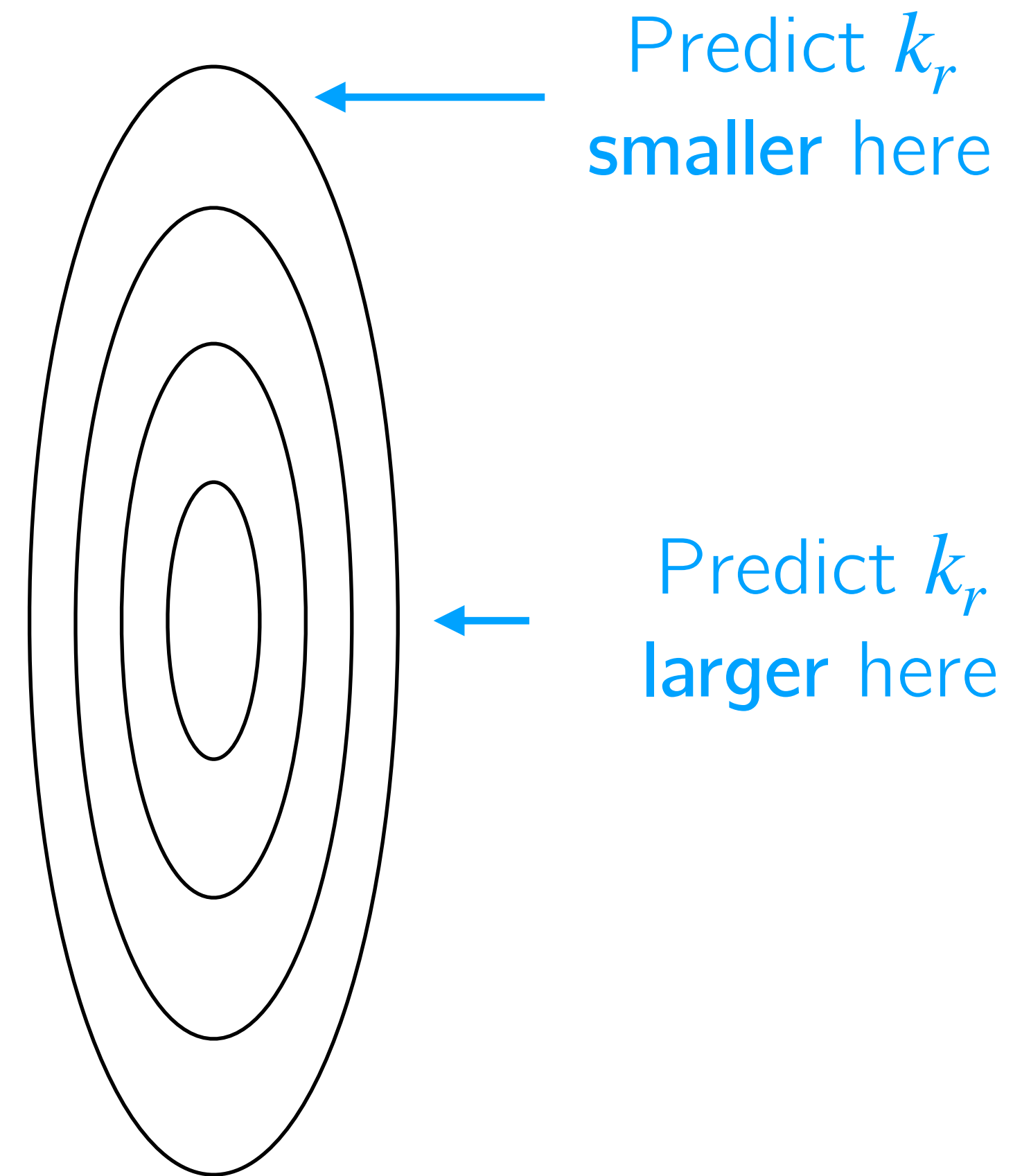
Mode moves along two diverging field lines,
(neglecting magnetic shear)



$|\nabla x|$ increasing

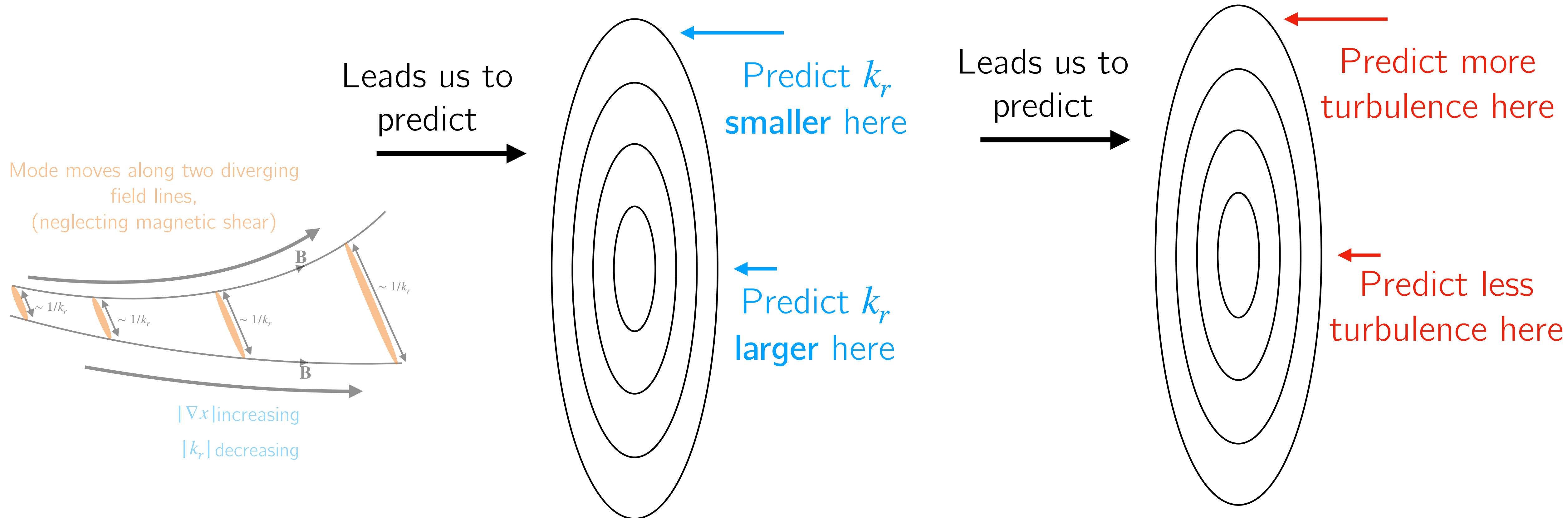
$|k_r|$ decreasing

Leads us to
predict



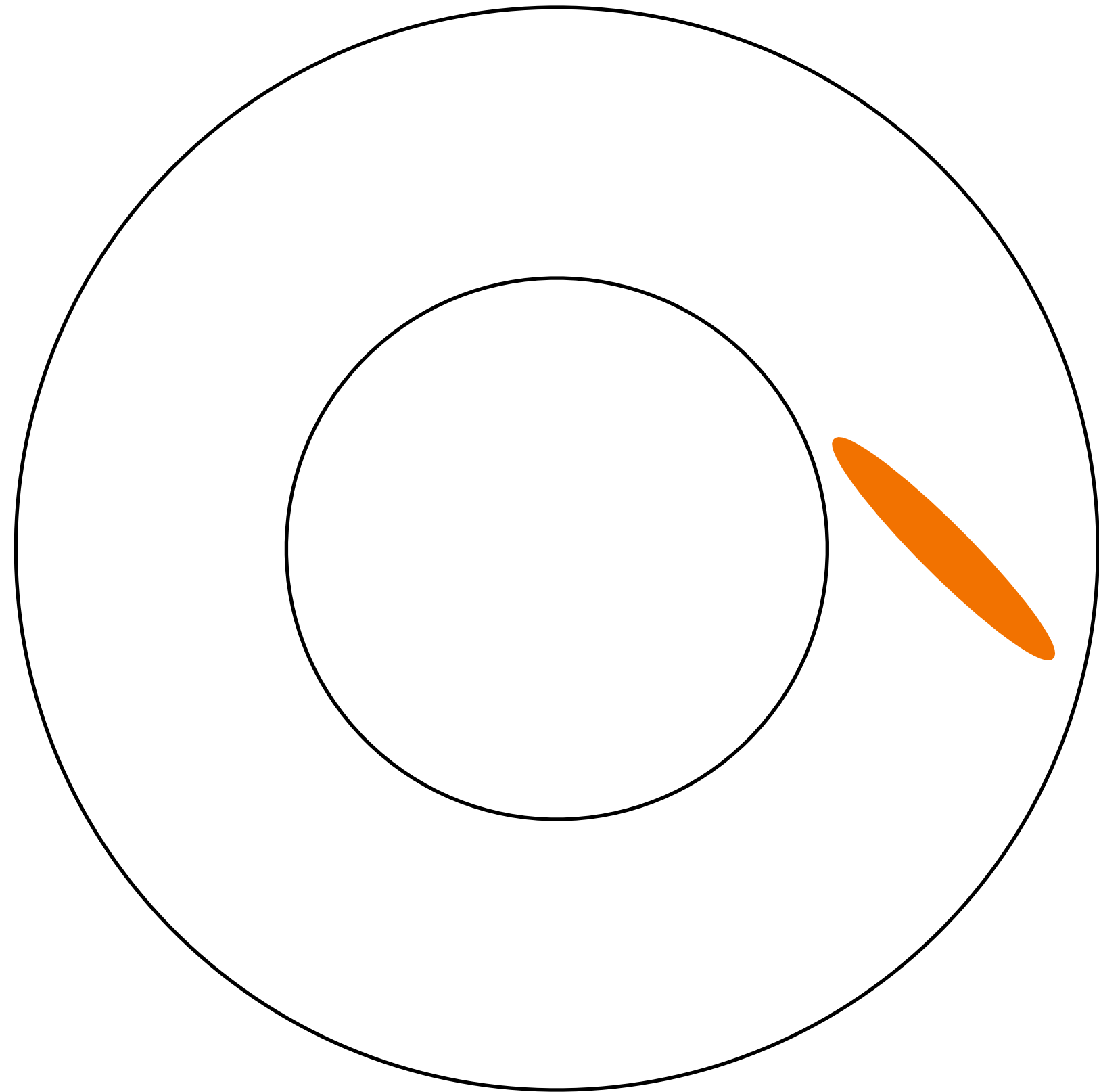
Flux expansion cartoon

How flux expansion affects the radial wavenumber

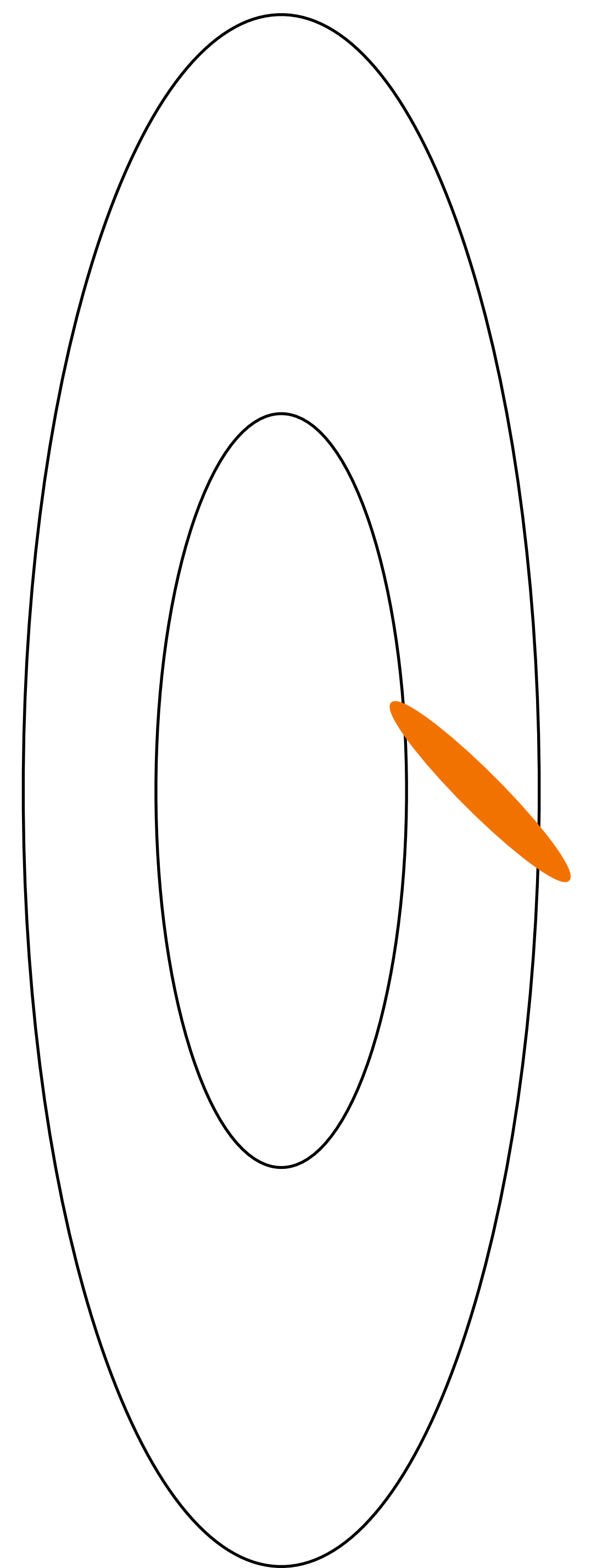


Flux expansion cartoon

Consider a mode on circular and elongated surface



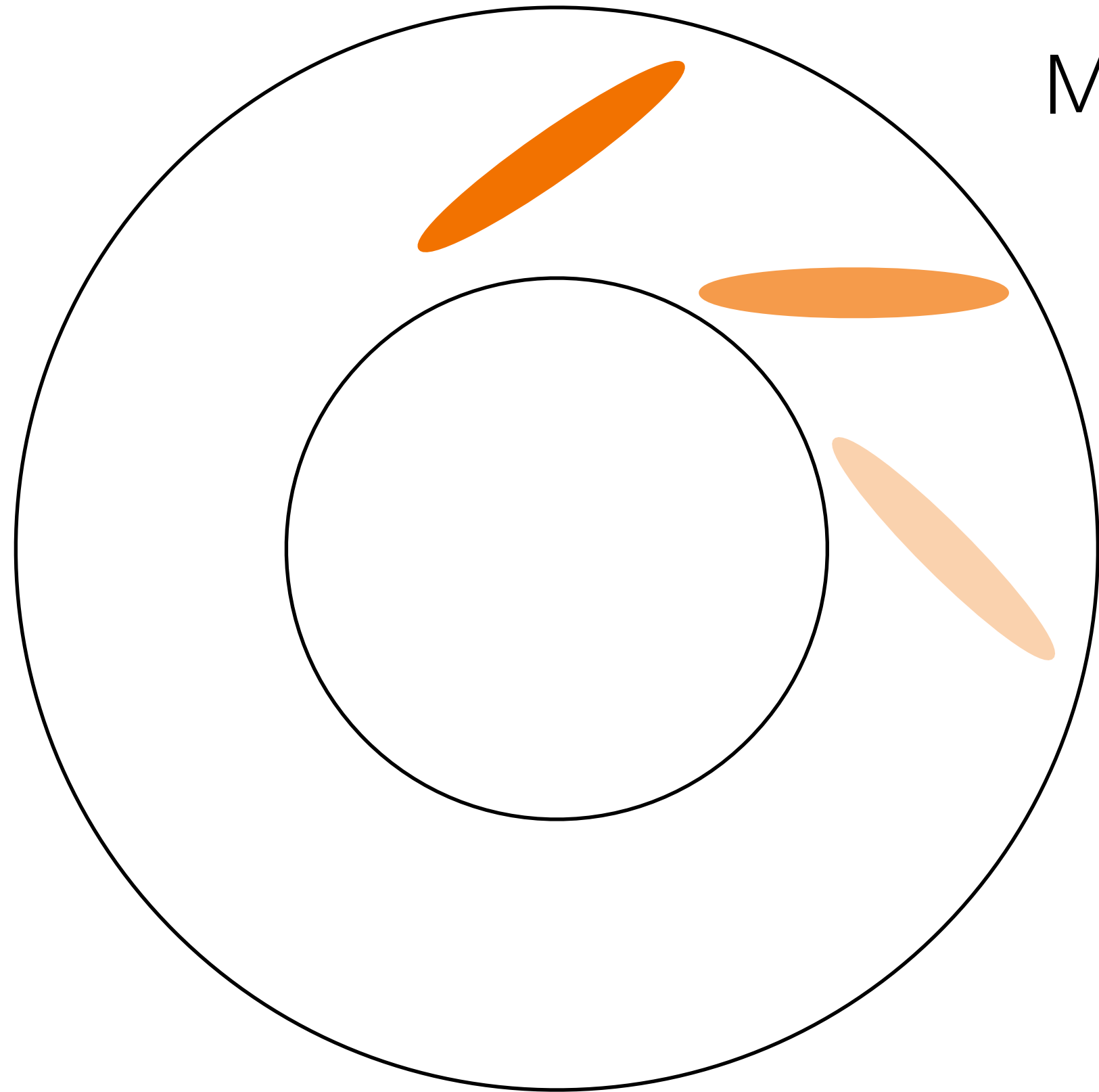
Mode starts at outboard midplane



$$k_{\perp}^2 = k_y^2 \left| |\nabla y|^2 + \theta_0 \nabla x \cdot \nabla y + \theta_0^2 |\nabla x|^2 \right|$$

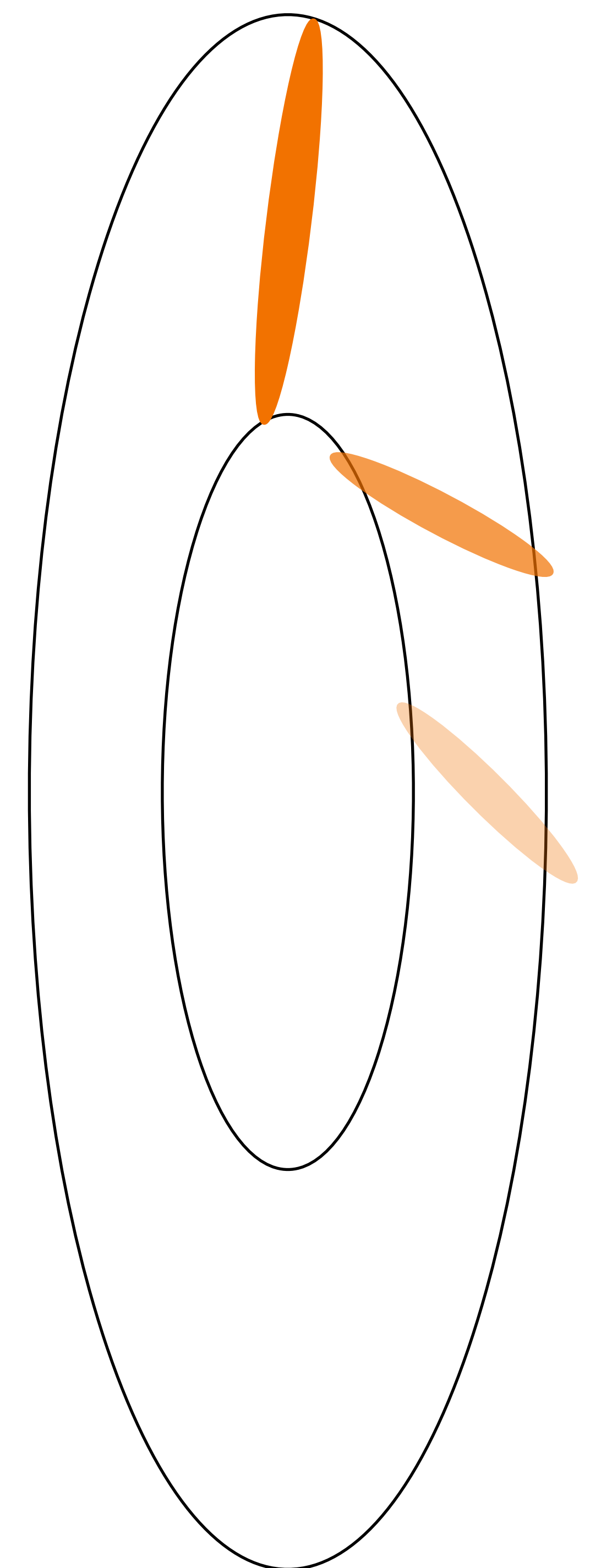
Flux expansion cartoon

Consider a mode on circular and elongated surface



Mode moves to outboard midplane
as flux expands

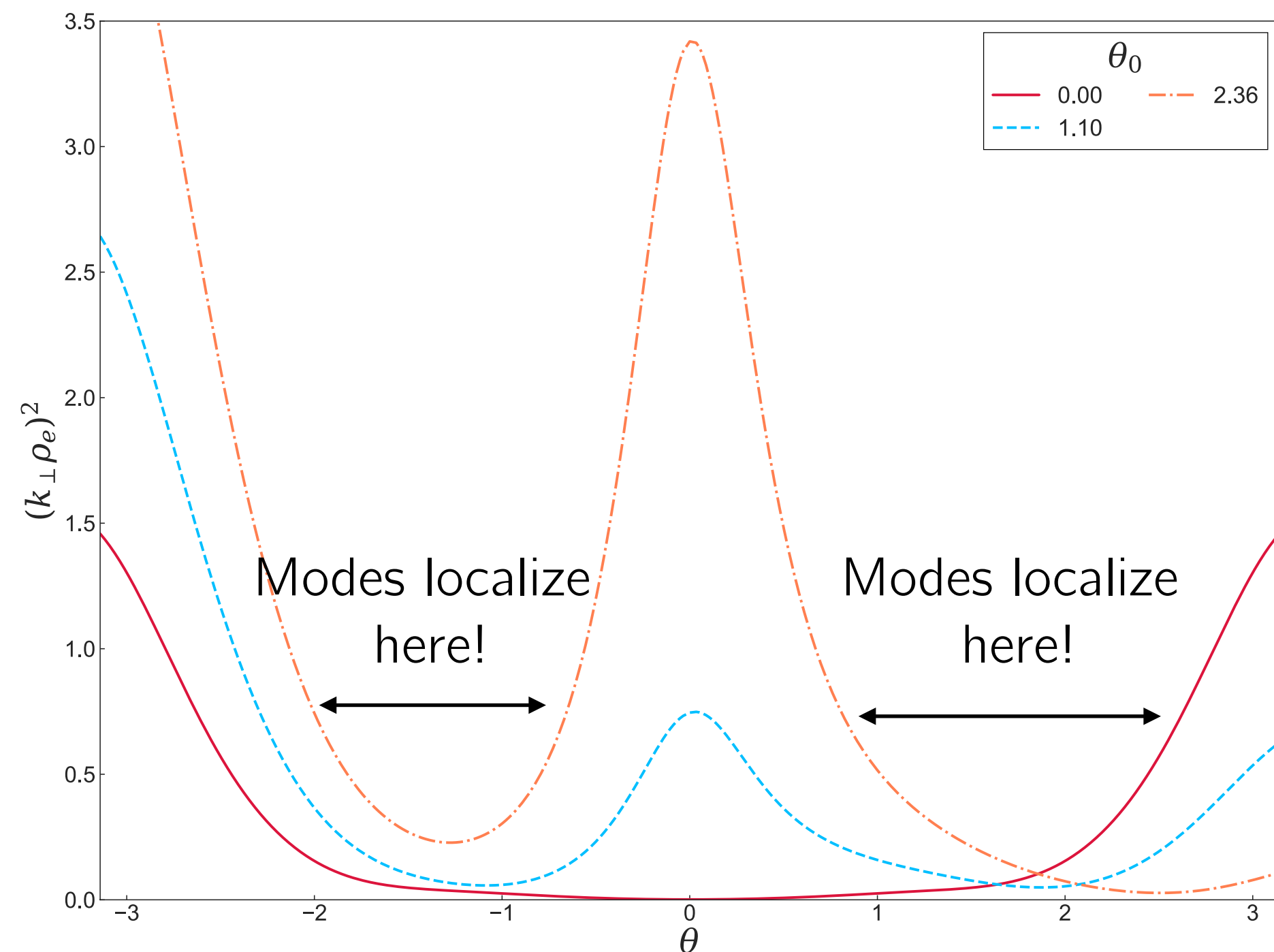
Mode starts at outboard midplane



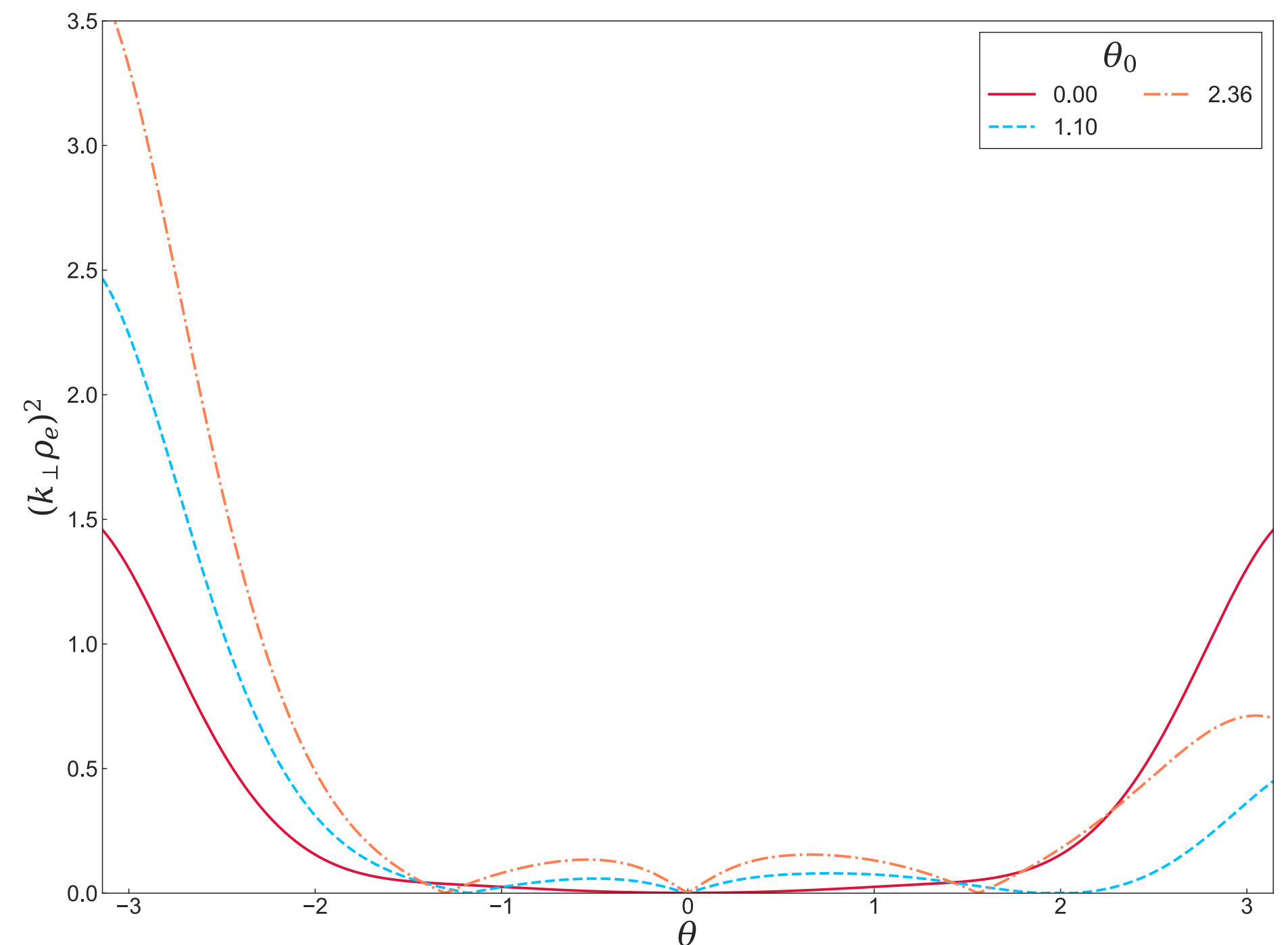
$$k_{\perp}^2 = k_y^2 \left| |\nabla y|^2 + \theta_0 \nabla x \cdot \nabla y + \theta_0^2 |\nabla x|^2 \right|$$

Evidence for this!

- Recall that $k_{\perp}^2 = k_y^2 \left(|\nabla y|^2 + \theta_0 \nabla x \cdot \nabla y + \theta_0^2 |\nabla x|^2 \right)$. By removing $|\nabla x|^2$ (flux expansion), we see can how much k_{\perp}^2 changes.
- Plotting $k_{\perp}^2(\theta, \theta_0)$ for JET pedestal with and without $|\nabla x|^2$:



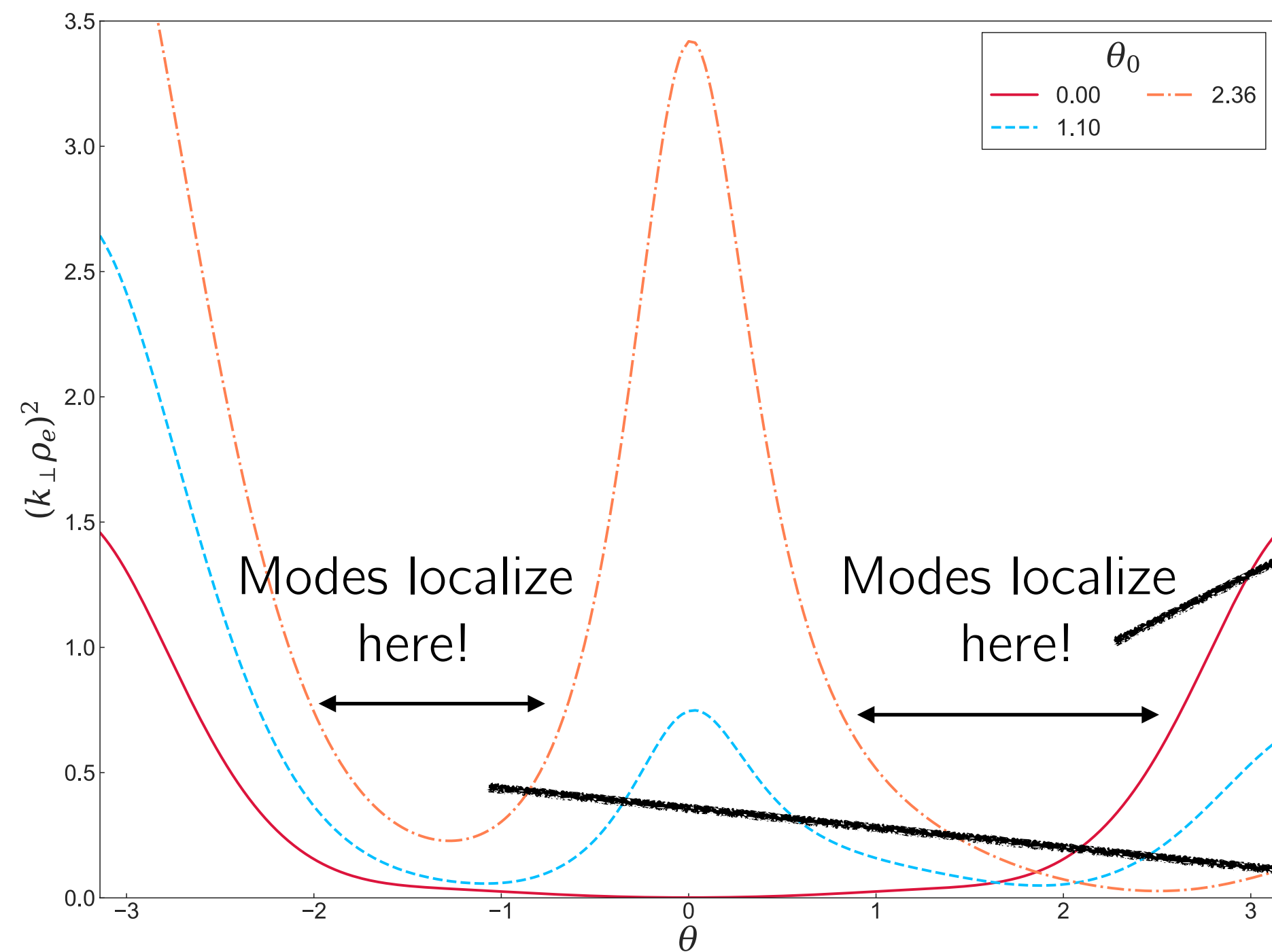
a) $(k_{\perp} \rho_e)^2$ versus θ for 3 values of θ_0 .



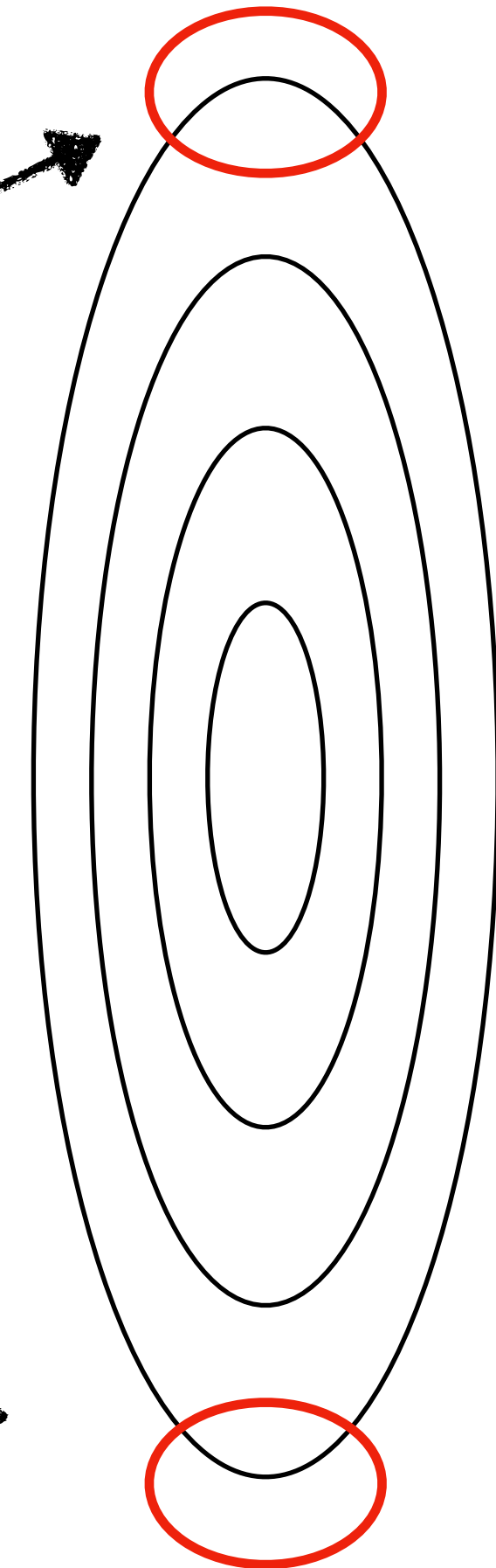
b) same as a) but with no flux expansion.

Evidence for this!

- Recall that $k_{\perp}^2 = k_y^2 | |\nabla y|^2 + \theta_0 \nabla x \cdot \nabla y + \theta_0^2 |\nabla x|^2 |$. By removing $|\nabla x|^2$ (flux expansion), we see can how much k_{\perp}^2 changes.



a) $(k_{\perp} \rho_e)^2$ versus θ for 3 values of θ_0 .



Generalized principles

Turbulence typically at location where flux expansion is high

